CHALMERS
UNIVERSITY OF TECHNOLOGY

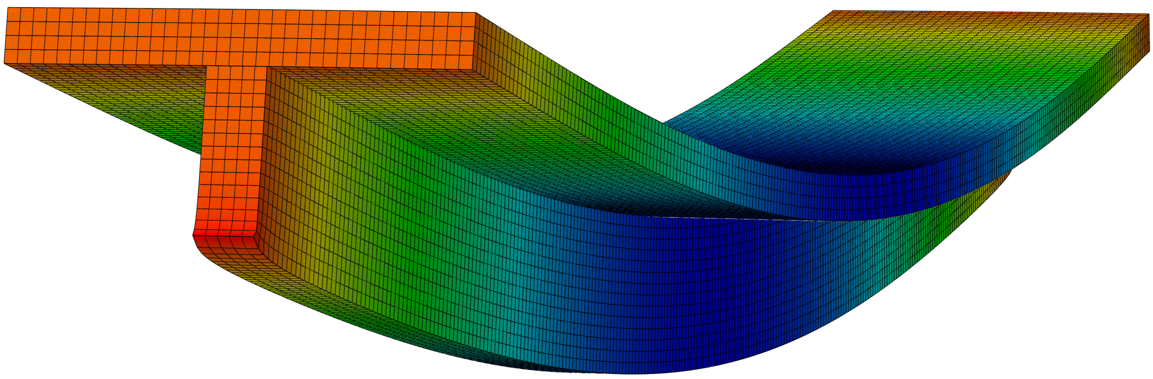

Long-term behaviour of Timber Concrete Composite elements

Finite element study of long-term deflections caused by creep and shrinkage

Master's thesis in Structural Engineering and Building Technology

CARL-JOHAN KÄLL
SAMUEL WIIK

DEPARTMENT OF ARCHITECTURE AND CIVIL ENGINEERING
CHALMERS UNIVERSITY OF TECHNOLOGY
Gothenburg, Sweden 2022
www.chalmers.se

Master's thesis 2022

Long-term behaviour of Timber Concrete Composite elements

Finite element study of long-term deflections caused by creep and shrinkage

CARL-JOHAN KÄLL
SAMUEL WIIK

Department of Architecture and Civil Engineering
Division of Structural Engineering
Chalmers University of Technology
Gothenburg, Sweden 2022

Long-term behaviour of Timber Concrete Composite elements
Finite element study of long-term deflections caused by creep and shrinkage
CARL-JOHAN KÄLL
SAMUEL WIIK

Supervisor: Linda Jakobsson, ELU Konsult AB
Supervisor: Johannes Lundgren, ELU Konsult AB

Examiner: Robert Jockwer, Department of Architecture and Civil Engineering

Master's Thesis 2022
Department of Architecture and Civil Engineering
Division of Structural Engineering
Chalmers University of Technology
SE-412 96 Gothenburg
Telephone +46 31 772 1000

Cover: Deflection of a Timber Concrete Composite element with a "T"-shaped cross section modelled in the finite element software Abaqus CAE.

Typeset in LaTeX
Printed by Chalmers Reproservice
Gothenburg, Sweden 2022

Long-term behaviour of Timber Concrete Composite elements
Finite element study of long-term deflections caused by creep and shrinkage
CARL-JOHAN KÄLL
SAMUEL WIIK
Department of Architecture and Civil Engineering
Chalmers University of Technology

Abstract

Timber Concrete Composite (TCC) is a hybrid structure for effective material utilization, combining the compression performance of concrete with the tension capacity of timber. There are multiple design possibilities in terms of cross-sectional design, production method and type of connection. Especially the latter has a significant impact on the behaviour. Additionally, the interaction of timber and concrete causes a complex long-term behaviour, with deflections often being a critical aspect.

The design approach presented in Eurocode 5 is based on an analytical calculation method called the γ-method (“gamma”-method). There, an effective cross-sectional stiffness is calculated based on the interaction degree between the timber and concrete. The γ-method has several limitations in terms of applicability and accuracy, and a more conformable solution procedure is achieved with a numerical analysis. In this work, the Finite Element software Abaqus is used as a numerical solver, where a modelling procedure for a “T”-cross-section is established. It is then used in a two-part parametric study to evaluate the long-term deflections of TCC elements.

In the first part of the parametric study, the impact of shrinkage and creep is evaluated for a chosen cross-section. The concrete shrinkage has a significant impact on the deflections, especially for high-stiffness connections. However, if the timber shrinks as well, the deflection increase is counteracted. The creep of timber and connection has a large impact on the estimated deflections. Contrary, the concrete creep factor has a much smaller influence for the studied cross-section. The second part of the parametric study investigate the concrete shrinkage impact together with cross-sectional design optimisations. In the studied case, increasing the concrete thickness is inefficient since the long-term load case is highly dependent on the self-weight, and the additional concrete weight counteracts the stiffness increase.

The conclusions of the study is that concrete shrinkage has a potentially large impact on the deflections, however the γ-method neglects its impact. Prefabrication of the concrete or using low-shrinkage concrete are suggested measures to reduce the deflection caused by its shrinkage. Additionally, further studies of lightweight concrete is suggested to reduce the dominant load-impact of the self-weight.

Keywords: TCC, long-term, deflection, shrinkage, creep, FE-modelling

Långtids-beteende av trä-betongsamverkansbjälklag
Finita element studie av långtids-deformationer orsakat av krympning och krypning
CARL-JOHAN KÄLL
SAMUEL WIIK
Instutitionen för arkitektur och samhällsbyggnadsteknik
Chalmers Tekniska Högskola

Sammanfattning

Trä-betongsamverkansbjälklag (på engelska TCC) är en hybridkonstruktion för effektivare materialutnyttjande, som fås genom att kombinera betongens goda egenskaper i tryck tillsammans med träets dragkapacitet. Det finns ett flertal möjligheter att påverka dess design, såsom tvärsnittsform, produktionsmetod och val av förband. Speciellt den sistnämnda har en betydande påverkan på beteendet. Dessutom medför interaktionen mellan trä och betong ett komplext beteende över lång tid, där nedböjning ofta är en kritisk aspekt.

Dimensioneringsmetoden som presenteras i Eurokod 5 baseras på en analytisk beräkningsmetod, γ-metoden ("gamma"-metoden). Där beräknas en effektiv tvärsnittsstyvhet som baseras på interaktionsgraden mellan träet och betongen. γ-metoden har ett flertal begränsningar vad gäller tilllämplighet och noggrannhet, och en mer överensstämmande lösningsmetod fås genom en numerisk analys. I detta arbete används finita element programmet Abaqus för en numerisk lösningsgång, där en modelleringsteknik för ett T-tvärsnitt tas fram. Denna används i en parametrisk studie i två delar för att bestämma nedböjning över långtid för ett TCC element.

I första delen av parametriska studien bestäms påverkan av krympning och krypning för ett valt tvärsnitt. Betongkrympningen har en betydande påverkan på nedböjningen, speciellt för styva förband. Däremot, om träet samtidigt krymper motverkas ökningen i nedböjning. Krypning av trä och förband har en stor påverkan på den beräknade nedböjningen. Krypfaktorn för betong har en mycket mindre påverkan för det studerade tvärsnittet. Andra delen av parametriska studien undersöker betongkrympningens inverkan tillsammans med optimeringar av tvärsnittets utformning. För det studerade fallet är en ökning av betongtjockleken ineffektivt eftersom långtids-lastfallet är starkt beroende utav egenvikten, och där den tillkommande betongvikten motverkar styvhetsökningen.

Slutsatserna som görs är att betongkrympningen har en potentiellt stor påverkan på nedböjningarna, trots detta försummar γ-metoden dess inverkan. Prefabricering av betongen eller att använda krympreducerad betong är föreslagna åtgärder för att minska nedböjningen från dess krympning. Ytterligare föreslås även vidare studier av lättbetong som ett sätt att minska den dominerande lastpåverkan från egenvikten.

Nyckelord: TCC, långtid, nedböjning, krympning, krypning, FE-modellering

Contents

List of Figures

List of Tables

List of Acronyms

Below is the list of acronyms that have been used throughout this thesis listed in alphabetical order:

CC-distance	Center Center distance
CLT	Cross laminated timber
EN	European Standard
Glulam	Glued laminated timber
ISO	International Organization for Standardization
LVL	Laminated Veneer Lumber
SLS	Serviceability Limit State
SS	Swedish Standard
TCC	Timber Concrete Composite
ULS	Ultimate Limit State

Acknowledgement

We have spent most of our time during this thesis at ELU's office here in Gothenburg and we would like to express our greatest gratitude to everyone working there for welcoming us so warmly. Special thanks goes out to Linda Jakobsson and Johannes Lundgren which additionally were our supervisors in this thesis and have helped us during the work. Lastly, thanks goes out to our supervisor at Chalmers, Robert Jockwer, who patiently has answered our questions and guided us in the process.

Carl-Johan Käll and Samuel Wiik, Gothenburg, May 2022

1

Introduction

The background, aim, limitations and method of the thesis are presented in the introductory chapter.

1.1 Background

As the greenhouse gas emissions caused by human activities are reaching a critical state, the construction industry plays an important role in taking the required actions to reduce its environmental impact. In the light of this, the interest in developing and using more sustainable construction materials is ever-increasing. The most predominant building material in the debate is the usage of timber, which has seen a large increase in interest over the last decade. However, due to its low density, constructing large buildings purely in timber entails problems with for instance stiffness, vibrations and acoustics. Therefore, the concept of hybrid structures, combining for example timber and concrete, is interesting to further investigate.

One of the combinations is the Timber Concrete Composite (TCC), which consists of timber slabs or beams with concrete cast upon it. The advantages compared to pure timber floors include better sound and vibration behaviour as well as higher stiffness. Additionally, TCC might improve the global stability if used in high-rise timber buildings, owing to the increased self-weight. However, the usage of TCC elements also entail several challenges such as achieving an adequate shear connection as well as a complex long-term behaviour in regard to shrinkage, creep, swelling and other time-dependent phenomena. Due to these challenges, the usage of TCC elements is still uncommon in Sweden, and there is a general lack of awareness and knowledge within the industry regarding the subject.

1.2 Aim

The broad aim of this thesis is to increase the knowledge of TCC elements and serve as a basis for possible future applications within the industry. More specifically, this includes an investigation of the long-term deformation behaviour caused by the different long-term effects of timber and concrete as well as the connection. The main questions the report treats are:

- What the most important long-term effects to consider in design are, and how large influence they have on the behaviour.
- How deflections caused by long-term effects can be minimized.
- Evaluation of current calculation methods for TCC, with emphasis on long-

term deflections.

- To find suggested design approaches for TCC in long-term.

1.3 Limitations

The focus of the studies is on TCC elements with a “T” cross-section, and other geometries will only be briefly presented. Furthermore, the analysis is performed for simply supported elements. The long-term deflections are the main interest, and acoustics and vibration performance will not be evaluated. Thereto, instability phenomena will not be considered.

The shear connection is a key aspect in the construction of TCC elements and its behaviour is therefore presented. However, since the connection performance is not the focus of the study, it is treated to a limited extent. Linear-elastic behaviour is assigned to all materials (concrete, connection, timber) which is a fairly accurate assumption since the analysis is performed for deflections in SLS.

Constant climate is assigned in the FE-model and therefore no effects from varying temperature and relative humidity is evaluated explicitly. The effect of varying climate, especially relative humidity, is taken into account by applying different service classes.

1.4 Method

The thesis begins with a literature study to acquire a deeper understanding of TCC elements, with extra focus on the long-term aspects. The aim of the study is also to specify the most important long-term factors to consider and based on it limit the extent of the FE-modelling. Experimental data to use when verifying the FE-model is also collected. Based on the knowledge obtained in the literature study, a FE-modelling technique is constructed using the software Abaqus CAE. The purpose of the model is to predict the long-term behaviour of TCC elements for different conditions, such as long-term effects and type of cross-section.

The validated FE-model is then used in a parametric study, where the impact of the long-term effects, shrinkage and creep, are evaluated for a specific cross-section. Based on the result, the concrete shrinkage is chosen for a more detailed study in a second parametric study, where various design choices are evaluated. From the two parametric studies and with the information gained from the literature study, conclusions on how to minimize the negative impacts from shrinkage and creep are made together with general design proposals.

2

Concept of TCC

The behaviour of a Timber Concrete Composite (TCC) element is greatly influenced by its cross-sectional proportions and the connection between the timber and concrete. The design choice affects the mechanical properties along with the stress- and strain distribution within the cross-section. Additionally, different production choices are possible.

When designing a TCC element, the hardest criteria to fulfil is usually the deflection limitation. Eurocode 5, SS-EN 1995-1-1:2004 (2009), presents a simplified analytical calculation method to use in design. However, several experimental studies that have been performed demonstrates shortcomings of the simplified design approach.

2.1 Characteristics

The structural principle of a TCC floor is that it takes the compressive forces in the concrete whilst the tension is taken by the timber. In that way, the materials are utilized efficiently in the cross-section unlike in a pure concrete slab, where the tension side is cracked, and the concrete there has little to none load-bearing functionality. Removing the tension-subjected concrete along with its reinforcement and replacing it with timber can in a well-designed cross-section make better use of the material properties.

In the cross-section, the concrete is mounted on top of a timber beam or slab, which in a floor structure results in the sought stress distribution, with compression at the top and tension in the bottom. However, a crucial factor to establish this behaviour is that the connection between the two materials is stiff enough to develop the composite action. Without a connection between the timber and concrete, the elements behave as two separate beams.

All of the three main mechanical properties (strength, stiffness and ductility) are heavily affected by the timber-concrete connection. They are also related to each other and therefore it is important to understand each of these properties to properly predict the cross-sectional behaviour. If a TCC element is well-designed, it shows multiple advantages compared to pure concrete- or timber beams. However, the weight of the concrete may induce large deflections.

2.1.1 Element types

TCC floors can be divided into two main categories, beam type and slab type. Ogrin and Hozjan (2021) describe that the difference between them is if a web and a flange can be distinguished in the cross-section. Apart from the visual difference between the two types of cross-sections, the location of the neutral axis differs between them. That will influence the tensile cracking behaviour of the concrete and therefore also affect which design procedure is suitable (Ogrin & Hozjan, 2021).

In a beam type cross-section, a web and a flange can be seen, which means that the width of the concrete is larger than the width of the timber. Such a cross-section is designed by having timber beams at a certain spacing, cc-distance, with continuous concrete on top. The timber beams could for example be made up of massive timber or glued laminated timber (Glulam). In a beam type TCC element, the neutral axis is most often located in the timber beam, due to the height of the cross-section. Figure 2.1 show a principal geometry of a beam type cross-section.

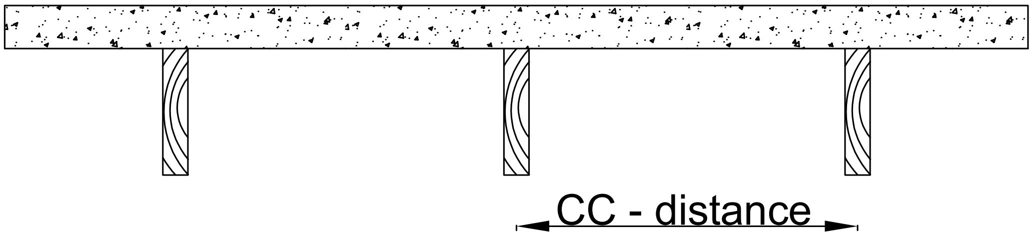

Figure 2.1: Example of beam type TCC cross-section.

The other main design alternative is the slab type cross-section, which is characterized by having an equal width of the timber and the concrete on top. The timber used is often either cross laminated timber (CLT) or vertically oriented timber boards in contact with each other. Slab type TCC elements usually have the neutral axis located in the concrete slab due to its higher equivalent area (Ogrin & Hozjan, 2021). An example of a slab type element can be seen in Figure 2.2.

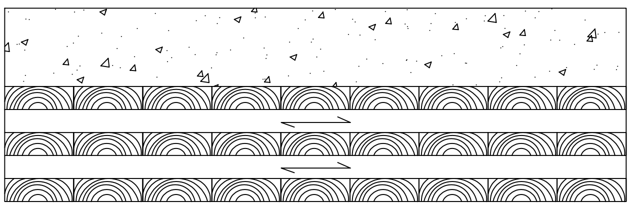

Figure 2.2: Example of slab type TCC cross-section.

2.1.2 Mechanical properties

The cross-sectional strength always needs to be considered in structural design. For TCC elements, the strength is limited by the maximum shear load that can be carried between the timber and concrete interface (Dias, 2018). Following International Organization for Standardization (1983), the maximum shear force is decided by the capacity up to a slip of 15mm or connection failure. Furthermore, what follows is that the acting shear force is related to the deformation behaviour and stiffness of the connection. Apart from the connection, the capacities of each material also govern the strength of the TCC element.

Another important property is the stiffness of the cross-section, which govern the deflection of the TCC floor. Since the deformation is heavily dependent on the composite degree, the connection rigidity has a large influence on the stiffness of the cross-section (Dias, 2018). Moreover, as the TCC is internally statically indeterminate, the stiffness of the connection also affects the stress distribution within the element. As a result of this, the connection stiffness is important to consider both in serviceability- and ultimate limit state.

In addition to the strength and stiffness properties, ductility is an important factor to consider in design (Dias, 2018). The ductility describes a structural element's ability to deform plastically before reaching failure. High ductility is generally preferred since it gives the structural system more redundancy in terms of large deformations before rupture. Additionally, in TCC elements ductile connections can increase the cross-sectional capacity since it allows for load-redistribution between the concrete and timber (Dias, 2018). The opposite of a ductile behaviour is brittle failure, which occurs suddenly and often without premonition.

The ductility of a TCC element is dependent on the type of connection used since concrete in compression and timber in tension both have brittle failure modes. The connection behaviour can vary between very ductile and flexible or stiff and with low ductility (Ceccotti, 2002). An example of a connector with low ductility is notched connections while steel connectors usually act ductile (Dias, 2018). Although the connectors have a large impact on the ductility, Ceccotti (2002) notes that a ductile element is not automatically achieved by using a ductile connector since the timber may still reach failure before the connection reaches plasticity. Then, the system could behave less ductile than anticipated in design.

There is no general consensus regarding what type of connection is preferred for TCC elements. Although high ductility is sought in design, it should not come at the expense of a stiffness reduction leading to excessive deformations of the structure in its service state. Furthermore, the connection should be strong enough to carry the shear forces in-between the materials and utilize their capacities.

2.1.3 Advantages

Compared to a pure timber- or concrete slab, the TCC exhibit a number of advantages, given that the design is properly done. Additionally, some advantages can be categorised as a general improvement of both:

- An effective utilization of the materials can be achieved in a TCC cross-section since the tensile and bending strength of timber is combined with the compressive strength of concrete.

- The construction process can be facilitated depending on the structural system and fabrication method. One example is that a continuous floor membrane can easily be created, either by casting concrete in-situ or by connecting prefabricated elements (Jockwer, 2022). Additionally, less reinforcement needs to be positioned in the process, compared to pure concrete slabs.

- The fire resistance of a TCC element is pronouncedly increased compared to pure timber slabs, since the concrete works as an effective barrier (Ceccotti, 2002). Research has also found that for some cases, the fire resistance of the TCC also improved compared to pure concrete slabs (Ceccotti, 2002). However, that is not a general case.

Compared to a pure timber slab, the advantages of TCC are:

- The concrete properties contribute to a stiffer cross-section with higher load-carrying capacity. Reported by Jockwer (2022), the increase in capacity and stiffness is about 60 % when comparing similar construction heights.
- The concrete contributes to an additional self-weight which could be beneficial for global stability if the construction is under risk of tilting. However, the increased load will contribute to deflections of the TCC element.
- The vibrational behaviour is improved. Ceccotti (2002) describes it as a reduction of “springiness” of the floor.
- Better sound insulation which means better acoustical performance of the air-transmitted noise (Ceccotti, 2002).
- The thermal mass of the concrete leads to an increase of the heat storage capacity, which buffer the temperature variations.
- The concrete casing protects the timber in the construction phase. With careful planning, the protection efforts can be reduced (Jockwer, 2022).

When instead comparing to a pure concrete slab, the following advantages of TCC are found:

- Reducing the concrete amount leads to a lighter structure since timber has a lower density than concrete. As a result of this, a higher efficiency in terms of load carrying capacity in relation to the self-weight is achieved (Ceccotti, 2002).
- A better damping which improves the impact noise insulation (Ceccotti, 2002).
- Possibilities to use the timber as an aesthetic enhancement of the ceiling.
- When replacing some of the concrete with timber the floor system gets a smaller carbon footprint

2.1.4 Disadvantages

Even though the stiffness of the cross-section is increased when adding the concrete to the timber beams, the self-weight of the structure is notably increased. As listed amongst the advantages, this might be favorable when looking at the global stability. However, it will also counteract the deflection reduction that the increased stiffness contribute to. As such, the concrete does not necessarily always improve the deflection behaviour.

Since TCC elements use two different materials which are most often not combined into composite construction elements, some challenges arise for its usage. Jockwer (2022) explains that problems may occur when the timber- and concrete sector needs to work together, since the procedures and building practises can vary. With proper communication and growing experience, the cooperation strengthens over time.

Another disadvantage when using TCC is the lack of practical experience and research. Even though there are multiple publications available that treat challenges such as the connection and long-term effects, the slabs' behaviour is still relatively unknown. Furthermore, it is not as well-tried as conventional structural elements and there might be a scepticism regarding its usage.

2.2 Stress and strain distribution

In a TCC element both the concrete- and the timber is subjected to external loads. The external forces need to be in equilibrium with the internal forces, which are bending moment in both the timber and concrete part together with the normal forces in both materials. In a simply supported cross section, without any external normal forces, the normal force is coming from the connection´s ability to restrict relative displacement between concrete and timber. The two normal forces are equal and counteract each other, where N_1 is a compression force and N_2 is a tensile force. The moment equilibrium is expressed in Equation 2.1 where z is the inner level arm between the two normal forces (Dias, 2018). To determine the forces in the timber-concrete cross-section it is not sufficient to only apply the equation of static equilibrium, since a TCC-element is always internally statically indeterminate. In addition to the static equilibrium equation, information about the curvature and strains are needed (Dias, 2018).

$$|N_1| = N_2 = N \tag{2.1a}$$

$$M_{external} = M_{concrete} + M_{timber} + N \cdot z \tag{2.1b}$$

TCC slabs are normally placed as simply supported floors and will therefore only be subjected to a positive bending moment. The bending moment causes both the timber and the concrete to be subjected to tensile stresses in the bottom and compression stresses at the top. However, as expressed in equation 2.1 it is not only the bending moments that keep the equilibrium in the TCC cross section, but also the normal force. The normal force changes the normal stress distribution compared to if there is no normal force in the system. The magnitude of the normal forces is determined by the level of composite action between the two materials, where a stiffer connection increases the normal stress caused by this force.

The interaction between concrete and timber can be divided into three main situations: no interaction, full interaction and partial interaction (Ogrin & Hozjan, 2021). The composite action affect the strain and stress distribution as principally illustrated in Figure 2.3. An increased composite efficiency makes the strain, and consequently deflection, decrease. The composite degree also affect the normal stress distribution. For no interaction, it is only the moment-components that are present, and both the timber and concrete will be subjected to tension and compression. With an increased composite action, the normal force that arise changes the stress distribution, and the global neutral axis moves towards the concrete. Thus, the concrete gets more compression stresses, which is generally desirable. However, an increased interaction is not necessarily equivalent to a decrease in stresses, since the stress distribution in a TCC element is a function of both normal stresses from bending (decrease) and from shear (increase) at the connection.

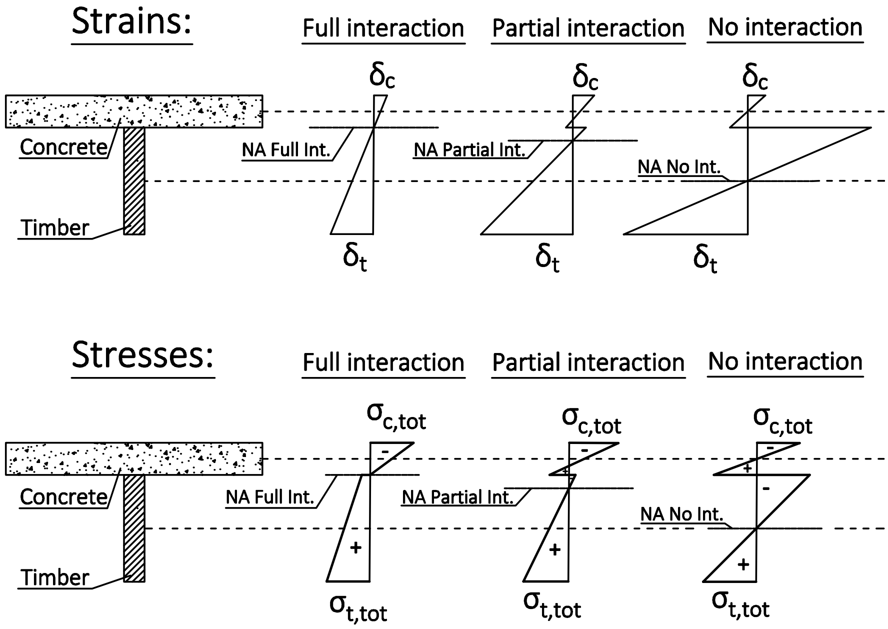

Figure 2.3: Principal strain- (above) and normal stress distribution (below) for full- partial- and no interaction.

2.2.1 No interaction

If there is no interaction between the concrete and timber, they work separately. Then, the slip between the two materials is clearly indicated, as can be seen in the strain distribution in Figure 2.4. When studying the normal stress distribution it can be seen that both components will be subjected to compression and tension. Since there is no shear forces transmitted at the interface, only the normal stresses from bending affect the total normal stress distribution. In an element with no interaction, the stresses from the bending moment will be larger compared to a cross section with higher interaction.

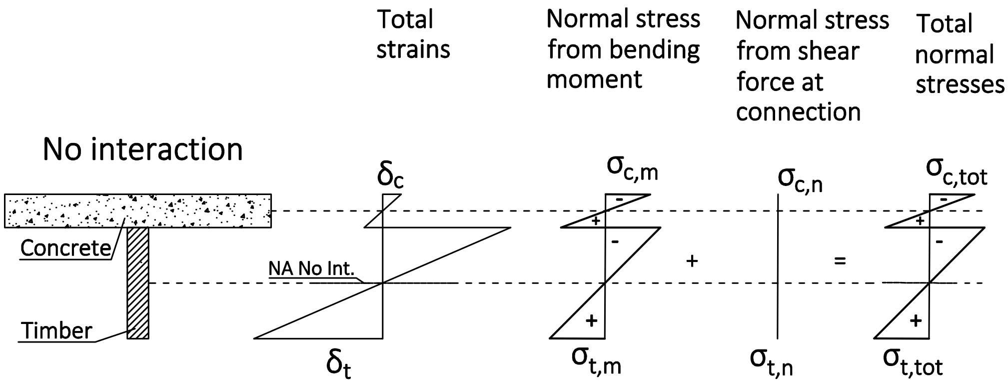

Figure 2.4: Principal strain distribution and normal stress components for no interaction.

2.2.2 Full interaction

With full interaction, the concrete and timber act as a unit. There is no slip between the materials and the strain distribution is therefore linear, see Figure 2.5. For equal loading, the strain, and therefore deflections, are smaller compared to no and partial interaction. With an increased interaction, the neutral axis is moved towards the concrete, which is illustrated when comparing Figure 2.5 to the case with no interaction, Figure 2.4. Additionally, the normal stress from the bending moment is lower for full interaction compared to when there is no interaction, since the bending stiffness (EI) of the cross section is increased. The full interaction induce high shear stresses in the connection and as a result a compression normal force appears in the concrete and a tension normal force in the timber. As such, the total normal stress distribution is the sum of the normal stresses from bending moment and from shear at connection.

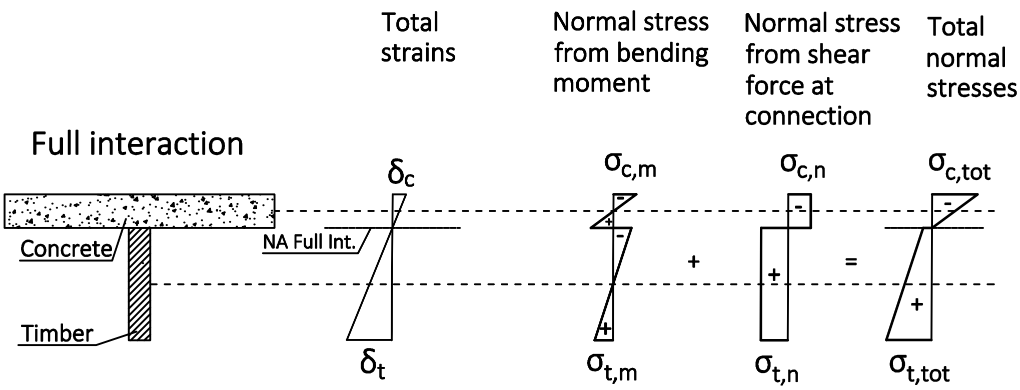

Figure 2.5: Principal strain distribution and normal stress components for full interaction.

2.2.3 Partial interaction

In practise it is very hard to achieve full interaction between the two materials (Ogrin & Hozjan, 2021). Instead the connection will work somewhere in between full- and no interaction, which is called partial interaction. The normal stresses due to bending will be larger compared to full interaction but smaller compared to no interaction. Opposite, the magnitude of the normal stresses due to the shear in the connection will be smaller than with full interaction, but larger than with no interaction. This causes most or all of the concrete (depending on the cross-sectional design) to be in compression, whereas the timber part will mostly be subjected to tension. Since the interaction makes the cross-section stiffer, the total strain will be smaller than for no interaction (given that the load is constant), see Figure 2.4..

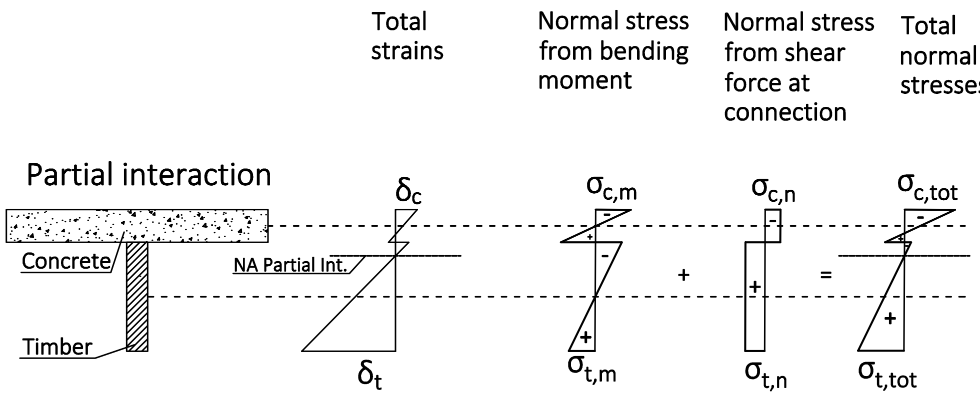

Figure 2.6: Principal strain distribution and normal stress components for partial interaction.

2.3 Production

TCC elements can be manufactured by two main procedures, either casting the concrete on site or using prefabricated slabs. Since the elements consist of two main components, the production phase is important to consider in design.

2.3.1 Cast on site

If the concrete is cast directly onto the timber beams, no composite action develops at the beginning and all the self-weight must be taken by the timber itself. Therefore, it is crucial to use a propping system during the time when the composite action is low, to reduce the initial deflection and to make the timber beam stiffer. The long-term deflection will also be decreased by using props since the time of loading of the concrete is delayed which will result in less creep (Lukaszewska, 2009). If the concrete is loaded at an early age, before it has a sufficient strength and stiffness, both deflection and stresses in the long-term will increase. For a cast on site TCC slab the props should be in place at least seven days (Lukaszewska, 2009).

2.3.2 Prefabrication

Prefabrication of TCC slabs can be performed in a number of ways. However, Jockwer (2022) distinguishes between two main types of prefabrication methods. The TCC slab can either be assembled directly by the concrete- or timber manufacturer, or transported as separate elements to the construction area and assembled on site.

In the first case, the concrete is cast on the timber beams in a factory and cured for a time before they are transported to the construction site. In the other case, it is the contractor that has the responsibility to connect the prefabricated concrete with the timber beams. The main difference between these two types of prefabrication methods is that in the second case, the concrete is not cast directly on the timber beams, instead they are connected when the concrete has cured.

An advantage of connecting the prefabricated concrete slab on the timber beams after it has cured is that a significant amount of the concrete shrinkage has already taken place before it is mounted on the timber beams, if it has been stored for a couple of weeks (Lukaszewska, 2009). This results in less deflection and stresses in the long-term compared to if the concrete is cast directly onto the timber beams, which is the case for the other prefabrication method (and also if the concrete is cast on site). As for the cast on site TCC slab, a propping system is required for the prefabricated elements when the prefabricated concrete slabs are assembled at the construction site. However, in order to reduce the long-term deformations, those props only need to be in place for a single day, compared to the minimum seven days required for the cast on site concrete (Lukaszewska, 2009). The reason for using the props during the first day of assembly is likely due to the time needed for the interaction between the elements to fully develop.

2.4 Design procedure

The design procedure for a TCC element is similar to standard construction elements in terms of the requirements put on it in the ultimate limit state (ULS) and serviceability limit state (SLS). However, due to the composite action between the elements, certain considerations are needed, especially for determination of the connection stiffness. Furthermore, regular analytical calculation methods are not applicable and for a detailed analysis, numerical approaches are suitable.

2.4.1 Slip modulus

Due to the slip occurring between partially connected elements, regular beam theory, where plane sections remain plane, can not be applied for TCC elements (Ceccotti, 2002). The relation between the shear load and resulting slip is for most connection types non-linear. Despite that, it is often sufficient to assume a linear value for the slip modulus in calculations (Ceccotti, 2002). However, it is crucial that the slip modulus is adapted for the type of analysis since its stiffness varies between design in SLS or ULS.

Ceccotti (1995) proposes a commonly used design approach for determining the slip moduli, included in Eurocode 5, (SS-EN 1995-1-1:2004, 2009). In serviceability limit state, the slip modulus, denoted K_{ser}, is determined by taking 40 % of the connection maximum load capacity. Since the method is simplified as linear, the value corresponds to a secant crossing the curve at 40 % load in a force-slip graph.

The slip modulus in ultimate limit state, denoted K_u, is determined by the same methodology, but instead at 60 % of the maximum load capacity. The secants are illustrated in Figure 2.7. Push-out test data should preferably be used for K_{ser} and K_u, but for design cases when no push-out test data is available, Eurocode 5 may be used. The proposed procedure is further explained in Section 5.1.1.

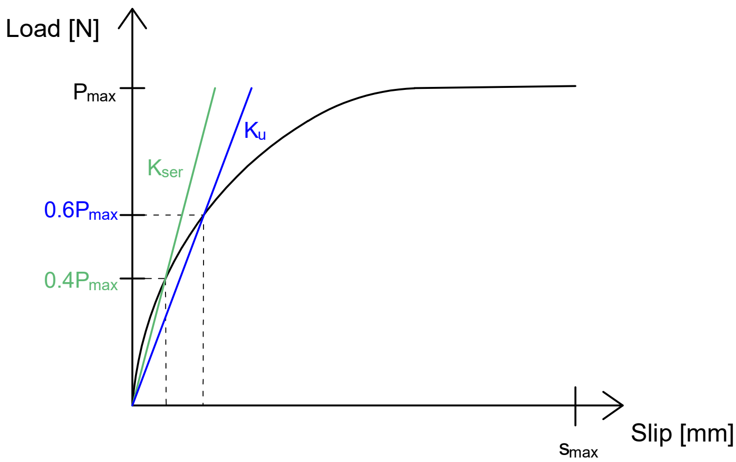

Figure 2.7: Principal slip illustration for determination of K_u and K_{ser}.

2.4.2 Calculation methods

The most commonly used analytical calculation model amongst the reviewed literature is following the method presented in Eurocode 5 Annex B, SS-EN 1995-1-1:2004 (2009), as done by for example Lukaszewska (2009). In the code, a procedure called the "effective bending stiffness method" more known as the γ-method ("gamma-method"), is described. Ogrin and Hozjan (2021) confirm that most of the developed calculation models for TCC element design are based on the γ-method. In addition to the formulas presented in Eurocode 5, several extensions of the γ-method have been proposed, for example by Kavaliauskas, Kazimieras Kvedaras, and Gurkðnys (2005) and Schänzlin and Fragiacomo (2007). The extensions are mainly focused on the long-term evaluation since that is the hardest to predict in the design procedure. Although several studies have been conducted in the subject, no consensus regarding the best model to consider the complexity of the long-term effects in TCC elements have been reached (Lukaszewska, 2009).

The γ-method is a simplified analysis method based on several assumptions, simplifications, and limitations. One assumption is that the connections are made with mechanical fasteners and with a constant or uniformly varying spacing. Furthermore, it is assumed that the load is only acting in the main bending direction. All assumptions are listed in Eurocode 5. Simplifications of the γ-method include a linear-elastic analysis of the structural behaviour for all of its components (Kavaliauskas et al., 2005). The formulas used in the γ-method are presented in Section 5.1.

A significant limitation of the model is that it can not take time-variations in the moisture content into consideration. The correlated deflection dependency, called mechano-sorptive creep, can therefore not be considered. This creep is further explained in Section 4.2.2. Furthermore, the moisture content also affects the shrinkage and swelling of timber and the mechanical properties of the timber. In addition to the inelastic strains caused by moisture content variations, the model also neglects the effect of concrete shrinkage. In several experimental studies, the neglection of these effects have been shown to result in significant under-estimations of the long-term deflection, especially in conditions resembling service class 3 (Ceccotti, Fragiacomo, & Giordano, 2006; Fragiacomo, Gutkowski, Balogh, & Fast, 2007; Hailu, 2015; Kavaliauskas et al., 2005; Lukaszewska, 2009; Yeoh, 2010).

Besides the γ-method, which allows for an analytical calculation model, the modelling can also be performed using numerical analysis. For a numerical analysis, FEM models can be constructed in various FE-softwares, for example Abaqus. Such models are often constructed in research to resemble experimental testing and then draw conclusions on how to configure the model in order to predict the real behaviour. Although FE-modelling is generally more convenient than large scale experimental testing, using numerical analysis in design is time-consuming and often cumbersome. It is however sometimes necessary to use when looking at complex behaviour that is not included in analytical solutions.

2.4.3 SLS

In serviceability limit state (SLS) design, the deflection of TCC beams is evaluated. Since this is commonly the hardest criterion to fulfil, it should preferably be performed before the strength (ULS) verification (Jockwer, 2022). The most severe deflections will most likely occur in the long-term analysis since inelastic strains such as creep are considered. However, not all long-term effects automatically increase the deflection, since for example expansion of concrete or shrinkage of timber will act to bend the TCC element upwards.

Ceccotti (1995) suggest a procedure based on the “Effective Modulus Method” to evaluate the long-term deflection behaviour. The approach is used in Eurocode 5, (SS-EN 1995-1-1:2004, 2009). It is based on the idea of reducing the modulus of elasticity in regard to the creep of the concrete, connection and timber, respectively. As such, the simplified model does not take into account the shrinkage or inelastic strains caused by the moisture variations. However, the latter can to some extent be considered when applying the service class of the timber. The equations used in design is presented in Section 5.1.4. Apart from the deflections, dynamic behaviour is also part of the SLS, but such analysis is not within the scope of this thesis.

2.4.4 ULS

In the ultimate limit state (ULS), a TCC element should be able to withstand the stresses that occur during its lifetime, both in short-term and long-term. The short-term ULS is a common design situation that most engineers are familiar with. It is also the design situation for which most experimental data is available, due to the number of tests performed (Ceccotti et al., 2006). Most commonly, the failure occurs in the timber due to high tensile stresses parallel to the grain.

The long-term evaluation of TCC elements is more complex since the stiffness varies in time, for example as a result of shrinkage or creep. Therefore, the stress distribution between the concrete, connection and timber also varies. One possible outcome of the stress-redistribution is considerable constraining effects, for example if the temperature rises and the concrete expands while the timber shrinks. In such case, even though the deflections would decrease, the shear force in the connections and the timber stress would increase (Ceccotti et al., 2006). The effect increases with stiffer connections. Although the redistribution may appear severe, Ceccotti et al. (2006) explain that the risk of failure is low due to the slow variations and the materials ability to disperse stress peaks. To evaluate the stiffness variation, Eurocode 5, SS-EN 1995-1-1:2004 (2009), suggest reducing the modulus of elasticity with respect to the creep of the materials. This is further explained in Section 5.1.5.

3

Components

A TCC element consists of three components: timber, concrete and the connection interlocking them. For each component, several types and modifications are possible, affecting the properties of the composite cross-section. There is no generally applied design rule regarding these design possibilities and such, a TCC element can be assembled in several different configurations.

3.1 Timber

The timber part of a TCC element can be made up of different wood-based products, with a clear geometrical distinction between the beam- and slab type elements. For the beam type TCC, construction timber, glued laminated timber (Glulam) or laminated veneer lumber (LVL) are commonly used. Any of these timber products can also be used in a slab type cross section by mounting them in a row. However, cross laminated timber (CLT) is most commonly used in that case. Construction timber is not an engineered wood product and thus, the other wood products can be seen as modified construction timber to acquire specific engineering properties.

Since SLS is often dimensioning for TCC elements, and especially deflection criterion, the modulus of elasticity is the material property that is of main interest when comparing the different timber products that can be used. The modulus of elasticity for different strength classes of construction timber, glulam and LVL are presented in Figure 3.1. The difference between those wood products together with cross laminated timber (CLT) are described in the coming sections.

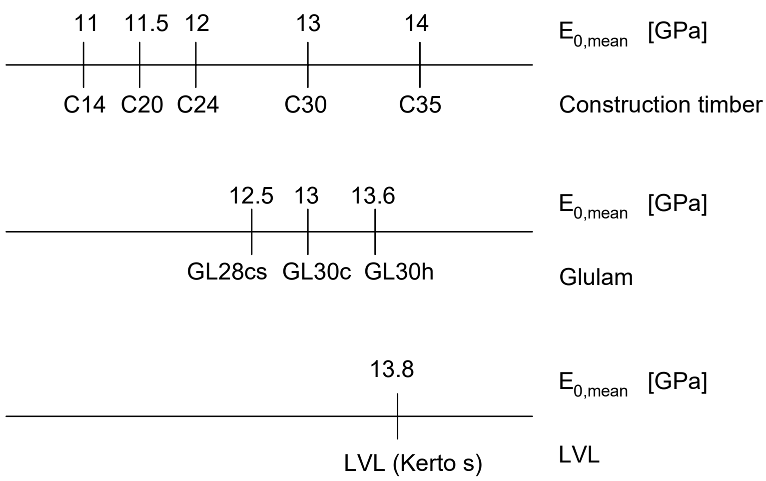

Figure 3.1: Modulus of elasticity for strength classes of construction timber, glulam and LVL.

3.1.1 Construction timber

The simplest form of timber used in design is sawn timber/construction timber, which is timber without any industrial processes involved to modify its properties. Wood is a natural material and when the wood is cut all the logs do not have the same properties. Instead, natural characteristics such as knots, presence of juvenile or reaction woods can affect its strength and stiffness properties (Swedish Wood, 2016c). To determine which part of the log that can be used for load-bearing structures (construction timber), a visual or a mechanical sorting is done.

The mechanical sorting is performed in line with SS-EN 338:2016 (2016) and the classes that can be identified for construction timber in Sweden are C14, C20, C24, C30 and C35. If no mechanical sorting is performed a visual sorting according to SS 230120:2010 (2010) can be done, with the classes T0, T1, T2 and T3 corresponding to the strength classes C14, C20, C24 and C30. The two most used timber classes are C14 and C24, and it is also these two classes that are stocked by most builder's merchants (Swedish Wood, n.d.).

Three main directions can be distinguished in the structure of wood, and therefore wood is an orthotropic material. These directions are longitudinal (L), radial (R), and tangential (T), presented in Figure 3.2. The longitudinal direction is along the length of the log (in the fibre direction), the radial direction is perpendicular to both the fibre direction and the annual rings while the tangential direction is perpendicular to the fibre direction and parallel to the annual rings. The orthotropic structure of wood causes the strength and stiffness properties to vary considerably in the three directions.

Twelve constants are needed to describe the elastic behaviour of wood, the elastic modulus E_L, E_R, E_T, shear modulus G_{LR}, G_{LT}, G_{RT} and Poisson's ratios v_{LR}, v_{RL}, v_{LT}, v_{TL}, v_{RT} and v_{TR} (Swedish Wood, 2016c). The difference in properties between the tangential and radial direction is small, and the Poison's ratio is often considered to be pairwise equal, and thus the timber can be described by six different variables. These are modulus of elasticity, shear modulus and poisons ratio parallel and perpendicular to the direction of the fibres, E_{II}, E_{perp}, G_{II}, G_{perp}, v_{II} and v_{perp}.

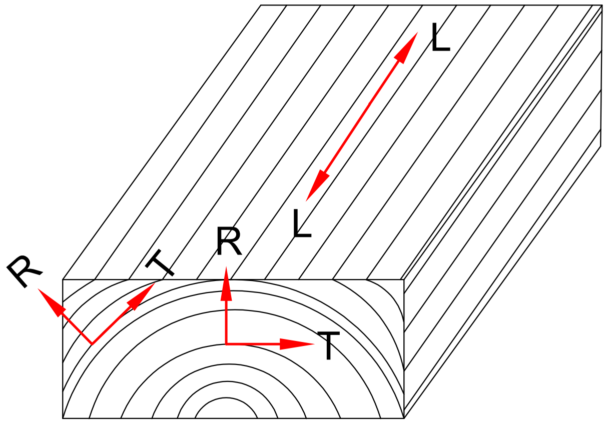

Figure 3.2: Illustration of Longitudinal (L), Radial (R) and Tangential (T) direction of timber.

3.1.2 Cross laminated timber (CLT)

Cross laminated timber (CLT) is a relatively newly developed engineered wood product, making its debut in the 1990s, it has since gained interest rapidly during the last decades (Swedish wood, 2019). The idea is to glue horizontally placed timber boards together in layers, with the grain direction being perpendicular in each new layer. Additionally, the lower and upper layer usually have the same fibre direction, resulting in an odd number of layers which in total range between 3-9 commonly. The timber boards usually have a thickness somewhere between 20-45mm and a thickness-to-width ratio of 1:4, resulting in widths between 80-200mm (Swedish wood, 2019). In Figure 3.3 a CLT cross section with 5 layers is presented.

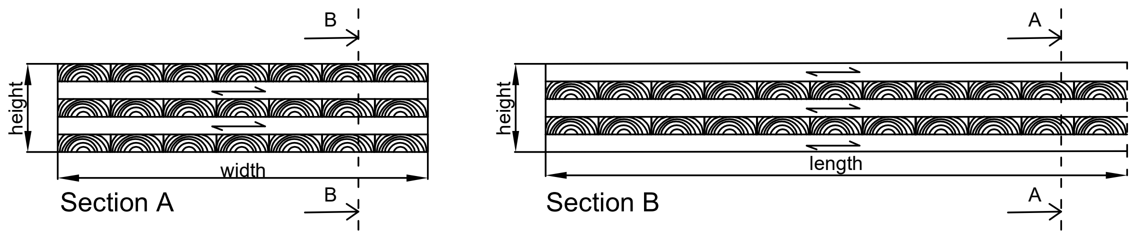

Figure 3.3: Example of 5-layered CLT cross-section.

Due to the perpendicularly placed layers, the stiffness variations between the orthotropic directions are partially evened out in CLT elements. In addition to the number of layers and board size, the mechanical properties are also influenced by the strength class of the timber boards used, which commonly range between C14-C30 (Swedish wood, 2019).

3.1.3 Glued laminated timber (Glulam)

Glulam is the oldest engineered wood product and has been in use for more than 100 years (Swedish Wood, 2016c). It is manufactured by gluing sawn laminations on top of each other, with its fibre direction along the length of the beam. The main advantage of using glulam is that better mechanical properties than in construction timber can be achieved, which is due to the lamination effect (Swedish Wood, 2016a). The lamination effect is the reduced probability of defects in the section when adding multiple layers instead of a solid section. Ordinary homogeneous construction timber consists of one layer and has therefore a higher probability of a defect that can impact the full cross section. However, the glulam itself is not significantly stronger than solid construction timber, as it is the variability in strength and stiffness properties that are reduced. Thus, a lower partial coefficient can be used for the strength. However, it should be noted that this does not apply for the stiffness properties. Even though the stiffness properties of glulam is not considerably higher than for construction timber, glulam may be preferred since it offers a larger variability in beam dimensions.

Glulam is divided into different strength classes, and those commonly in stock in Sweden are GL28cs, GL30c and GL30h (Swedish Wood, 2016b). GL30c and GL30h correspond to construction timber with strength class C30, and the difference between them lies within the notations c and h. The small letter h (homogeneous) is glulam where all lamellas have the same strength class, whereas letter c (combined) is where the inner lamellas have a smaller strength class (Swedish Wood, 2016a). A result of this is that the combined cross section will have a lower strength and stiffness compared to a homogeneous section. GL28cs is glulam with a characteristic bending strength of 28 MPa, with inner lamellas of lower strength compared to the outer, and the s (split) describe that the glulam beam is split from a larger one.

3.1.4 Laminated veneer lumber (LVL)

LVL was developed more than 50 years ago and has similar properties as glulam (Swedish Wood, 2016c). LVL is produced by gluing veneer sheets together, which creates a thick structural element with a lower variability in strength and stiffness properties compared to an equal sized element with only one layer, similar as for the glulam beam.

The veneer sheets are generally placed with the fibre-direction along the longest side, but if stiffness is sought in multiple directions, some sheets are placed in the perpendicular direction. Therefore, two different types of LVL are usually distinguished, type S and type Q, where some of the veneers in type Q are placed perpendicular to the longest side which is not the case for type S (Swedish Wood, 2016c). This could be suitable for LVL loaded flatwise to be able to distribute the load not in only one direction, such as in floor structures. For TCC beam type elements the LVLs' are placed edgewise, and therefore only type S is of interest for this application.

3.2 Concrete

Concrete consists of water, cement, aggregates and admixtures, which hardens over time (Soutsos & Domone, 2017). It has a high compression strength but the tensile strength is very low. In TCC elements, the aim is that the concrete should be in the compression zone, to minimize the need for reinforcement. Even tough all the concrete is in the compression zone, some reinforcement (minimum reinforcement) is still needed to withstand the tensile forces from shrinkage of concrete (Ogrin & Hozjan, 2021). If the connection has low stiffness or the concrete slab is very thick in comparison to the timber part, the lower part of the concrete might be in the tensile zone. Then, minimum reinforcement is not sufficient and additional reinforcement is needed.

The concrete used in TCC elements is usually normal-weight concrete, which has a density of approximately 2400 kg/m^3. The tensile strength of concrete is often neglected since it is usually only 1/10 of the compression strength (Soutsos & Domone, 2017). In Eurocode 2, SS-EN 1992-1-1:2005 (2008), concrete is divided into 14 strength classes, ranging between C12/15 and C90/105. From the strength classes both compression strength and the modulus of elasticity can be determined, since these two properties are related.

3.2.1 Modification possibilities

The composition of concrete can be modified to gain certain beneficial properties. For example altering its long-term behavior, such as shrinkage. Below, two different modifications possibilities are presented, that can be used to modify the long-term performance of TCC.

Low-shrinkage concrete

Shrinkage of concrete is a long-term phenomenon that is important to consider since it contributes to an extra deflection of TCC elements over time. It is dependent on the amount of water that is leaving the concrete during the hydration process (Soutsos & Domone, 2017). The consequences of shrinkage and further explanation of this phenomenon, is found in Section 4.1.3.

Low-shrinkage concrete generates considerably smaller shrinkage strains compared to ordinary concrete, achieved by adding a shrink-reducing admixture or using saturated lightweight aggregates (Cusson & Margeson, 2010). A low-shrinkage admixture decreases the drying shrinkage of concrete, whereas lightweight aggregates reduces the autogeneous shrinkage and can therefore be a good option in concrete with a low water-cement-ratio. In an article by Zhan and He (2019), the effect of different low-shrinkage admixtures were tested, and the result varied between 20-80 % reduction of concrete shrinkage by adding the shrink-reducing admixture. It was noted that the result was heavily affected by the composition of the concrete components.

Lightweight concrete

Lightweight concrete has a lower density compared to normal-weight concrete, achieved by using lightweight aggregates (Soutsos & Domone, 2017). By using lightweight concrete, it is possible to reduce the long-term deflection, since the self-weight of the concrete is a large contributor to the long-term deflection of TCC elements (Ogrin

& Hozjan, 2021).

In a study by Jorge, Schänzlin, Lopes, Cruz, and Kuhlmann (2010) lightweight and normal-weight concrete was compared both in short-term and long-term. An important long-term effect is the influence of shrinkage, and it is concluded that lightweight concrete shrinks more than normal-weight concrete and thus causing an increased deflection. Further, lightweight concrete has a lower stiffness in the elastic range compared to normal-weight concrete, which also has a negative influence on the deflection. However, the lightweight concrete creeps less, which contrarily decreases the deflections.

After analysing both the difference in shrinkage and creep behaviour, together with the lower long-term stiffness between normal-weight concrete and lightweight concrete, it was found that lightweight concrete had a clear and distinct benefit (Jorge et al., 2010). That means that the lower self-weight for lightweight concrete has such decisive influence that it could be a suitable measure to decrease the long-term deflection for TCC elements.

3.3 Connections

The connection between the timber and concrete is a crucial part of the TCC behaviour as it influences the stress distribution and composite action of the indeterminable system. Dias (2018) list three mechanical properties that an ideal connector should have:

(i) Strength to carry the shear forces that forms at the connection surface.

(ii) Stiffness to do so without considerable slip.

(iii) Ductility to enable load redistribution and avoid brittle failure of the connector.

None of the connectors available today fulfil all of the desired properties, with the stiffness requirement being the least commonly satisfied (Dias, 2018). As a consequence, simple design methods are generally not valid.

For a simply supported beam, the shear forces are largest close to the beam ends and decreases closer to the middle, with neglectable shear at the maximum moment section. Dias and Jorge (2011) notes that since the largest shear force arise close to the supports, that is where the connector must withstand the largest force and develop the largest deformation. If the connector fails, the load must instead be transferred by the remaining connectors, which increases the load and might result in a fast and brittle failure. To avoid that course of events, connections with a deformation capacity larger than the allowable slip could be used (Dias & Jorge, 2011). Such connections have large ductility which allows for redistribution of the shear forces. However, using ductile connectors make the deformation behaviour non-linear and harder to predict in design.

There are multiple different connection systems available, with a range of different mechanical properties. The behaviour of the connections is commonly illustrated in a load-slip graph, correlating the shear force at the interface to the slip between the elements, as could be seen in Figure 2.7. Although the behaviour of the connectors differs, a general case is that stiffer connections have smaller ultimate deformation capacity while the less stiff connections can deform more (Dias & Jorge, 2011).

Dias (2018) presents that dowel type connections are the configuration with the most reported studies with notches being the second most researched. Together, the two types make up more than 75 % of the found publications. Other connection types are therefore relatively sparingly researched. An example of such a connection is the adhesive connection, which could also be referred to as a glued connection.

3.3.1 Dowel type

The dowel type of connectors includes screws, nails, dowels, and other similar metallic fasteners, an example of a dowel type connection can be seen in Figure 3.4. It is not only the most researched but also the easiest type of connection to use in practise (Dias & Jorge, 2011). The behaviour of dowel connections is distinctively non-linear with a short linear relation before a fast increase in deformation. Their low strength and stiffness are somewhat compensated by the high ductility of the connection, following their deformation behaviour. Out of the dowel type connections, screws are the most common, owing to their axial strength which removes the risk of separation at the interface (Dias, 2018) . The mechanical properties of the screws can be enhanced by inserting them with an inclination and therefore better utilize their high axial capacity (Jockwer, 2022).

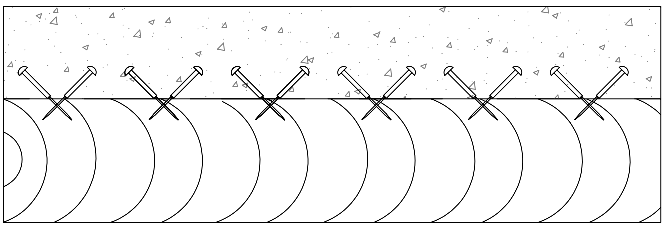

Figure 3.4: Example of a dowel-type connection, based on (Ogrin & Hozjan, 2021)

3.3.2 Notches

Notched connections are achieved by cut-outs in the timber where concrete is casted to create a mechanical interlock. An example of a notched connection can be seen in Figure 3.5 There are various shapes possible such as having inclined sides or not. Notched connections have mechanical properties opposite those of the dowel type fastener, with a high strength and stiffness but a very brittle failure due to low ductility. Dias and Jorge (2011) describe its behaviour as perfectly linear elastic up until rupture. The simplicity of the connection makes it very effective in relation to the high stiffness that is achieved (Dias, 2018). In order to reduce the brittleness of the failure, the notches are often complemented with dowel type of fasteners, which increase the ductility as well as the axial capacity (Dias, 2018). Increasing the axial capacity makes the connection performance more reliable since separation of the elements is prevented.

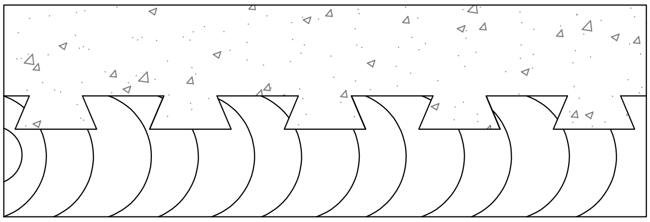

Figure 3.5: Example of a notched connection, based on (Ogrin & Hozjan, 2021)

3.3.3 Adhesive

As with the notched connection without steel fasteners, a glued (adhesive) connection experience brittle failure when its full capacity is reached. An example of an adhesive connection can be seen in Figure 3.6. However, up until the point of failure, the connection is very stiff and develops close to full composite action, which allows for easier calculations (Dias, 2018). Additionally, the continuous connection makes the shear stress uniform at the interaction surface, and local stress concentrations can be avoided.

Dias (2018) highlights the potential that multiple studies have shown regarding the usage of adhesive connectors but conclude that further studies need to be carried out before applying it in real designs. Challenges mentioned include the brittle failure, quality control and long-term behaviour. Tannert, Endacott, Brunner, and Vallée (2017) has treated the latter in tests over 4.5 years of loading. The results showed a good structural performance with no degradation of the bond during the investigated loading time. However, in the study the need for additional research is distinctively noted.

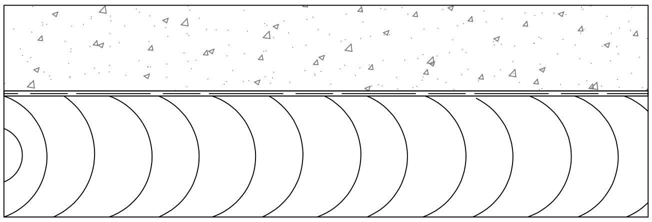

Figure 3.6: Example of adhesive connection, based on (Ogrin & Hozjan, 2021)

4

Long-term effects

Long-term effects of a TCC element are important to consider, especially in SLS, since these effects usually are a main contributor to the deflection (Tannert et al., 2017). Since a TCC consists of 3 different components (timber, concrete and connection) with various properties, it will be subjected to multiple long-term effects. For timber and concrete the long-term effects will change the strains in the two materials, and this strain change is described in Equation 4.1 for timber and Equation 4.2 for concrete. The long-term effects for the connections will instead result in an increase of the slip between the two materials, which is described by Equation 4.3.

$$\epsilon_{t,tot} = \epsilon_{t,C} + \epsilon_{t,MSC} + \epsilon_{t,SM} + \epsilon_{t,ST} + \epsilon_{t,E} \tag{4.1}$$

Where:
$\epsilon_{t,tot}$ is the total timber strain from long-term effects
$\epsilon_{t,C}$ is the timber strain from creep
$\epsilon_{t,MSC}$ is the timber strain from mechno-sorptive creep
$\epsilon_{t,SM}$ is the timber strain from shrinkage/swelling due to moisture content variations
$\epsilon_{t,ST}$ is the timber strain from shrinkage/swelling due to temperature differences
$\epsilon_{t,E}$ is the timber strain from change of modulus of elasticity of the timber due to moisture content variations

$$\epsilon_{c,tot} = \epsilon_{c,C} + \epsilon_{c,S} + \epsilon_{c,ST} \tag{4.2}$$

Where:
$\epsilon_{c,tot}$ is the total concrete strain from long-term effects
$\epsilon_{c,C}$ is the concrete strain from creep
$\epsilon_{c,S}$ is the concrete strain due to autogeneous and drying shrinkage
$\epsilon_{c,ST}$ is the concrete strain from shrinkage/swelling due to temperature differences

$$s_{con,tot} = s_{con,C} + s_{con,MSC} \tag{4.3}$$

Where:
$s_{con,tot}$ is the total connection slip from long-term effects
$s_{con,C}$ is the connection slip from creep
$s_{con,MSC}$ is the connection slip from mechano-sorptive creep

It can be seen from these three equations that different long-term effects affect different TCC components. All these long-term effects will be described in Section 4.1, 4.2 and 4.3.

4.1 Shrinkage and swelling

Shrinkage and swelling occurs in the concrete and the timber for various reasons, for example as a consequence of moisture and temperature differences. Additionally, concrete undergoes autogeneous and drying shrinkage during the hardening process of the fresh concrete.

4.1.1 Shrinkage/swelling due to moisture content variations

In a TCC, the moisture content variations only affect the timber, through either shrinkage or swelling.

Timber

Wood is a hygroscopic material and is therefore affected by the temperature and relative humidity of the surrounding climate when reaching an equilibrium moisture content. Soutsos and Domone (2017) describe that timber usually reaches a moisture content of 12 % if it is stored in an indoor environment of 20 degrees Celsius.

The equilibrium moisture content in wood is explained by desorption and adsorption curves, as principally illustrated in Figure 4.1. Desorption is the removal of water from the timber and adsorption is absorption of water. The curves varies depending on material and temperature. If timber undergoes desorption, the final equilibrium moisture content will be higher compared to if the timber would be subjected to adsorption up to the same equilibrium relative humidity.

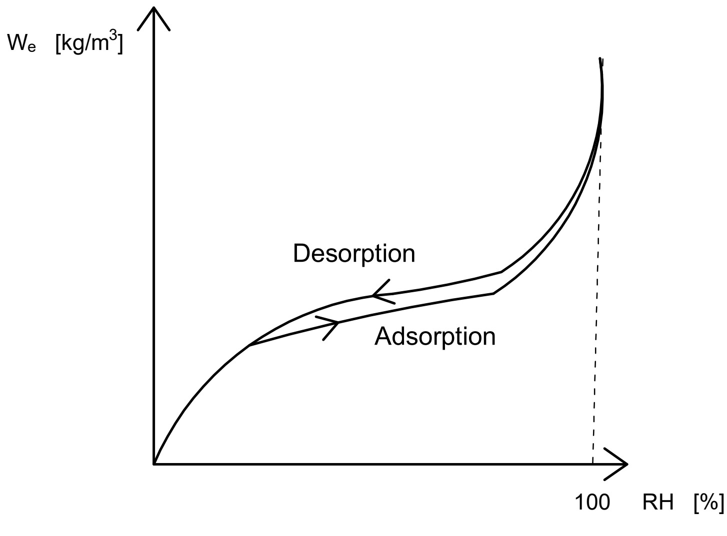

Figure 4.1: Principal drawing of sorption isotherm of timber.

The water is either adsorbed or removed from the wood through the cell wall, where the water is stored in the micro fibrils (Swedish Wood, 2016c). If the moisture content is reduced, water leaves them which makes the micro fibrils come closer to each other and thus the timber shortens, which is called shrinkage. If the opposite conditions are present, the volume of the timber is increased, referred to as swelling. The changes in volume and strength only occur below a certain moisture content, called the fibre saturation point (Soutsos & Domone, 2017).

Since timber is an orthotropic material, the movement from shrinkage or swelling is different in the different directions, due to the location of the micro fibrils in the timber element (Swedish Wood, 2016c). The largest timber movement, either shrinkage or swelling, will be in the tangential direction, thereafter radial and longitudinal direction in descending order. The three timber directions are illustrated in Figure 3.2. Values for shrinkage strain for a change in moisture content by 1 % are presented by Swedish Wood (2016c) in the three directions, tangential direction: 0.0030, radial direction: 0.0015 and longitudinal direction: 0.0001

When the timber beam shrinks, the concrete beam will be subjected to compression forces whereas the timber will be subjected to tension forces, which is illustrated in Figure 4.2. Since the neutral axis of the TCC cross-section is above the neutral axis of the timber beam itself, a negative bending moment will arise. As a consequence, the length reduction of the timber beam induce an upwards bend of the TCC beam.

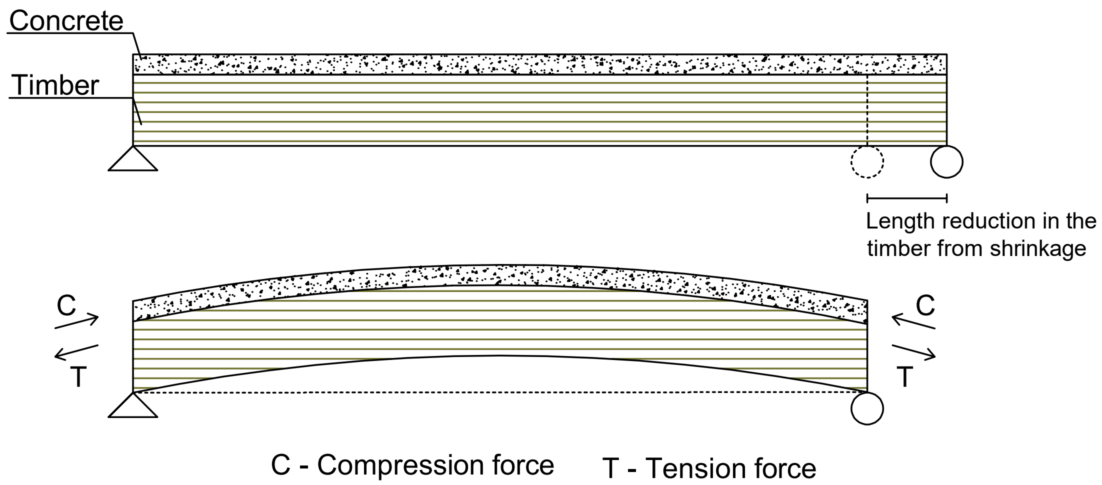

Figure 4.2: Principal deformation of TCC due to timber shrinkage, based on (Dias, 2018)

4.1.2 Shrinkage and swelling due to temperature variations

Both timber and concrete exhibit strain changes due to temperature variations.

Timber

Increasing the temperature in timber enhance the oscillations of molecules which causes a larger distance between them, refereed to as swelling (Soutsos & Domone, 2017). If the temperature is lowered, the opposite takes place, and the timber shrinks. The shrinkage or swelling that occur due to temperature alterations is considerably smaller than the corresponding moisture content variations (Soutsos

& Domone, 2017). For normal temperature ranges, the dimensional changes from temperature differences are often neglected (Swedish Wood, 2016c).

Concrete

As for timber, concrete is subjected to dimensional changes when subjected to temperature variations. The dimensional change can be expressed as strain per unit temperature change, and the value of this strain differs between concrete mixtures based on the coefficient of thermal expansion of the cement paste and aggregates (Soutsos & Domone, 2017). Since the aggregate volume is often 70-80 % of the total concrete volume, it is the expansion coefficient of the aggregates that dominate the thermal expansion behaviour of the concrete.

4.1.3 Concrete shrinkage

Shrinkage of concrete is a load-independent volume reduction caused by chemical reactions during cement hydration and water removal during drying (Soutsos & Domone, 2017). The shrinkage during cement hydration is called autogenous shrinkage, whereas the shrinkage that take place due to the exchange of moisture with the environment is called drying shrinkage. The method presented in Eurocode 2, SS-EN 1992-1-1:2005 (2008), takes both the autogenous and drying shrinkage into account, and is based on experimental data. The equations are presented in Appendix A. However, it is hard to define an exact value of the drying shrinkage with certainty.

Autogenous shrinkage

The autogeneous shrinkage takes place during the first days of the curing when the hydration process is at its highest rate. Hydration is the process when water and cement react, and this chemical reaction leads to the shrinkage called autogenous shrinkage (Soutsos & Domone, 2017). According to Eurocode 2, autogenous concrete shrinkage is taken into account as a strain increment which is dependent on the strength properties of the concrete.

Drying shrinkage

Opposite to the autogenous shrinkage, the drying shrinkage depends on the surrounding environment. For normal-strength concrete, all the water in the concrete matrix will not take part in the hydration process between the cement and the water. Then, if the environment is drier than the concrete, the excess water leaves the concrete, resulting in a volume reduction called drying shrinkage. This shrinkage is the most significant shrinkage phenomena, especially for normal-strength concrete (Soutsos & Domone, 2017).

Drying shrinkage is dependent on many factors, but the most important factors are the water-cement-ratio, geometry of the concrete specimen and the environmental conditions of the surrounding climate (Haedicke, Schober, Rautenstrauch, Müller, & Doehrer, 2007). Concrete with high water-cement-ratios has more free water which causes more drying shrinkage. The geometry of the concrete specimen has a large influence on the drying shrinkage, since if the water must be transported a long distance before it can be released, the shrinkage rate is lowered. Lastly, a very humid climate results in less drying shrinkage since the concrete specimen emits less water to reach equilibrium with its surrounding.

4.2 Creep

Creep is a load-dependent strain which increases with time, in contrast to elastic and plastic deformations that occur instantaneously (Dowling, 2013). It is also described by Dowling (2013) that creep is not only affected by the time of loading but also increases with temperature, change in moisture content and loading cycles. The rate of the creep depends on the material, but in general the rate is highest in the beginning. According to Soutsos and Domone (2017), creep can be classified into two creep strain components. Creep strain during constant moisture content, viscoelastic creep, and an extra creep strain for varied moisture content, mechano-sorptive creep.

4.2.1 Viscoelastic creep

Viscoelastic creep is the creep that occurs during constant moisture content and it takes place for all three materials in a TCC element; timber, concrete and the connection.

Timber

The creep of timber can be shown with a creep curve, see Figure 4.3. The first deformation is the elastic deformation, which occurs instantaneously. Thereafter a deformation dependent on time increases the deflection, and consists of both a delayed elastic deformation and a viscous deformation. The delayed elastic deformation is the time dependent deflection that is reversible during unloading.

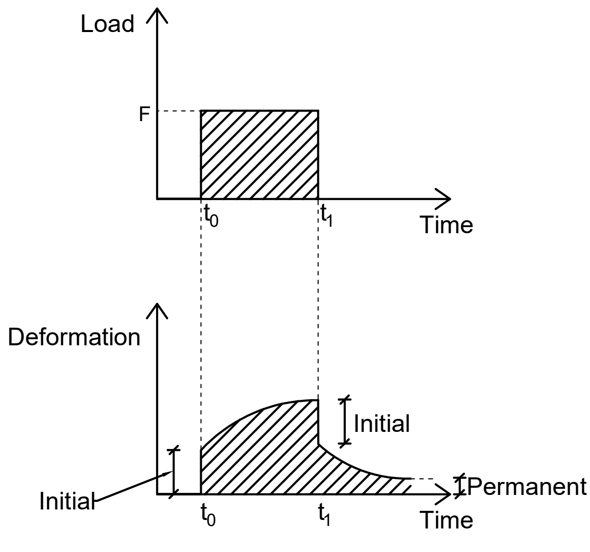

Figure 4.3: Creep deformation of timber.

There are many factors that influence the creep rate, such as stiffness and load directions, but also temperature and moisture differences (Swedish Wood, 2016c). The creep deformations increase with decreased stiffness and the creep rate is also very much affected by the load directions. Granello and Palermo (2019) describe that loading perpendicular to the grains can result in eight times more creep than parallel to the grains. In Eurocode 5, SS-EN 1995-1-1:2004 (2009), the creep effect on the displacement is taken into account by reducing the modulus of elasticity with a creep factor, denoted k_{def}, which depends on surrounding climate. Three different climates are considered in Eurocode 5, called service classes.

Concrete

The concrete creep increases with time, but in addition to time the creep rate is also dependent on if it is drying at the same time. The total creep strain can therefore be estimated as the sum of the basic creep strain and the drying creep strain (Soutsos & Domone, 2017). Other parameters that affect the creep of concrete is moisture content at loading, magnitude of applied load, concrete strength and temperature. In Eurocode 2, SS-EN 1992-1-1:2005 (2008), the creep is taken into account by a creep coefficient, which relates the creep deformation to the elastic deformation. These equations are presented in Appendix A.

Connection

As a consequence of the creep in the connection, the slip modulus will be reduced. Lukaszewska (2009) refer to three different reports where the long-term effects of connections in timber concrete composite systems have been studied. It could be seen that the creep of different connections followed the same pattern, where the creep was higher for the connections compared to the timber. In Eurocode 5, SS-EN 1995-1-1:2004 (2009), the creep of the connection is taken into account by reducing the slip modulus with a creep factor that is two times the creep factor of the timber.

4.2.2 Mechano-sorptive creep

In contrast to the viscoelastic creep, mechano-sorptive creep is the additional creep that occur due to variation in moisture content. In a TCC element the timber and the connection will be subjected to mechano-sorptive creep, but not the concrete.

Timber

Varying moisture content may have a considerable effect on the behaviour of timber and the deformation due to the mechano-sorptive creep could be many times larger than the creep in constant humidity (viscoelastic creep) (Swedish Wood, 2016c). When the beam is subjected to dehydration (desorption), the beam deflection increase while adsorption reduces the deflections. Hailu (2015) describes that the mechano-sorptive creep has a large impact in high humid climates, but when the moisture content is below 15 % the influence is considerably lower. The mechano-sorptive creep can not be taken into account very accurately in Eurocode 5. However, it can be considered to some extent by using a more severe service class than what the average moisture content corresponds to.

Connection

The mechano-sorptive creep of wood also influences the creep of the connections, due to the interface between the two materials (Fragiacomo et al., 2007). Thus, the slip modulus of the connections will be reduced with a higher creep coefficient when subjected to a varied relative humidity compared to a constant. The effect of mechano-sorptive creep of the connections is larger for an increased number of cycles and humidity cycles with larger amplitudes (Fragiacomo et al., 2007).

4.3 Moisture content impact on modulus of elasticity of timber

The modulus of elasticity of timber, and thus the stiffness, depends on the moisture content. As for the shrinkage and swelling of wood, the largest change in stiffness properties takes place below the fibre saturation point, and the stiffness properties are reduced linearly with increased moisture content (Soutsos & Domone, 2017; Swedish Wood, 2016c). A change in moisture content by 1% can change the modulus of elasticity up to 1.5% (Swedish Wood, 2016c). In Eurocode 5, the impact of the moisture content on the modulus of elasticity of timber is considered within the service class (Swedish Wood, 2016c).

4.4 Stress redistribution

Since a TCC element is internally statically indeterminate, the long-term behaviour of the different components affect each other, and stress redistribution between the materials occur. However, the determining design requirement for TCC elements are generally the deflection limitations. Therefore, the stress redistribution caused by the long-term effects will not be thoroughly analysed but it is briefly presented in the following Sections, 4.4.1 and 4.4.2.

4.4.1 Creep

In a TCC element, the creep behaviour of the three different components affect the response of the system. In regular design, the creep factor is considered by reducing the elastic modulus, resulting in a less stiff element. Schänzlin and Fragiacomo (2007) explain the deformation compatibility as a loop, where the concrete and timber behaviour affect each other. Starting with the creep of concrete, the stiffness and therefore stresses in concrete reduces. Since the external acting moment is constant regardless the internal stress distribution, the timber stresses increases when the concrete stiffness reduces, to maintain equilibrium. Higher stresses in timber then leads to additional creep which in turn reduces its stiffness and stresses. Following the same analogy, the stresses in concrete then increases. Then, additional creep in concrete occurs and the loop restarts.

It is important to consider that creep occurs in both materials (and the connections) simultaneously. The loop explained above should therefore only be used to understand how different creep rates affect the overall stress distribution. If all components have the same creep rate, the stress distribution will remain constant through the materials while the deflections increase. In the case of non-uniform creep, the stress redistribution increases with larger differences in creep (Dias, 2018). Stress redistribution as a result of creep will be further presented in Section 5.1.5.

4.4.2 Shrinkage and swelling

Inelastic strains causing shrinkage or swelling of the materials in the TCC element also affects the stress distribution within the cross-section. As an example, concrete shrinkage is partly resisted by the timber and thus tensile forces arise in the concrete section whilst the timber is compressed. The resultant of these normal forces acts with an eccentricity to the neutral axis of the composite cross-section and cause an additional component of the equilibrium requirement, see Equation 2.1. The normal force times the eccentricity is referred to as the composite bending moment and acts opposite the direction of the bending moments from the concrete and timber cross-section (Dias, 2018).

Since the concrete in a TCC element is designed to act in compression, the tensile forces caused by the concrete shrinkage leads to a reduction of the normal forces. Likewise, the timber tensile force will be reduced by the compressive forces from the concrete shrinkage. Therefore, a reduction of the normal forces occurs. To maintain equilibrium in the composite system, the bending moment will be increased and the maximum stress in the system will also increase (Dias, 2018). The load carrying capacity of the complete cross-section will therefore be reduced, especially since the tensile stress increases in the outermost timber fibre. However, the load on the connectors decreases.

The behaviour from concrete shrinkage is similar to the swelling of timber and result in the same reaction. However, Dias (2018) explain that the opposite occurs if the timber shrink (or concrete swell). Then, the normal force will increase and therefore the bending moment and the maximum stress decrease. The drawback is an increase of load on the connectors. Since the inelastic strains have a clear influence on the forces within the system, it is important to consider in ULS design if there is a risk of failure in any of the components. The behaviour is summarized in Table 4.1.

Table 4.1: Stress redistribution from inelastic strains (Dias, 2018).

	Internal forces	Connectors	Deflection
Concrete shrinkage or timber swelling	Reduced normal force, increased maximum stress	Reduced load	Increased deflection
Timber shrinkage or concrete swelling	Increased normal force, decreased maximum stress	Increased load	Reduced deflection

5

Design methods

Two possible design approaches for a TCC element are presented, an analytical analysis and a numerical analysis. The analytical analysis method applied in Eurocode 5, SS-EN 1995-1-1:2004 (2009), are often referred to as the γ-method ("gamma"-method) and it is a simplified calculation method. A numerical analysis is generally more time-consuming, but it is possible to capture more complex behaviour and result in a more detailed analysis. When modelling several long-term phenomena, the numerical solution gives more flexibility in regard to what is possible to include in the study.

Construction elements need to be designed regarding both serviceability limit state (SLS) and the ultimate limit state (ULS) as well as in short- and long-term. Each state and -term has specific conditions to consider in design since the material properties varies in time. Additionally, the connection slip modulus also varies between the SLS and ULS analysis.

5.1 Analytical analysis (γ-method)

The simplified approach for design of TCC used in Eurocode 5 is a method suggested by Ceccotti (1995). In the analysis, linear behaviour of the concrete, timber and connection is assumed in the instantaneous stage. This simplification may not be very accurate, especially if dowel type of connections is used, which have a highly non-linear behaviour. In order to take this into account, two different connection stiffnesses are applied in SLS and ULS verifications, as introduced in Section 2.4.1. A more detailed analysis of the slip modulus is presented in Section 5.1.1. Further information regarding the applicability of the γ-method was reviewed in Section 2.4.2.

The equations in the γ-method applied for calculations of TCC cross-sections are presented in Equations 5.1-5.9, based on formulations in Eurocode 5 Annex B, (SS-EN 1995-1-1:2004, 2009). Equation 5.1 defines the effective bending stiffness.

$$(EI)_{eff} = E_c I_c + \gamma_c E_c A_c a_c^2 + E_t I_t + E_t A_t a_t^2 \tag{5.1}$$

Where subscript c is used for the concrete and t for the timber. Then, E_i is the modulus of elasticity, I_i is the second moment of inertia and A_i is the area. The shear coefficient, γ, and the distance parameter, a_i, is calculated by Equations 5.2, 5.3 and 5.4.

$$\gamma_c = \frac{1}{1 + \frac{\pi^2 E_c s}{k L^2}} \tag{5.2}$$

$$a_c = \frac{h_c + h_t}{2} - a_t \tag{5.3}$$

$$a_t = \frac{\gamma_c E_c A_c (h_c + h_t)}{2(\gamma_c E_c A_c + E_t A_t)} \tag{5.4}$$

For the shear coefficient, γ, s is the spacing and k is the stiffness of the connectors while L is the length of the TCC element. The distance parameters are presented with the cross-sectional geometrical properties in Figure 5.1.

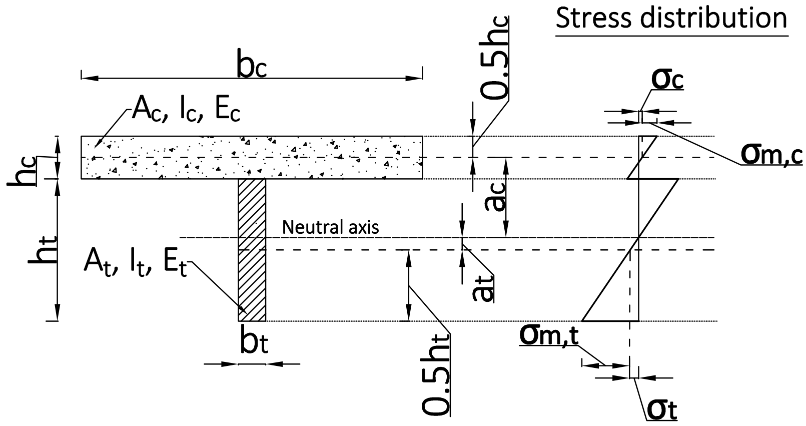

Figure 5.1: Geometrical illustration of properties based on Eurocode 5, (SS-EN 1995-1-1:2004, 2009)

As can be derived from the equations, a shear coefficient of 0 results in no interaction in the connection and the materials will work independently. Consequently, the effective bending stiffness will have its minimum value. Contrary, if the shear coefficient is 1, which is true for the case with infinitely stiff connectors, the bending stiffness will reach its maximum. For all types of connection, the calculated γ-value will be somewhere between 0 and 1, with stiffer connections being closer to 1 and therefore full composite action.

If unevenly spaced connectors are used, an empirical approximation with an effective spacing can be applied, see Equation 5.5 (Ceccotti, 2002). The estimation is good in regards to the deflection calculations but does not capture the real slip behaviour.

$$s_{eff} = 0.75\, s_{min} + 0.25\, s_{max} \quad \text{with} \quad s_{max} \leq 4\, s_{min} \tag{5.5}$$

Both the maximum and minimum spacing measurements are defined at the midpoints between each stiffener. The maximum spacing, s_{max}, may be taken as the largest value of either $s_{max,con}$ or $s_{max,sym}$, and the minimum spacing s_{max}, is defined as the smallest value of $s_{min,con}$ or $s_{min,end}$. The different spacings are illustrated in Figure 5.2, where $s_{max,con}$ and $s_{max,sym}$ is the largest distance between two adjacent connector-midpoints or the distance between the beam symmetry line and the nearest connector-midpoint, whereas $s_{min,con}$ and $s_{min,end}$ is the minimum spacing between two connector-midpoints or the distance between the outermost connector-midpoint and the support.

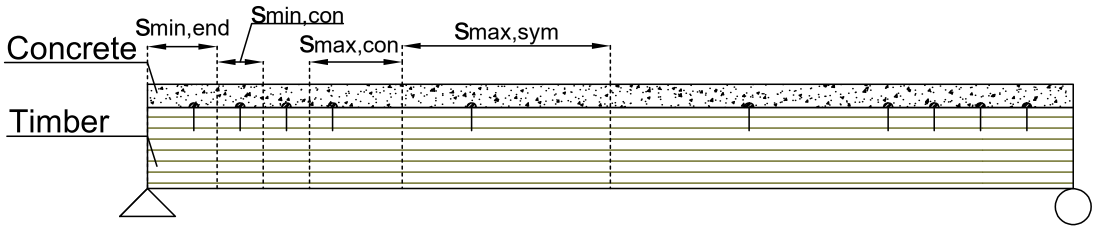

Figure 5.2: Illustrative definition of s_{max} and s_{min}.

With the effective stiffness determined, the standard equation for a simply supported beam may be used to calculate the maximum (mid-span) deflection, Equation 5.6.

$$\delta = \frac{5qL^4}{384(EI)_{eff}} \tag{5.6}$$

Furthermore the stresses in the cross section can be determined with Equation 5.7 and 5.8. σ_i is the stress-component from the shear force at connection which increases with stiffer connections, whereas σ_{mi} is the flexural component that decreases with stiffer connections. The total stress is the sum of the two stress components, calculated for both materials (timber,t, and concrete,c). In Section 2.2 the stress components was further discussed, and a schematic stress distribution, illustrating the methodology could be seen in Figure 5.1.

$$\sigma_i = \frac{\gamma_i E_i a_i}{(EI)_{eff}} M \tag{5.7}$$

$$\sigma_{m,i} = \frac{0.5 E_i h_i}{(EI)_{eff}} M \tag{5.8}$$

If of interest, the shear force in the fastener can be calculated using Equation 5.9.

$$F = \frac{\gamma E_i A_i a_i s}{(EI)_{eff}} V \tag{5.9}$$

With the basics of the γ-method presented, the input values to be used will be presented and discussed in the following Sections 5.1.1-5.1.5. Additionally, for the long-term evaluation, some suggested extensions will be introduced as well.

5.1.1 Slip modulus

When no test data is available for the slip moduli, Eurocode 5, SS-EN 1995-1-1:2004 (2009), propose to double the value for regular timber to timber connections to get the serviceability limit state slip modulus, K_{ser}. The stiffnesses are tabulated for different types of connections and depends on the timber density and connector diameter. However, this approach has been shown to give very variable accuracy, sometimes giving values close to the test data but in other cases being far off.

In a study performed by Ceccotti et al. (2006), the analytical data based on the Eurocode 5 approach lead to a 40-50 % underestimation of the slip moduli. Despite the values being on the conservative side, the difference in result is noteworthy and the unaccounted stiffness may lead to unexpected behaviour such as a more brittle failure. As a result, Ceccotti et al. (2006) recommends using experimentally determined data. The formulation for the slip modulus in the ultimate limit state, K_u, in Eurocode 5 is based on the aforementioned K_{ser} value, see Equation 5.10.

$$K_u = 2/3\, K_{ser} \tag{5.10}$$

Since the SLS value has been shown to have variable reliability, it is reasonable to assume that the same apply for the ULS formula. Additionally, even if the K_{ser} value has been concluded to be a good estimation, the nonlinear behavior of connections makes the equation in Eurocode 5 very simplified and may sometimes be significantly different from the real behavior.

Dias (2005) present an example that illustrates the possible difference for a dowel type connection, which is known to behave nonlinear. In the example, the slip calculated based on Eurocode 5 was about 8 mm while the experimentally obtained slip reached almost the double, at 15 mm. The difference is explained by the vastly different behavior before and after yielding. Since the connection in the presented case yields for a higher value than K_{ser}, K_u is based on a linear behavior even though the stiffness is drastically reduced after yielding occurs.

Another connector where the Eurocode 5 formula is not proper to use is notched connections, which inhibits close to linear behavior up to failure and the stiffness may therefore be assumed to be constant, see Equation 5.11 (Dias, 2018). Following the theory of glued connections, it is reasonable to assume that the same applies for those as well.

$$K_u = K_{ser} \tag{5.11}$$

Despite experimental data being preferred over the suggested approach in Eurocode 5, consideration should be taken in regard to the test data collection. Dias (2005) explains that the method for which the test data is collected, International Organization for Standardization (1983), might lead to large variations in result for the same connection. This is due to the testing being performed based on an estimated maximum load capacity, F_{max}, and the estimation is allowed to differ up to 20 % from the actual result for the test to be valid. Since K_{ser} is defined at 40 % of F_{max}, the estimation can have a large influence for materials with nonlinear behaviour around that magnitude. In an example, Dias (2005) present that stiffness variations of 100 % for K_{ser} can be found between the allowable lower and upper limit of estimation correctness in the test procedure of a lag screw joint.

5.1.2 SLS - short-term

Verification of the TCC element in short-term analysis is computationally more convenient than the long-term analysis since the material time dependency does not need to be considered. The γ-method presented in Section 5.1 can be followed with the corresponding slip modulus applied. For calculation of initial deflection of the beam, a slip modulus according to SLS should be applied, K_{ser}. The material properties are presented in Equations 5.12. The short-term SLS check is seldom performed in design practice since deflections will most often be larger in the long-term, unless the timber shrinkage causing the TCC element to bend upwards is dominant. The mean values of the material stiffness moduli should be applied in the SLS calculations.

$$E_c = E_{cm} \tag{5.12a}$$

$$E_t = E_{0,mean} \tag{5.12b}$$

$$K = K_{ser} \tag{5.12c}$$

5.1.3 ULS - short-term

The ULS calculations for the short-term verification is similar to the procedure for SLS. The exception being the slip modulus for the connection being taken as K_u instead. As for the SLS calculations, the stiffness moduli for timber and concrete should be taken as their respective mean values, rather than the characteristic values (Ceccotti, 2002), see Equations 5.13. Hailu (2015) explains that the reason for this is that no characteristic values are available for the slip modulus of the connection and therefore mean values should be used for all stiffness properties. Logically, the most realistic behaviour is captured when the mean values are used, and therefore, the current approach gives the stress distribution most likely to occur.

$$E_c = E_{cm} \tag{5.13a}$$

$$E_t = E_{0,mean} \tag{5.13b}$$

$$K = K_u \tag{5.13c}$$

5.1.4 SLS - long-term

For analysis in long-term, the procedure becomes more simplification-based, due to the difficulty to analytically capture the real response of the TCC element. As presented in Chapter 4, there are numerous long-term effects that affect the behaviour. Concrete shrinks and creep whilst the timber and connection are heavily dependent on the moisture content in terms of mechano-sorptive creep and shrinkage/swelling.

The model presented in Ceccotti (1995) and used in Eurocode 5, SS-EN 1995-1-1:2004 (2009), is referred to as the “effective modulus method”. In it, the creep is considered by reducing the stiffness of the concrete, timber and connection, respectively, see Equations 5.14.

$$E_{c,fin} = \frac{E_{cm}}{1+\phi(t,t_0)} \tag{5.14a}$$

$$E_{t,fin} = \frac{E_{0,mean}}{1+k_{def}} \tag{5.14b}$$

$$K_{fin} = \frac{K_{ser}}{1+2k_{def}} \tag{5.14c}$$

The creep factor for concrete, ϕ, is calculated according to the guidelines presented in Eurocode 2, SS-EN 1992-1-1:2005 (2008), attached in Appendix A. The approach considers the time of loading, ambient conditions and multiple other factors affecting the long-term deformation behaviour of concrete. Furthermore, the creep factor of concrete can be evaluated for any point in time and not only as a final value.

For timber, the factor used to consider the creep, k_{def}, is mainly based on the service class and its value is tabulated in Eurocode 5, (SS-EN 1995-1-1:2004, 2009). Even though the service class considers the ambient conditions such that more variable and higher relative humidities result in higher service classes, the approach is very general and indefinite. For demanding climates, with large variations of relative humidity, several studies have indicated that the mechano-sorptive effects are critically underestimated in the current approach (Hailu, 2015).

As for the timber, the connection stiffness is reduced using k_{def}. However, Eurocode 5, suggest that the value of k_{def} should be doubled for the connection, reducing the stiffness even more. The suggestion is followed in several studies (Ceccotti et al., 2006; Kavaliauskas et al., 2005). However, some research does not consider this factor (Lukaszewska, 2009). Since the Eurocode 5 model is very simplified and the experimental test recurrently generates larger deflections than the presented effective modulus method, it is difficult to evaluate if the Eurocode 5 suggestion of doubling the creep factor for timber is a good approximation. However, since the results tend to critically underestimate the deflections, more conservative values seems reasonable to apply.

Apart from the "effective modulus method", followed in Eurocode 5, additional analytical calculation procedures are presented and evaluated by several researchers (Dias, 2018; Fragiacomo et al., 2007; Kavaliauskas et al., 2005). Although several methods on how to properly evaluate the long-term effects have been investigated, no consensus have been reached amongst researchers, which demonstrates the complexity of the analysis.

5.1.5 ULS - long-term

Since the components in a TCC element have different long-term behaviour, the stress distribution varies in time with the stiffness variations. Unlike the concrete creep model presented in Eurocode 2, SS-EN 1992-1-1:2005 (2008), the creep behaviour of timber presented in Eurocode 5, SS-EN 1995-1-1:2004 (2009) only considers the final creep factor. Therefore, additional models need to be considered in order to capture the variations of creep over the life-time of timber. Such rheological models are presented and evaluated by Schänzlin and Fragiacomo (2007) and Dias (2018). Both studies concluded that the concrete creeps significantly faster during the first years, compared to the timber. Additionally, both the concrete and timber display a clear non-linear deformation behaviour.

Schänzlin and Fragiacomo (2007) and Dias (2018) notes that apart from the initial and final point in time, the period between 3 and 7 years should also be considered in design. During this age, the concrete has reached approximately 95 % of its final creep whilst the timber has only developed around 60 % of its equivalent creep, which is illustrated in Figure 5.3. Furthermore, during this period, the two materials display a similar relative creep rate (Dias, 2018). For ages longer than 7 years, the concrete creep is very small whilst the timber creeps its remaining 40 %.

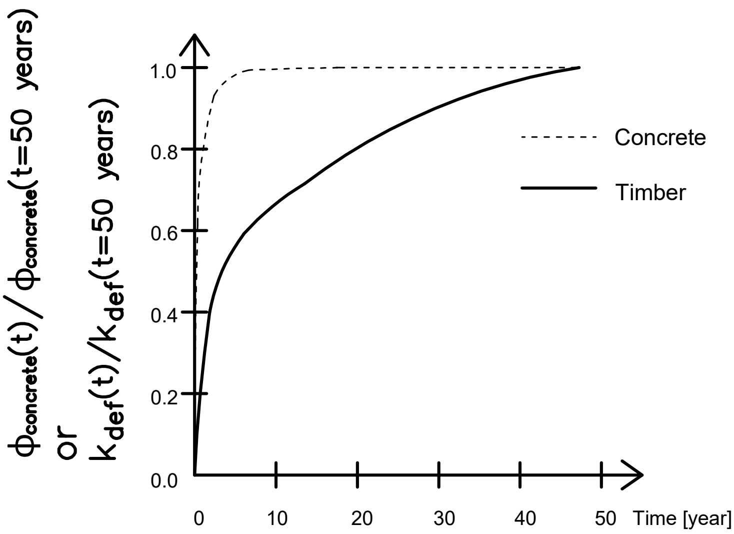

Figure 5.3: Principal concrete and timber creep, based on (Dias, 2018).

Schänzlin and Fragiacomo (2007) explains that in the general case, where the concrete initially creeps faster than the timber, the timber will be subjected to the highest tensile stresses during the first 3 to 7 years. The stress redistribution due to creep is explained in Section 4.4.1. As the concrete creeps, its stiffness is reduced, then the timber stiffness increases relative to the total stiffness of the cross-section. As a result, the timber attracts more load and therefore its stresses increase. In the final stage, when the timber has crept additionally, the load on the concrete will have increased relative to the intermediate case.

A further developed computational method compared to the recommended approach in Eurocode 5, SS-EN 1995-1-1:2004 (2009), is presented by Schänzlin and Fragiacomo (2007), see Equation 5.15.

$$E_{c,fin} = \frac{E_{cm}}{1 + \psi_c \phi(t, t_0)} \tag{5.15a}$$

$$E_{t,fin} = \frac{E_{0,mean}}{1 + \psi_t k_{def}} \tag{5.15b}$$

$$K_{fin} = \frac{K_{ser}}{1 + 2k_{def}} \tag{5.15c}$$

The ψ-coefficients are determined through parametric studies and varies with the evaluated time as well as the type of TCC element used (beam or slab). The forthcoming updated version of Eurocode 5 will display a more comprehensive analysis of ψ-coefficients compared to the current version in which a more simplified approach is suggested. In the present Eurocode 5, SS-EN 1995-1-1:2004 (2009), the ψ-coefficient is simply taken as the quasi-permanent load factor, ψ_2. Although Schänzlin and Fragiacomo (2007) does not consider any factor of the connection stiffness, the same theory can be applied to establish appropriate values for its creep as well.

Despite the conclusion that the stress distribution in the intermediate time frame is important to consider in design for the ULS, Dias (2018) points out that there is no record of any failure occurring during that period of time. The suggested explanation is that the ULS will most likely not be governing in design, and therefore the deflections in SLS will determine the required cross-sectional dimensions. The relatively small increase of stress between 3 to 7 years will therefore not likely require an increase in element size.

5.2 Numerical analysis

The behaviour of structures are mathematically described by partial differential equations, and when the problem becomes too complex it is not possible to solve them by an analytical analysis. Instead, an approximate solution is needed which can be obtained by solving the structural problem numerically. A common way to solve partial differential equations numerically in the engineering field is to use the finite element method (FEM) (Ottosen & Petersson, 1992). There are many different FEM programs that are used today, and one commonly used in research is Abaqus. In this thesis Abaqus CAE is used together with the Standard solver.

When using a numerical approach it is possible to model complex long-term behaviour. Creep and shrinkage are important rheological phenomena when studying a timber-concrete composite beam during long-term, but they affect the three materials in the composite beam differently. To be able to capture the moisture changes variation at each location of the beam and the behavior over time, a numerical model is suitable (Khorsandnia, Valipour, Shrestha, Gerber, & Crews, 2013).

The searched output from a numerical analysis are often deflection and stresses, which both are dependent on the strains. When studying a beam under long-term loading both elastic strains and strains from creep and shrinkage need to be considered. Each of the long-term effects, that has been described in Chapter 4, will contribute to a change in the total strains (Eisenhut, Seim, & Kühlborn, 2016).

The best approach to model the long-term effects as correctly as possible in Abaqus would be to define the different constitutive relations for all long-term effects by user-defined subroutines. The subroutine that is used to describe new material properties in Abaqus is called UMAT and the programming language used is Fortran. By writing a user-defined UMAT it is possible to describe constitutive relations that does not exist in the user interface of Abaqus. Defining constitutive relations for all the materials and their corresponding long-term effects is a very demanding task, as it requires a great experience in modelling technique and detailed knowledge about the long-term performance of each material.

Since the scope of the thesis is to do a parametric analysis of the general behaviour caused by common long-term effects, no user-defined subroutines will be written. As such, the already defined constitutive relations in Abaqus will be used. A result of this limitation is that variations in climate over time can not be considered, which is similar to the approach in the γ-method. However, unlike the γ-method, the numerical solution is able to include the inelastic strains from shrinkage and/or swelling in the analysis.

6

Modelling procedure in Abaqus

The numerical analysis in this study is performed using the FEM-program Abaqus CAE with the standard solver. A solid model is used since this was the simplest to use for various connection types. The drawbacks of a solid model is the relatively long computational time and fine mesh-size needed. In the coming sections, the modelling method is presented along with a validation of the model.

6.1 Conditions

No variations in temperature and relative humidity is considered. Due to these limitations, all long-term effects can not be explicitly considered, such as mechano-sorptive creep and strain due to temperature changes. If these variations would be considered a very complex FE-model is needed, which is not necessary to fulfill the aim of the study.

6.2 Input data

The following data are defined in the model; geometry of the slab, material properties, loads, boundary- and symmetry conditions and the level of interaction between the concrete and timber part. Abaqus does not have any defined built in system of units, and the chosen units are presented in Table 6.1.

Table 6.1: Table of SI units used in Abaqus.

Quantity	Unit
Length	Millimeter, [mm]
Force	Newton, [N]
Mass	Tonne, [ton]
Time	Second, [s]
Stress	Mega-Pascal, [MPa] [N/mm^2]

6.2.1 Geometry

The "T"-shaped TCC beam type cross-section consists of a concrete slab and timber beam, modelled as solid elements. A Cartesian coordinate system is chosen with the three directions, X, Y and Z, illustrated in Figure 6.1.

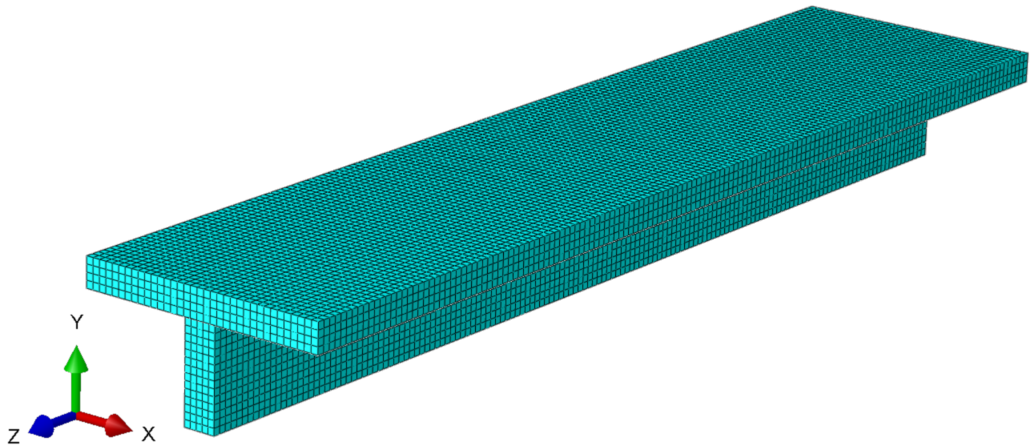

Figure 6.1: Coordinate system and meshed TCC beam type element in Abaqus.

6.2.2 Material properties

Material properties of concrete are taken from Eurocode 2, SS-EN 1992-1-1:2005 (2008), and the material properties for different wood products can be found in SS-EN 338:2016 (2016). The concrete is defined as *isotropic* while the orthotropic behaviour of timber is captured by the material type *Engineering constants*. There, a local coordinate system needs to be defined.

6.2.3 Loads

The loads used in the model are the self-weight of the TCC and an applied uniform load. The self-weight is included by adding a gravitational acceleration of load type *gravity*. Following Table 6.1, it should be applied as mm/s^2. The uniform load is applied at the upper surface of the concrete, visualized in Figure 6.2.

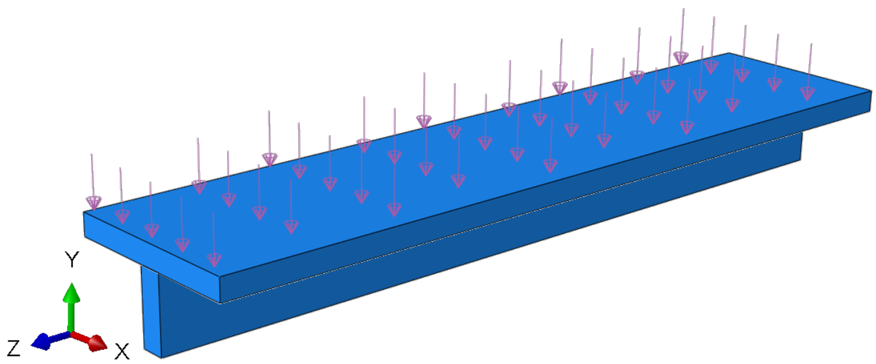

Figure 6.2: Applied uniform load on TCC element in Abaqus.

6.2.4 Boundary- and symmetry conditions

A simply supported beam is studied, but only half the beam is modelled to decrease the computational time. Thus, a roller support is modelled together with a symmetry condition in the other end (corresponding to the middle of the beam). The roller support is modelled by a constraint in the X- and Y-direction. The symmetry condition is achieved by a constraint in the Z-direction and constraints of the rotation around X and Y. The boundary conditions as shown in Abaqus is displayed in Figure 6.3.

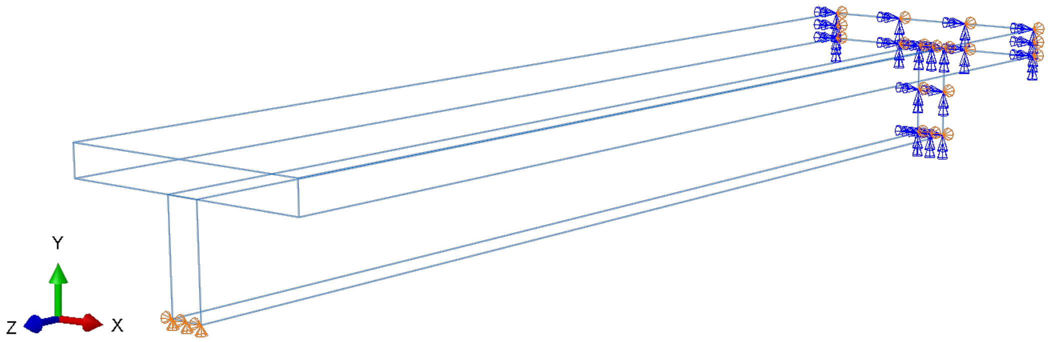

Figure 6.3: Boundary conditions of TCC element in Abaqus.

6.2.5 Interaction

In a TCC element, the interaction properties between the materials has a large impact on the performance. The connectors that defines this behaviour is expressed with a slip modulus. The interaction between concrete and timber consists of two phases, the initial bonding, and the friction. Initial bonding is the interaction achieved by the connectors, for example dowels and notches. If the connection fails, only the friction contributes to the shear transfer between the materials. Jaaranen and Fink (2021) states that the frictional contribution is generally not considered in models, since the effect is often neglectable for a global analysis.

The properties of the connectors usually behave non-linear for large loads as discussed in Section 3.3. It is generally valid to neglect this non-linearity for long-term analysis, since the shear force is small in comparison to the shear strength of the connections (Lukaszewska, 2009). Therefore, the interaction is modelled with a linear elastic behaviour. Two main modelling techniques for connections can be distinguished, continuous and discrete interaction.

6.3 Continuous interaction

When using a continuous interaction, the location of the connections does not need to be modelled, instead the connectors are smeared along the interface between the two materials. As such, glued connections are naturally continuous. However, connection types with discrete spacing could also be modelled as continuous. An advantage of using continuous interaction for the model is the reduction of computational time and time for modelling (Lukaszewska, 2009). It is a good approximation when the spacing of the connectors is uniform and the distance between them is rather small. An illustrative example of the contact area for a continuous interaction is shown in Figure 6.4. How to model the two extremes full- and no interaction and partial interaction with a continuous modelling technique is presented in Section 6.3.1, 6.3.2 and 6.3.3.

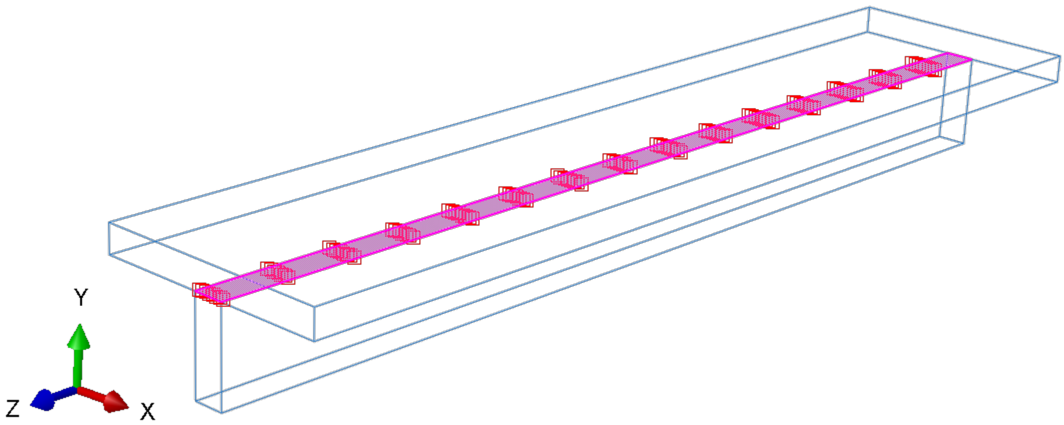

Figure 6.4: Continuous interaction of TCC element in Abaqus.

6.3.1 Full interaction - Tie

Full interaction can be modelled in Abaqus with the constraint type *tie*. This connection does not allow any relative movement between the two components, instead they behave as a unit. When using the *tie* constraint, a master and a slave surface needs to be defined. If a smaller surface interacts with a larger surface, then the smaller surface should be the slave surface and the larger should be the master (Simulia - Abaqus 6.14, 2014). If this distinction cannot be done, then the surface with largest stiffness should be considered as the master surface. For a beam type TCC the first criterion is fulfilled, but for a slab type CLT the second criterion is only valid. Both the criteria implicate that the concrete should be the master surface and the timber the slave surface.

6.3.2 No interaction - Hard contact

If no fasteners are bonding the two materials together and no friction is considered, there is no interaction between the two materials. Which means that the timber and the concrete work separately. In Abaqus, no interaction can be modelled by creating an interaction with certain properties in the normal- (global Y-direction) and the tangential (global X- and Z-direction) direction at the material interface. In the normal direction *hard contact* is chosen as the pressure overclosure relationship, which means that no tensile forces can be transmitted between the two parts. The interaction property in the tangential behaviour is chosen as *frictionless*. The interaction is modelled by creating an interaction with type *surface-to-surface contact* which means that a master and a slave surface must be defined, as for the *tie* constraint.

6.3.3 Partial interaction - Cohesive

Partial interaction is modelled with a similar procedure as no interaction, the difference is that a *cohesive* behaviour is added to the interaction properties. The *cohesive* behaviour is described by traction-strain stiffnesses in three directions, $K_{n,n}$, $K_{s,s}$ and $K_{t,t}$, with units N/mm^3. $K_{n,n}$ is the stiffness in normal direction (global Y-direction) whereas $K_{s,s}$ and $K_{t,t}$ are the stiffnesses in tangential directions (global X- and Z-directions). The stiffness in the normal direction is set to be zero, whereas the stiffness in the two other directions are related to the connections and the spacing between them. In practice the stiffness in the normal direction is not zero, especially not for dowel type connectors which has a significant axial capacity. However, in the model it is a fair simplification since the elements are modelled to always keep contact, as a simplification. The traction-strain stiffness for the two tangential directions in a TCC connection with equal spacing are calculated by dividing the slip modulus of one connection with its influence area.

6.4 Discrete interaction

A discrete interaction modelling technique considers the location of each connector. This procedure is more time consuming both when creating the model but also for the computational time (Lukaszewska, 2009). It also requires more information about the location of the connectors and can be a hindrance when performing a parametric study. However, at the same time the model becomes more realistic. A discrete modelling of the interaction is more important when there is an uneven distribution of the connectors, for example in the case with more connectors near the supports, where the shear forces are the largest.

Partial interaction with discrete modelling technique can be achieved by applying spring elements at the locations of the connectors. The springs are then assigned a spring stiffness in the direction of the span length, which corresponds to the slip modulus of the connection. To insert a spring element, reference points have to be defined at the locations on the timber and concrete part where the connectors are placed. A graphical display of springs in Abaqus is shown in Figure 6.5.

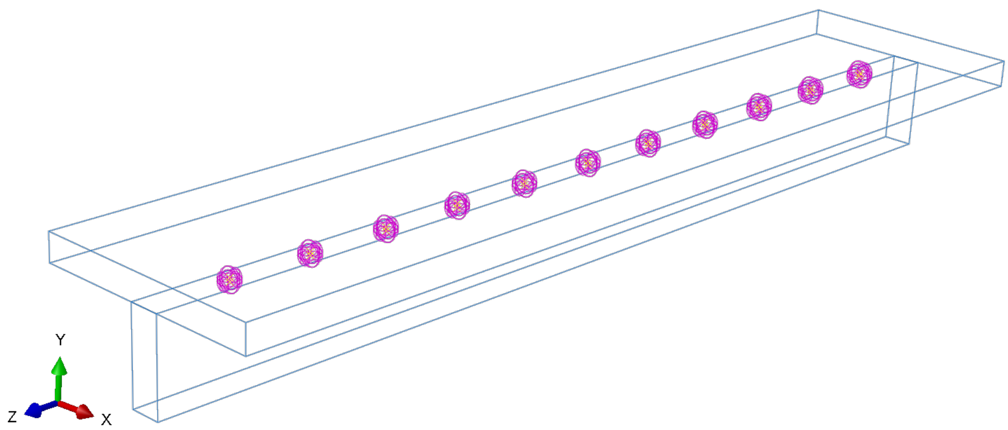

Figure 6.5: Discrete interaction (springs) of TCC element in Abaqus.

6.5 Long-term effects

When modelling the long-term effects of TCC slabs in Abaqus, a constant climate is assumed. As such, the changes in moisture content resulting in mechano-sorptive creep and strains from temperature differences are not considered. The effects that are included are creep of the three materials together with shrinkage of concrete and shrinkage/swelling of timber. As described in Section 5.1 the effects that the analytical procedure, described in Eurocode 5, SS-EN 1995-1-1:2004 (2009), the γ-method, take into account is the creep of the three materials. Hence, the additional aspects in the Abaqus model are the shrinkage and swelling.

6.5.1 Shrinkage

The shrinkage of concrete consists of both the drying shrinkage and autogenous shrinkage as described in Section 4.1.3. In Eurocode 2, SS-EN 1992-1-1:2005 (2008), the shrinkage is calculated as a strain and it is inserted as an negative expansion coefficient in Abaqus.

If the timber is installed with a higher moisture content than the equilibrium moisture content, shrinkage of the timber occurs. The shrinkage of timber can be taken into account by a shrinkage strain as described in Chapter 4. Since the vertical deflection is of interest, the shrinkage strain in the longitudinal direction is implemented in Abaqus. As for concrete, the corresponding strain is implemented as an expansion coefficient.

6.5.2 Creep

Creep of all the materials are taken into account by reducing the modulus of elasticity of the timber and connection by the factor k_{def} (doubled for the connection) and the creep factor for concrete, ϕ. The formulas for the final modulus of elasticity and slip modulus are expressed and described in Sections 5.1.4 and 5.1.5.

6.6 Validation of model

To validate the modelling technique, experiments found in literature are used. The different experimental setups are both modelled in the FE-program Abaqus and calculated with the γ-method. Hence, the real experimental results and γ-method can be used to validate the FE-model. The behaviour is compared both in short-term and long-term, with deflection as evaluation aspect. Several experimental setups have been used to validate the model, and three of these are presented in this report, one performed by Lukaszewska (2009) and two experiments from Hailu (2015).

The experiment performed by Lukaszewska (2009) is referred to as experimental setup 1, which is used to validate the model in short-term. The two experiments performed by Hailu (2015) are used to validate the model both in short-term and long-term, and are referred to as experimental setup 2 and 3. The validation by using experimental data or the γ-method is described briefly in the coming sections, while a more in-depth description is found in Appendix B for all three experiments separately.

For each FE-model, a convergence study was run to make sure the mesh was sufficiently fine, while not taking too long to run. An example of meshing and deflection shape of the modelled beam is presented in Figure 6.6

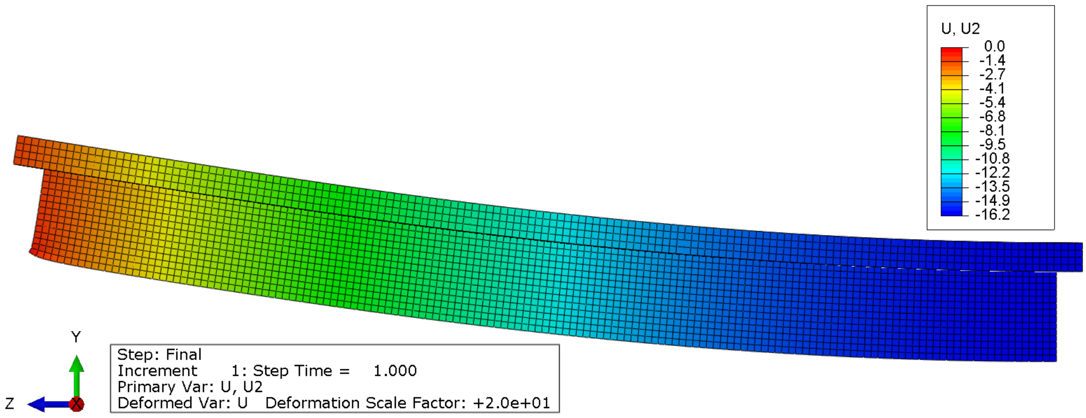

Figure 6.6: Example of mesh-size and deflection-result in Abaqus.

6.6.1 Experimental data

The experiments that the modelling technique was validated towards in short-term had different connection types, connector locations, material properties and geometries (with "T"-shaped cross-sections). By validating the model by a vast range of experiments it is possible to determine if the modelling technique works for a general TCC beam type element. When modelling experimental setup 1, 8.7 % more deflection was obtained compared to the real experimental value, and for setup 2 and 3 there was an overestimation of the deflection of 8.2 % respectively an underestimation of 2.2 %. Generally it could be concluded that the FE-model gave larger deflections compared to the experimental, except for setup 3. That test was performed by Hailu (2015), where it is described that this experiment showed unexpectedly large deflections. Therefore the results from experimental setup 3 is more unreliable than setup 1 and 2. As a conclusion of the short-term validation, the FE-modelling technique gives a reasonably good approximation of the behaviour, and the modelled short-term deflection seems to be on the conservative side.

When validating the model in long-term it is important to find experiments that are monitored for at least a couple of years. The creep of timber and connectors are implemented in the model as final creep factors, and therefore the model will not be a very good representation if the experiments have a relatively short time-span. Further, it is desirable to find long-term experiments with a non-varying climate, since mechano-sorptive creep and strain differences due to temperature changes are not considered explicitly in the Abaqus model. No long-term experiments that fulfil these conditions were found in the literature, since most of the experiments had been monitored for less than a year. Therefore, only two experiments were used for the validation of the long-term modelling.

The two experiments, referred to as experimental setup 2 and 3, were performed over a period of 1400 days and was subjected to heavily varied relative humidity. For both setups, the considered modelling procedure does not capture the long-term behaviour very well. The underestimation between the FE-model and the experimental values was approximately 25 % for setup 2 and 39 % for setup 3. As for the short-term modelling, experimental setup 3 differed more from the expected behaviour and the results in setup 2 is deemed more credible. However, an underestimation of 25 % is still a fairly large difference, and the main reason is likely the highly varying climate that the modelling technique can not capture properly when using service class 3. This demonstrate that even though service class 3 is considered, the long-term deflection might not be captured correctly, when such heavy variations in relative humidity occurs.

The aim of the TCC model is to be able to understand the behaviour of TCC elements both in short-term and in long-term, and capture which long-term effects that have the largest influence on the deflections. The modelling technique used in the parametric study will not function as a design tool of TCC elements for long-term analysis. Therefore, it is not essential to have a model that match the experimental values perfectly. Most important is that the proposed modelling technique of TCC beams can capture its behaviour. Therefore, even though the modelling technique was not able to match the long-term deflection it is still deemed as a good tool for analysing the influence of different long-term effects.

6.6.2 Gamma-method

In addition to the actual experimental values of the deflections in short-term and long-term, the analytical procedure proposed in Eurocode 5 Annex B, SS-EN 1995-1-1:2004 (2009), the γ-method, is also used to validate the modelling procedure. Since the FE-modelling technique is based on the effective modulus approach used to consider creep in the γ-method, comparing the FE-model with the γ-method should give similar results, also in the long-term. The difference between the analysis are that in the FE-model, strains caused by shrinkage can be included, which is not possible in the γ-method. However, since the concrete slab is not connected with the timber until after 200 days in the two experiments from Hailu (2015), the concrete shrinkage is neglected. Additionally, the timber moisture content is not lower at the end than at assembly, and thus timber shrinkage is not considered either.

As expected, the γ-method and the FEM models showed similar results for both the short- and long-term, respectively. Therefore, the modelling technique is a good representation of the γ-method, while having additional advantages such as possibility to consider shrinkage strains and more complex geometries.

6.6.3 Behavioural validation

In addition to the experimental test data and the γ-method, the modelling procedure is evaluated by examining the behaviour under changing conditions. In the parametric study, the model outcome is compared to the studied theory, to see if the analysis result match the expected outcome. In that way, the modelling method is continuously evaluated and verified for the investigated parameters. As an example, the slip is studied in Abaqus, which should be largest at the simply supported edge, where the shear is the largest. At the symmetry edge, there should not be any slip since no shear force is present. In Figure 6.7, the slip in Abaqus is shown following this behaviour.

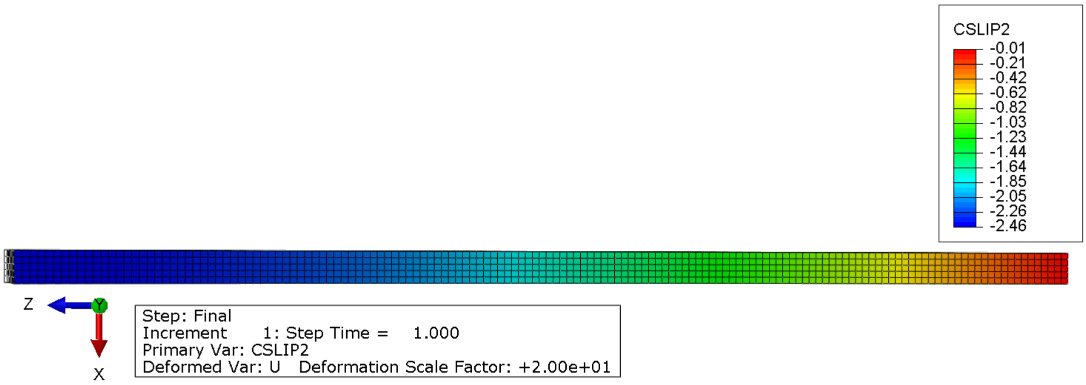

Figure 6.7: Example of slip-result in Abaqus (view from "above").

7

Parametric study

Based on the validated FE-modelling technique, a parametric study is performed to analyse the shrinkage and creep behaviour, and what parameters that affect the deflections. The parametric study is divided in two main parts, the first part is presented in Section 7.1, 7.2, 7.3 and 7.4, whilst the second part is in Section 7.5. First, the shrinkage and creep behaviour are investigated in a general case, to get an overview on how big of an impact those long-term effects have and conclude which ones are the most important to consider. Then, in the second part, one of the parameters is more thoroughly investigated in a more realistic design case, with varying cross-section to match a deflection limit.

In the first part of the parametric study, all the analyses are based on the same cross-section, but with varying connector stiffness and span length. Additionally, the investigated long-term parameters, shrinkage and creep (stiffness), are varied as well. However, the same geometry and material properties are used, and the self-weight is always included. Further, the variable load magnitude is kept constant at 2 kN/m^2 since varying the load level does not affect the principal behaviour of a linear material. The chosen design is based on the experiments performed by Hailu (2015); Lukaszewska (2009), from which a compiled average cross-section has been determined. The geometry is presented in Figure 7.1 and the beam is simply supported.

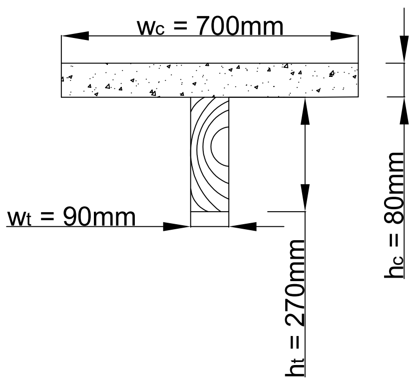

Figure 7.1: Cross-section used in the first part of the parametric study.

One long-term effect (shrinkage or creep) for one material (concrete or timber) will be studied at a time. The first step for each investigated long-term effect is to study how the connection stiffness affect the deflections. For those analyses, the span length is set to 6 meters which is chosen as the "standard" case and result in long-term deflections around L/200-L/300. After deducing the connection stiffness impact on the behaviour, the analysis is run for varying span lengths to study how that affect the behaviour. Lastly, the impact of varying long-term effects in the “other” material is studied, which for example means that variations in creep for both concrete and timber is studied simultaneously.

Two different sets of material properties are used in the studies, for concrete see Table 7.1 and timber Table 7.2. In the shrinkage analysis, the stiffness is chosen as to simulate reasonable long-term values of the concrete and timber. Since the stiffness varies with the creep factor and service class, the chosen values are set within the common range. In the creep analysis, the short-term stiffness properties and their corresponding long-term reduced values are presented. The remaining conditions (connector stiffness, span length and "other" long-term effects) are presented separately for each analysis, since those parameters are varied. In the creep analysis, shrinkage is set to zero.

Table 7.1: Concrete properties used in the first part of the parametric study.

Type of analysis:	MoE, E [MPa]	Poisson's ratio, ν [-]	Density, ρ [kg/m^3]
Shrinkage	15000	0.2	2450
Short-term	33000	0.2	2450
Creep φ=1.5	13200	0.2	2450
Creep φ=2.5	9428	0.2	2450

Table 7.2: Timber properties used in the first part of the parametric study.

Type of analysis:	E_1, [MPa]	E_2=E_3, [MPa]	G_{12}=G_{13}, [MPa]	G_{23}, [MPa]	Poisson's ratio, ν [-]	Density, ρ [kg/m^3]
Shrinkage	5000	250	300	25	0	450
Short-term	13800	500	600	50	0	450
Creep SC 2	7667	278	333	28	0	450
Creep SC 3	4600	167	200	17	0	450

In order to facilitate the modelling when changing the span lengths, the interaction was set using the cohesive interaction type instead of modelling each spring. For uniformly spaced connectors, this assumption is notably accurate and a basis for the γ-method used in analytical design. The compliance of the two modelling methods have been verified for the chosen model. In the studies where the connection stiffness is presented, the values correspond to connectors with an equal spacing of 250 mm.

To demonstrate the long-term behaviour, upper and lower values are used in the analysis, for example by applying an upper and lower shrinkage strain or creep factor. This way, the relative difference in deflection can be evaluated by calculating the percentage of increase (or decrease) in deflection, see Equation 7.1. In some figures, this relative difference will be presented and for those graphs dashed lines are used, “- - -“. The detailed result of each analysis is tabulated in Appendix C.

$$D_{relative} = \frac{upper - lower}{lower} \tag{7.1}$$

7.1 Concrete shrinkage

To study the potential effect of concrete shrinkage, an element with *no* shrinkage is compared to one with *normal* shrinkage. In the model, shrinkage can be considered through a negative expansion coefficient, corresponding to the strain, ε. The shrinkage strain set as the upper and lower values is used to illustrate the behaviour of a TCC element and the influence of concrete shrinkage. However, the values should not be interpreted as the physically possible extreme values.

The lower shrinkage coefficient is set to zero, meaning no shrinkage occurs after interaction between the timber and concrete has been established. In practice, such a situation is difficult and inconvenient to achieve since shrinkage occurs for a long time. However, the shrinkage has a much higher rate shortly after the casting than when the concrete has cured for some time. It is therefore plausible to assume that under the right conditions, the concrete shrinkage becomes neglectable. This is supported by Lukaszewska (2009) which states that if the concrete is stored for some weeks before it is mounted on the timber beams, the concrete shrinkage can partly or fully be neglected.

For the upper limit, a shrinkage of 0.04 % was used as a *normal* shrinkage value, based on assumptions of reasonable conditions and previous calculation experience. The value was deduced with use of the Eurocode 2, SS-EN 1992-1-1:2005 (2008), analytical calculation of concrete shrinkage, see Appendix A. Although, it is physically possible for the concrete to shrink more than the set upper limit, such cases are assumed to be avoided in design due to the possible inconvenience.

7.1.1 Connection stiffness

First, the concrete shrinkage impact is studied for various connection stiffnesses, with properties according to Table 7.3. The values of the connection stiffness should be interpreted as the long-term slip modulus.

Table 7.3: Properties for analysis of concrete shrinkage with varying connection stiffness.

Property:	Connection stiffness [kN/mm]	Span length [m]
Value:	1, 4, 10, 25, 75, 200	6

In Figure 7.2, the connection stiffness is shown to have a large impact on the structural response to the concrete shrinkage. In the graph, the percentages presented on the y-axis is calculated according to Equation 7.1, and thus represent the relative deflection increase when comparing *no* and *normal* shrinkage. The largest deflection increase due to the shrinkage occurs for high-stiffness connectors whilst it has a small influence for low stiffnesses. The deflection increases more than 50 % for the stiffest connections in the performed analysis.

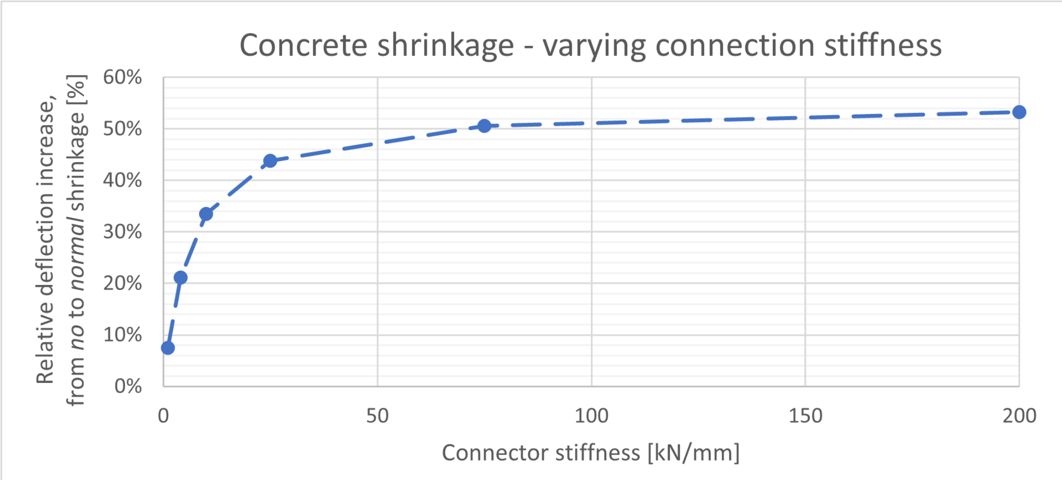

Figure 7.2: Relative deflection increase from *no* to *normal* concrete shrinkage, with varying connection stiffness.

The captured behaviour in the model correlates well to the theory for the composite action, presented in Section 4.1. When no interaction between the timber and concrete is applied, the concrete is allowed to shrink freely (when disregarding the minimum reinforcement) and the timber is unaffected. Since no stress redistribution occurs and the effective stiffness of the cross-section remains constant, the deflection is unchanged. For the opposite case, with full interaction, the concrete shrinkage results in a redistribution of forces within the cross-section. Since the shrinkage force is applied above the neutral axis of the section, the additional bending moment will cause the deflections to increase.

7.1.2 Stiffness and span length

To further investigate the parameters that influence the concrete shrinkage, an analysis of the connection stiffness for different span lengths are performed. Since the connector stiffness had a clear influence of the results, the analysis was run for four different connection slip modulus, in order to capture any potential discrepancy in results. The full properties are presented in Table 7.4.

Table 7.4: Properties for analysis of concrete shrinkage with varying connection stiffness and span length.

Property:	Connection stiffness [kN/mm]	Span length [m]
Value:	2.5, 7.5, 15, 25	2, 3, 4, 5, 6, 7, 8, 9, 10

The stiffness magnitudes were chosen to simulate the influence of long-term creep, where the stiffness is markedly reduced. Therefore, the lowest stiffness of 2.5 kN/mm corresponds to around 7-12 kN/mm in the initial case, depending on assumed service class and whether the creep reduction factor, k_{def} is doubled or not, as discussed in Section 5.1.4. That stiffness corresponds to that of a simply installed dowel type connection. The highest modelled stiffness, which is 10 times higher at 25 kN/mm, therefore corresponds to an initial stiffness of 70-120 kN/mm, which can be achieved with for example notched connections. Even higher stiffnesses than that can be achieved when using adhesive connectors or even stiffer notches, but the chosen stiffnesses are deemed sufficient to investigate the structural behaviour.

The result presented in Figure 7.3 shows the absolute increase in deflection in regard to the deflection limit for each span, which was set to L/300. The formula used is presented in Equation 7.2. Values calculated in this way is presented with dashed-dotted lines, "-.-.-". Note that in the previous graph, Figure 7.2, the relative deflection increase was presented, which is not calculated in the same way.

$$D_{limit} = \frac{upper - lower}{L/300} \tag{7.2}$$

The reason for using different formulas is that the span length has a major impact on the deflection caused by the bending strains. Thus, for longer span lengths, the relative deflection increase caused by shrinkage is overshadowed by the increase in deflection due to the long span, with a large bending strain. This also proves that the beam is under-designed for the longer span widths. For the set cross-sectional dimensions, a span length of around 6 meters is most realistic.

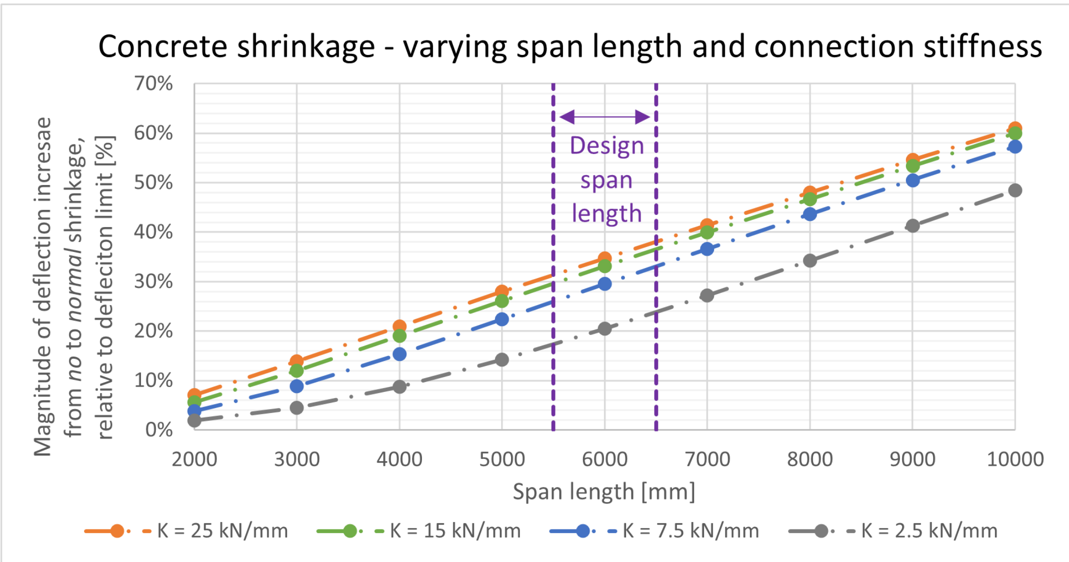

Figure 7.3: Magnitude of deflection increase from *no* to *normal* concrete shrinkage, relative to deflection limit.

In the graphs, a close to linear dependency on the span length is shown and similar behaviour is seen for all connection stiffnesses. As concluded previously, shrinkage increases the deflection the most for stiff connections. A conclusion from the linear behaviour is that the shrinkage strain is independent from the bending strain, which match the studied theory. At a span length of 6 meters, which is the span that the geometry is best suited for, the deflection caused by concrete shrinkage is 34 % of the maximum allowed deflection (L/300) for the stiffest connection. The corresponding value for the least stiff connection is 20 %. Thus, the concrete shrinkage seems to have a clear impact on the deflections.

7.1.3 Concrete shrinkage conclusions

Shrinkage of concrete is shown to potentially have a large influence on the long-term deflection of the TCC beam. The connection stiffness is a decisive parameter for how large impact the shrinkage strain has, since the interaction degree determine how much the concrete is allowed to shrink. Higher stiffness of the connection causes larger deflection increase when the concrete shrinks. However, that does not mean that the final deflections are larger when having stiff connectors, since the initial deflection is much smaller in that case. The absolute increase in deflection caused by the shrinkage was seen to vary linearly with the span length, when the geometry of the cross-section was constant.

In order to properly evaluate the long-term deflection, the magnitude of the shrinkage should be considered and neglecting the concrete shrinkage, as the γ-method suggest, could potentially cause significantly under-dimensioned TCC elements. Using low shrinkage concrete or letting the concrete shrink for some time before connecting it to the timber is two ways of reducing the deflection impact of the concrete shrinkage. The latter is only possible if prefabricated concrete slabs are used.

7.2 Timber shrinkage

In addition to the concrete shrinkage study, the effect of timber shrinkage is investigated. As explained in Section 4.1.1, a change in timber moisture content results in dimensional changes. Increase in moisture content causes swelling while a reduction makes the timber shrink. The most probable situation is that the timber is delivered with a moisture content equal to or higher than the equilibrium. Therefore, the timber is not likely to swell when looking at a long-term perspective. Contrariwise, if the timber shrinks, the reaction will be opposite that of concrete shrinkage, since the timber shrinkage acts to bend the TCC element upwards, see Figure 4.2.

Since the impact of the connection stiffness and span length has already been investigated for the concrete shrinkage, the same analysis parameters will not be investigated again. That behaviour is assumed to be similar but with opposite effect, following the load-independent strain theory. Instead, the correlation between concrete and timber shrinkage is presented.

The longitudinal expansion coefficient is 0.0001 for each percent change in timber moisture content. Therefore, at 4 % reduction in moisture content, the timber shrinkage is equal to the set *normal* value of the concrete shrinkage. The analysis is run for moisture content reductions up to 8 % since initial moisture contents that cause changes higher than that is unlikely to be installed. The properties in the analysis shown is presented in Table 7.5.

Table 7.5: Properties for analysis of concrete- and timber shrinkage.

Property:	Connection stiffness [kN/mm]	Span length [m]	Moisture content reduction [%]
Value:	7.5	6	0, 2, 4, 6, 8

The first notable result is that the magnitude of the deflection increase from *no* to *normal* concrete shrinkage is the same for all timber moisture contents, which can be seen by the constant inclination of the graphs in Figure 7.4. Another conclusion based on the results is that the timber shrinkage also has a proportional influence on the result, since the distance between each graph is constant for the equally increased timber moisture content reductions.

A third interesting note is that the deflection for no concrete nor timber shrinkage (0 % moisture content reduction) is the same, 20 mm, as for *normal* concrete shrinkage and a moisture content reduction of 4 %. The result then proves that a 4 % reduction in timber moisture content is equal to the set *normal* concrete shrinkage, which means that the strains counteract each other.

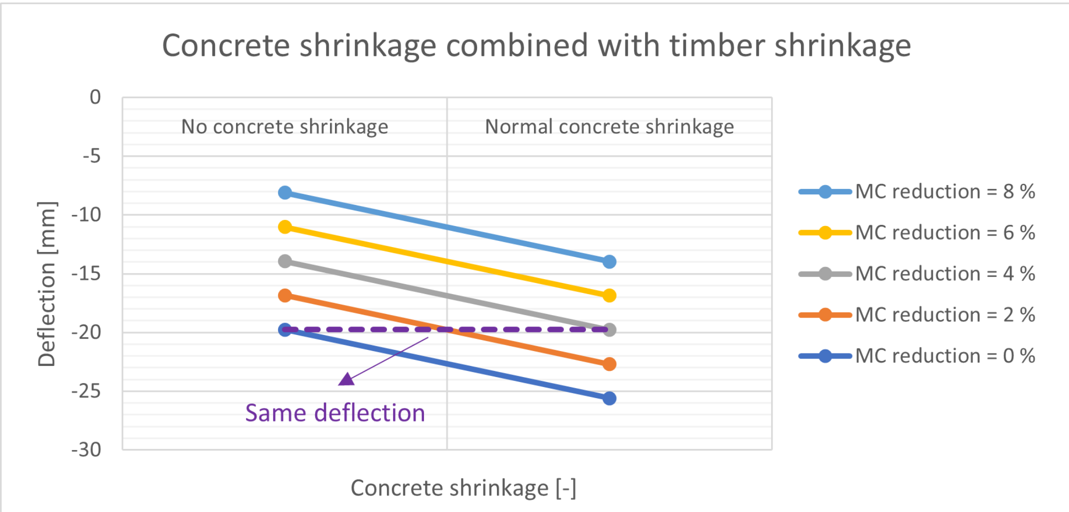

Figure 7.4: Deflections with varying timber and concrete shrinkage.

7.2.1 Timber shrinkage conclusions

The timber shrinkage has an opposite effect on the TCC structure than the concrete shrinkage, since it reduces the deflections. A *normal* concrete shrinkage corresponds to a timber shrinkage strain caused by around 4 % moisture content reduction, and for such a case the deflection effects cancel out each other. Since the concrete shrinkage was shown to potentially have a large influence on the deflection, the same behaviour holds true for the timber shrinkage, but instead it reduces the deflection.

In production, it is common that the timber is delivered with a moisture content higher than the equilibrium condition. Generally, the hope is to minimize this difference since the moisture that is within the timber then is built into the structure. Having moisture in the structure could potentially cause degradation problems such as mould or corrosion. Although the drawbacks of built-in moisture still holds for TCC elements, significant gains in relation to the structural performance can be achieved by the timber shrinkage that occurs in the long-term. If the timber shrinkage is of a similar magnitude as the concrete shrinkage, the effect of both in terms of deformations may be neglected, which allows for a simpler structural analysis, for example using the γ-method. However, if the value of the timber moisture content at assembly is unknown it would be suitable to neglect its effect on the timber shrinkage, since overestimations of the timber shrinkage makes the deflection design un-conservative.

7.3 Timber and connection creep

In the analysis of the timber and connection creep, the deflection difference between service class 2 and 3 is investigated. Studies have shown that even for TCC elements in service class 2 according to the Eurocode 5, SS-EN 1995-1-1:2004 (2009), definition, a creep reduction factor, k_{def}, equivalent to service class 3 may be more appropriate (Ceccotti et al., 2006; Lukaszewska, 2009). In addition, there might be design situations for which the service class is hard to determine. Therefore, it is of interest to analyse the influence in deflection of choosing either service class 2 or 3. The study will be performed similarly to the shrinkage analysis and the deflection in service class 2 corresponds to the lower- and service class 3 to the upper value.

The creep is considered by reducing the stiffness according to Section 5.1.4. Values for the creep formula is presented in Table 7.6 (note that the value for the connection is double the k_{def}).

Table 7.6: Creep reduction factors for timber and connection.

	Timber	Connection
Service class 2	0.8	1.6
Service class 3	2	4

7.3.1 Connection stiffness

First, the influence of the connection stiffness is investigated. The stiffness of the connectors are presented with their un-reduced values, K_{ser}, and is chosen in order to correlate to different connector types. It is important to note that the presented connection stiffness is not the direct values used in the analysis, since they are before application divided by $(1 + 2 \cdot k_{def})$. The lowest stiffness, 7.5 kN/mm corresponds to a simple screw connection whilst the higher values of 20 and 45 is more advanced dowel type of connectors, for example with inclined screw pairs or small notches. A stiffness of 100 kN/mm could be achieved with more robust notches. The properties are presented in Table 7.7.

Table 7.7: Properties for analysis of timber and connection creep with varying connection stiffness.

Property:	Connection stiffness [kN/mm]	Span length [m]	Concrete creep factor [-]
Value:	7.5, 20, 45, 100	6	1.5

In the results, the relative deflection increase for service class 3 compared to service class 2 is about 55-59 % for the studied set-up, see Figure 7.5. No distinctive trend in behaviour between the different connector stiffnesses can be distinguished. The relatively large increase in deflection is explained by the fact that the service class affect both the timber properties and the connection stiffness. Especially the latter is influenced by the difference since for service class 2, the slip modulus is divided by 2.6 whilst it for service class 3 is divided by 5, which results in almost half the stiffness of the previous service class.

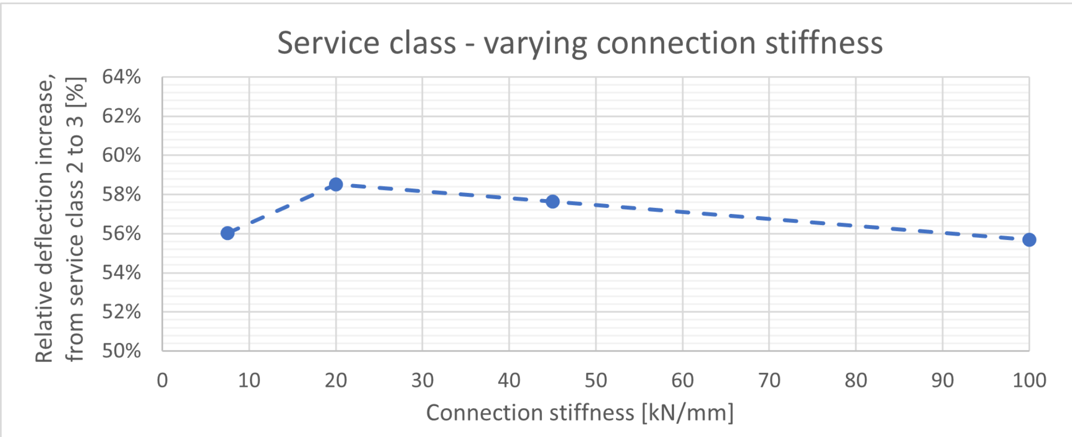

Figure 7.5: Relative deflection increase from service class 2 to 3, with varying connection stiffness.

7.3.2 Concrete creep factor and span length

The second analysis for the influence of the service class is made with varying span length and concrete creep. They are combined to show a more comprehensive behaviour while still being displayed in a single graph. The connection stiffness is set as constant. Input data can be found in Table 7.8.

Table 7.8: Properties for analysis of timber and connection creep with varying concrete creep and span length.

Property:	Connection stiffness [kN/mm]	Span length [m]	Concrete creep factor [-]
Value:	7.5	2, 4, 6, 8, 10	1.5, 2.5

Figure 7.6 shows that there is a small difference in result between the different creep factors. The graphs shows that a lower concrete creep decreases the relative deflection increase between service class 2 and 3 with about 2-4 % points. An explanation might be that for a smaller concrete creep, the concrete is stiffer and therefore more capable of counteracting the timber and connector stiffness reduction. For the span length, no clear behavioural dependency can be distinguished, although the relative deflection increase for spans above 4 meters is increasing slightly.

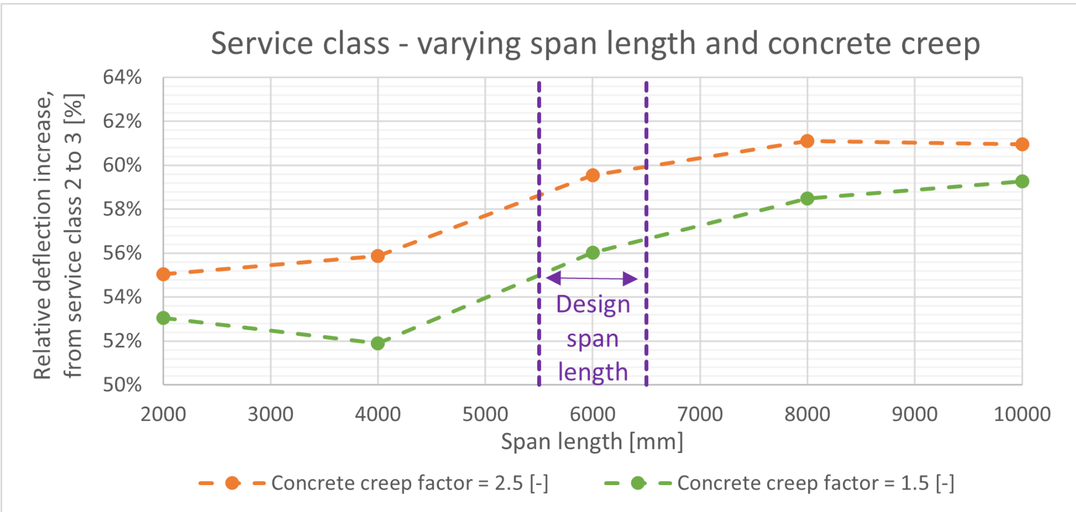

Figure 7.6: Relative deflection increase from service class 2 to 3, with varying concrete creep factor and span length.

Although the relative deflection increase is similar for all span length, the absolute value increases faster than linearly, which can be seen in Figure 7.7. That is different than the shrinkage behaviour, which had a linear deflection increase. This is explained by the fact that shrinkage is a stress-independent strain whilst the creep is affected by the bending stresses. Since longer span lengths result in higher bending stresses, the deflection caused by creep increases faster than linearly. For a span of 6 meters, which suits the geometry of the cross-section the best, the difference between service class 2 and 3 corresponds to around 60 % of the allowed deflection.

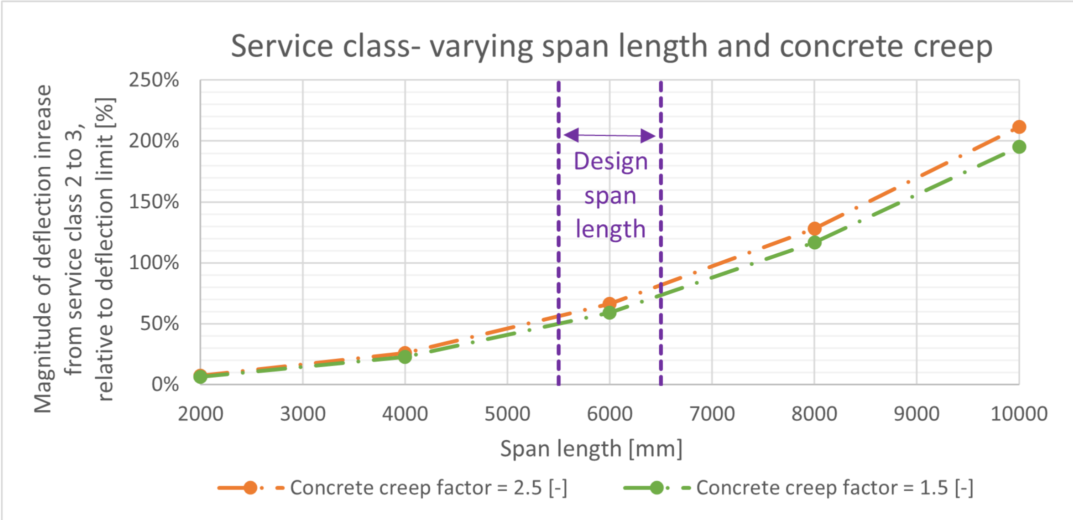

Figure 7.7: Magnitude of deflection increase from service class 2 to 3, relative to deflection limit.

7.3.3 Timber and connection creep conclusions

The relative deflection difference between service class 2 and 3 is around 50-60 % for the used geometry and material properties. The connection stiffness did not have a clear impact on those values. Changing the concrete creep and span length affected the relative deflection increase slightly, but not in a substantial manner. The magnitude of deflection increase caused by changing from service class 2 to 3 is around 60 % of the deflection limit (L/300).

The assumed service class is shown to have a large influence on the deflection and should therefore be carefully considered in design. Previous research studies have concluded that the creep reduction factor applied by following the Eurocode 5 definition underestimate the long-term deflections. Additionally, some studies have shown that assuming values for service class 3 match the experimental data better, even though the climate corresponds to the Eurocode 5 definition of service class 2. Therefore, a conservative design approach might do best in considering service class 3 in order to not get significantly larger deflections than calculated for.

7.4 Concrete creep

To evaluate the influence of the concrete creep, the behaviour of a concrete creep factor of 1.5 and 2.5 is compared. The two creep factors are treated as a lower and upper value, respectively. A creep factor smaller than 1.5 is seldom conveniently achieved while values larger than 2.5 is assumed to be avoided in design due to the large time-dependent deformations.

In production, a low creep factor can be achieved by increasing the time before loading of the concrete, for example by prefabricating. For cast on-site concrete, the time with props needs to be increased to reduce the creep factor. Further parameters that affect the concrete creep is the strength class and the relative humidity. The approach to calculate the creep factor used in Eurocode 5, SS-EN 1992-1-1:2005 (2008), is presented in Appendix A. The analysis follows the same procedure as the investigation of timber creep in relation to the service classes.

7.4.1 Connection stiffness

First, the influence of the connection stiffness is analysed. As for the service class investigation, four different connector stiffnesses are compared, 7.5, 20, 45 and 100 kN/mm. The analysis is made with timber and connection properties corresponding to service class 3 and the properties are presented in Table 7.9.

Table 7.9: Properties for analysis of concrete creep with varying connection stiffness.

Property:	Connection stiffness [kN/mm]	Span length [m]	Service class [-]
Value:	7.5, 20, 45, 100	6	3

As for the service class, the connection stiffness has a relatively small impact on the relative deflection increase, as can be seen in Figure 7.8. For lower stiffness, the relative difference in deflection is around 8 %, under the current configuration, while it for the higher connection stiffnesses reduces to a value of 6 %. The trend can be explained as if the concrete stiffness has a larger influence for less stiff connections. This behaviour might then be correlated to the interaction between the materials and for higher stiffnesses, the relative timber contribution increases and thus the deflection decrease.

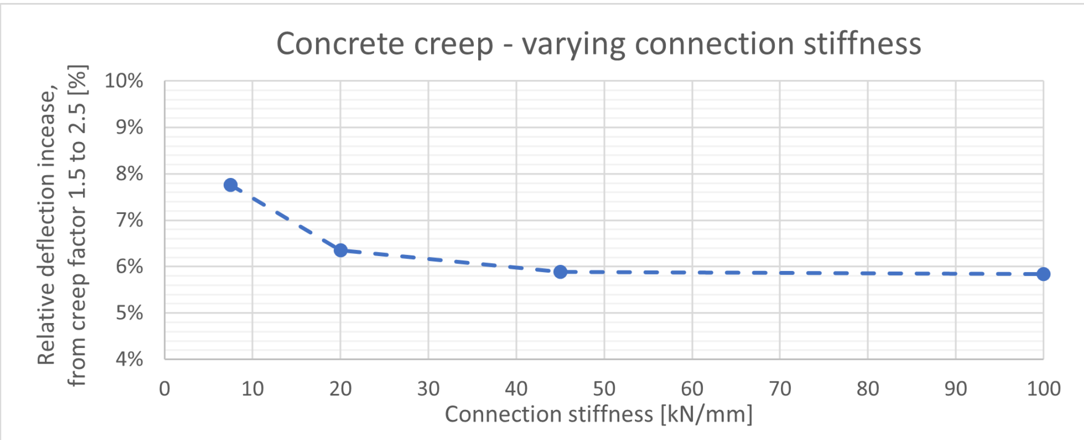

Figure 7.8: Relative deflection increase from concrete creep factor 1.5 to 2.5, with varying connection stiffness.

7.4.2 Service class and span length

The influence of the service class and span length is investigated in the second analysis, which is run for timber and connection stiffnesses corresponding to both service class 2 and 3, see properties in Table 7.10.

Table 7.10: Properties for analysis of concrete creep with varying timber and connection creep and span length.

Property:	Connection stiffness [kN/mm]	Span length [m]	Service class [-]
Value:	7.5	2, 4, 6, 8, 10	2, 3

Figure 7.9 shows that the behaviour in relation to the length is similar for the two service classes, with a peak at 4 meters and then a steady decrease in influence. However, the relative difference is only around 1-2 %-points and thus the result is not distinctively influenced by the span length. Further, the relative increase in deflection is also affected by 1-3 %-points depending on the service class of the timber. The difference is likely connected to the overall stiffness reduction of service class 3, and that the timber and connection is not as effective in counteracting the concrete creep. A correlative behaviour to what was seen in the inverse analysis in Figure 7.6.

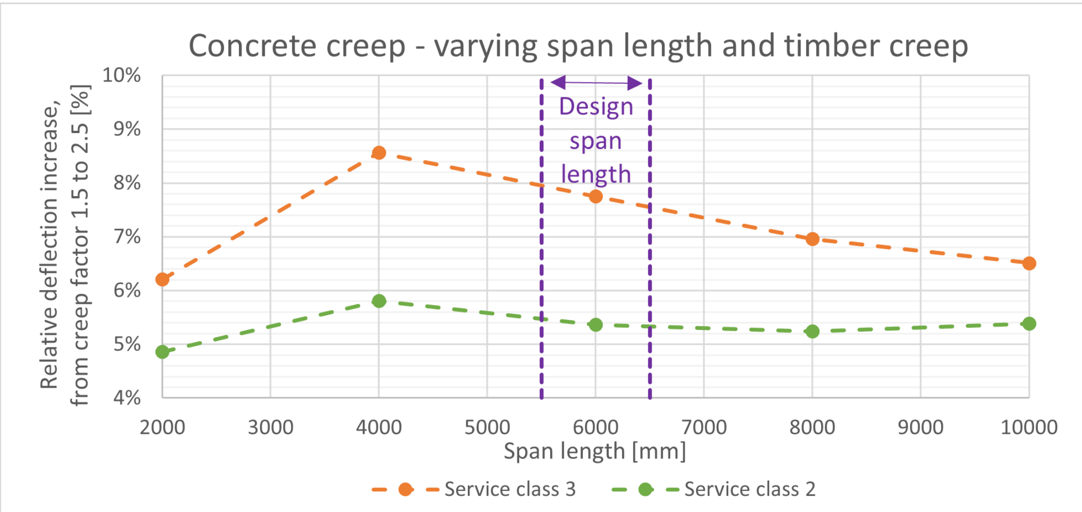

Figure 7.9: Relative deflection increase from concrete creep factor 1.5 to 2.5, with varying service class and span length.

In Figure 7.10 the deflection increase in relation to the span length requirement is plotted. The behaviour is similar to that of the timber creep, with a non-linear increase for longer span widths. The difference between using service class 2 and 3 for the timber is significant since the stiffness properties of the timber and connection have been found to be distinctive. Since the TCC element has an overall lower stiffness when service class 3 is applied, the structure is more sensitive to additional stiffness reductions caused by the concrete creep. For the reasonable span length of 6 meters, the additional deflection when having a creep factor of 2.5 instead of 1.5 is around 6 % and 13 % of the allowed deflection, for service class 2 and 3 respectively.

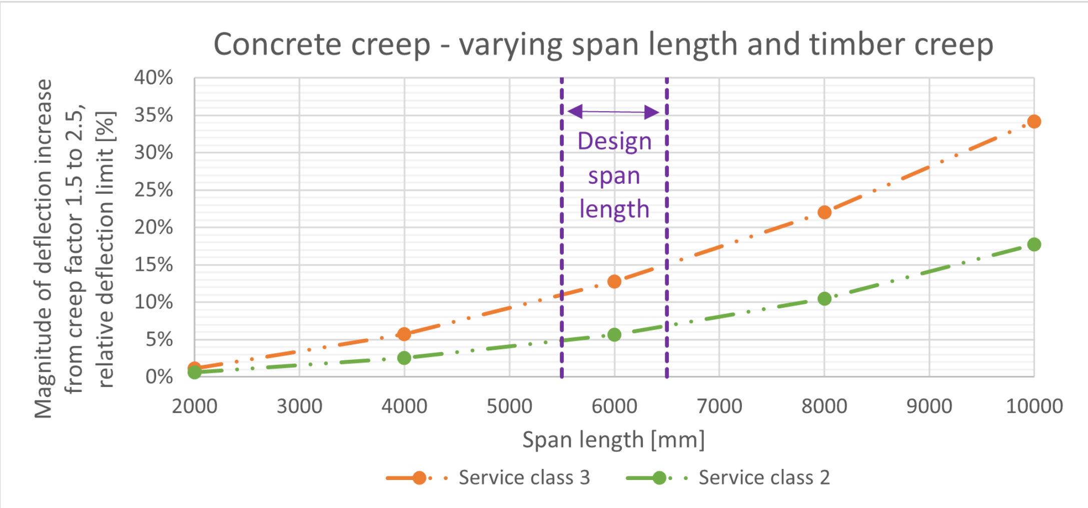

Figure 7.10: Magnitude of deflection increase from concrete creep factor 1.5 to 2.5, relative to deflection limit.

7.4.3 Concrete creep conclusions

The concrete creep factor is shown to influence the system with a deflection increase up to 9 % with the applied configuration, when changing the factor from 1.5 to 2.5. The connection stiffness, applied service class and span length affect the result slightly, around 1-3 %-points. Generally, lower stiffness of the timber and/or connectors increase the relative deflection difference for a higher concrete creep factor. When comparing the deflection difference between a creep factor of 1.5 and 2.5, it corresponded to up to 13 % of the total allowed deflection, which is significantly lower than the difference between service class 2 and 3 for the timber and connection, in the previous analysis.

Since values lower than 1.5 is inconvenient to achieve in practise, mainly due to long curing times before loading, the results show that the concrete creep factor does not have a major impact if it is in the range of common values. Therefore, increasing the time before loading the concrete to reduce the concrete creep factor is a way to decrease the deflections of a TCC element, but it does not affect the result majorly for geometries similar to the one in this study.

7.5 Design optimization with concrete shrinkage

The first part of the parametric study investigated how shrinkage and creep affect the long-term performance of a TCC beam in a general sense. It was concluded that the concrete shrinkage could potentially have a large impact on the deflections, despite it being neglected in the proposed Eurocode 5 design rules. The concrete shrinkage will therefore be more thoroughly analysed for different cross-sectional designs in this, second part of the parametric study. Similar investigations could be performed for the other long-term phenomena as well, but the creep influence is deemed harder to adjust in design and therefore no further studies of its impact is performed.

The impact of concrete shrinkage can be greatly reduced by letting the concrete slab shrink freely before connecting it to the timber beams. Consequently, the method is only applicable when prefabricated elements is used. For the chosen concrete slab dimensions used in the two parts of the parametric study, and with standard indoor environment, approximately 30-40 days are needed for the concrete to shrink 50 % of its total shrinkage strain. To make the deepened analysis more realistic to apply in design, “no” shrinkage is replaced by “small” shrinkage, where 50 % of the ”normal” shrinkage strain is applied. The second part of the parametric study is therefore performed for concrete strains of -0.0004 (*normal*) and -0.0002 (*small*).

In the first part of the parametric study, the same cross-section was used for all analysis. Contrariwise, in the second part the geometrical design is iteratively modified to match the deflection limit and thus the cross-section is optimized for each analysis. The deflection limit is set to L/300 and the analysis will be made for a 5 m span, which gives a maximum deflection of 16.67 mm. Thus, the geometry of the cross-section will be adopted to be as close to the deflection limit as possible, rendering more comparable design results. The span length is chosen based on an average beam length used in the investigated experimental setups. Since the long-term behaviour is of interest, the quasi-permanent load case is considered.

Considering the creep, a factor of 2.5 is used for the concrete and service class 3 for the timber and connection, the corresponding material properties can be found in Table 7.11 and 7.12. The properties of the timber is updated from the first part of the parametric study to reassemble the properties of a LVL beam. As in the previous part of the parametric study, the behaviour for different connection stiffnesses will be investigated. The material usage in the different cross-sections can then be compared to study how a TCC element can be designed most efficiently.

Table 7.11: Concrete properties in the second part of the parametric study.

MoE, E, [MPa]	Poisson's ratio, ν [-]	Density, ρ [kg/m^3]
9428	0.2	2450

Table 7.12: Timber properties used in the second part of the parametric study.

E_1, [MPa]	E_2, [MPa]	E_3, [MPa]	G_{12}=G_{13}, [MPa]	G_{23}, [MPa]	Poisson's ratio, ν [-]	Density, ρ [kg/m^3]
4600	143	43	200	1	0	450

Table 7.13 and 7.14 shows which dimensions that was set to change in each of the performed design alternatives. The different dimensions are illustrated in Figure 7.11. In order to study the effect of each geometrical change, only one dimension was changed at a time and the results are presented and discussed accordingly. As can be noted from the two tables, a different amount of analysis is made for each geometrical property. This is connected to the performance of the alteration and is further discussed in the coming sections. Note that the width of the concrete slab is equal to the distance between the timber beams and thus, changing its width affects the cc-distance between the girders. The detailed result of each design alternative is presented in Appendix C.

Table 7.13: Geometric properties in the second part of the parametric study, Design 1-4.

Design:	1	2	3	4
Timber width, w_t	*Varied*	*Varied*	*Varied*	*Varied*
Timber height, h_t	270 mm	225 mm	270 mm	225 mm
Concrete thickness, h_c	80 mm	80 mm	80 mm	80 mm
Concrete width/c-c, w_c	700 mm	700 mm	500 mm	500 mm

Table 7.14: Geometric properties in the second part of the parametric study, Design 5-9.

Design:	5	6	7	8	9
Timber width, w_t	70 mm	70 mm	70 mm	70 mm	70 mm
Timber height, h_t	*Varied*	*Varied*	225 mm	270 mm	225 mm
Concrete thickness, h_c	80 mm	80 mm	*Varied*	80 mm	80 mm
Concrete width/c-c, w_c	700 mm	500 mm	700 mm	*Varied*	*Varied*

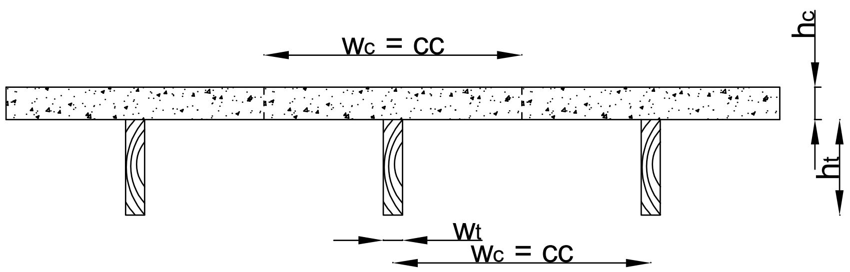

Figure 7.11: Illustration of dimension-notations.

7.5.1 Timber width variation

Changing the timber width is deemed as the simplest solution for optimization since the cross-sectional height, which is often limited, is not affected. Neither is the cc-distance between the beams. However, for the moment of inertia, an increased thickness is not as effective as increasing the height of the element. Four analyses were made changing the width of the timber beam, see Design 1-4 in Table 7.13. The result for two different heights, 270 and 225 mm, as well as cc-distances, 700 and 500 mm, were studied. The required width to fulfil the deflection limit for the four analysis are presented in Figure 7.12 and 7.13.

Figure 7.12: Required timber width for Design 1 and 2.

Figure 7.13: Required timber width for Design 3 and 4.

All tested geometries display a similar behaviour and unsurprisingly, the widest beam is required for the lowest beam with largest cc-distance, Design 2. It can be noted that the shape of the graphs for a spacing of 700 mm is very similar to the corresponding result for a spacing of 500 mm. However, the longer spacing requires around 45-60 % wider beams when comparing the 270 mm (Design 1 and 3) and 225 mm (Design 2 and 4) high beams respectively.

From the graphs, it can also be concluded that the lower beams, Design 2 and 4, are more affected by the concrete shrinkage since the width is reduced up to 29 % when changing from *normal* to *small* shrinkage. For the higher beam in Design 1 and 3, the difference is instead up to 22 %. However, the difference is not that large for all connection stiffnesses. The largest difference occurs for medium-stiff connections at 20-40 kN/mm, whilst the impact for low-stiffness connectors, 5-10 kN/mm are not as significant. Based on the result in the first part of the parametric study, it is expected that the shrinkage has a larger impact for stiffer connections.

To study which of the solutions that are the most material-efficient, the area of each designed timber beam is calculated. To be able to compare the different cc-distances, the area is divided by the spacing to get a value corresponding to the area required per width of the finished floor. Unsurprisingly, the design with higher beams requires less material, since increasing the height is the most efficient way to increase the stiffness of the beam. The required timber area for each design is presented in Figure 7.14, note that only the case for *normal* shrinkage is plotted.

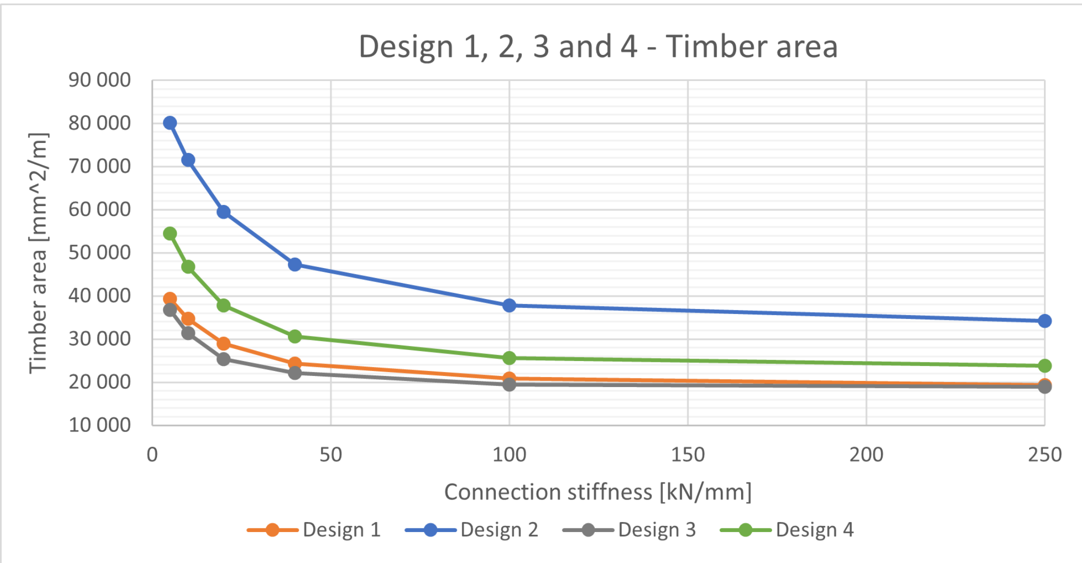

Figure 7.14: Required timber area for Design 1, 2, 3 and 4, with *normal* concrete shrinkage.

For the beams with a spacing of 700 mm, Design 1 and 2, the required area for the less stiff connectors is doubled when decreasing the timber height from 270 mm to 225 mm. With stiffer connections the difference gets smaller and the increase is about 65 % for the stiffest connection. The difference is not as drastic for the beams with a spacing of 500 mm, where the area increase varies from 50 % for the weakest connections to 20 % for the stiffest.

If the result is instead compared between the different cc-distances, it is noted that the smaller spacing (Design 3 and 4) requires less area than their corresponding 700 mm-spaced beams (Design 1 and 2). For the 225 mm high timber beam, Design 2 and 4, the area increase for the longer spacing is about 30-35 %. For the 270 mm high beam, Design 1 and 3, the difference is only about 5-10 %. Unlike for the varied timber heights, the connection stiffness does not have a significant correlation to the required area between the different spacings.

When comparing all four solutions, the most material-effective is the high beam (270 mm) with small spacing (500 mm), Design 3. However, the difference between that one and the corresponding beam with 700 mm spacing, Design 1, is not very large. Decreasing the timber height increases the total material usage since the reduction in height needs to be compensated by an increased width, which is not as efficient in terms of stiffness. The design that requires the most material is the 225 mm high beam with a spacing of 700 mm, Design 2, which for the least stiff connections use more than double the timber compared to the most efficient design.

7.5.2 Timber height variation

The height of an element has a larger influence on its moment of inertia than the width. Increasing the timber height should therefore be more material efficient than increasing the width, given that no stability issues or other problems arise. However, the total cross-sectional height available is often limited in design. In Design 5 and 6, see Table 7.14, the cross-sectional height of the timber was varied for two different beam spacings. The width was set to 70mm since this was concluded as an approximate average value in the timber width variation analysis. Figure 7.15 shows the required height for Design 5 and 6, with a respective spacing of 700 and 500 mm.

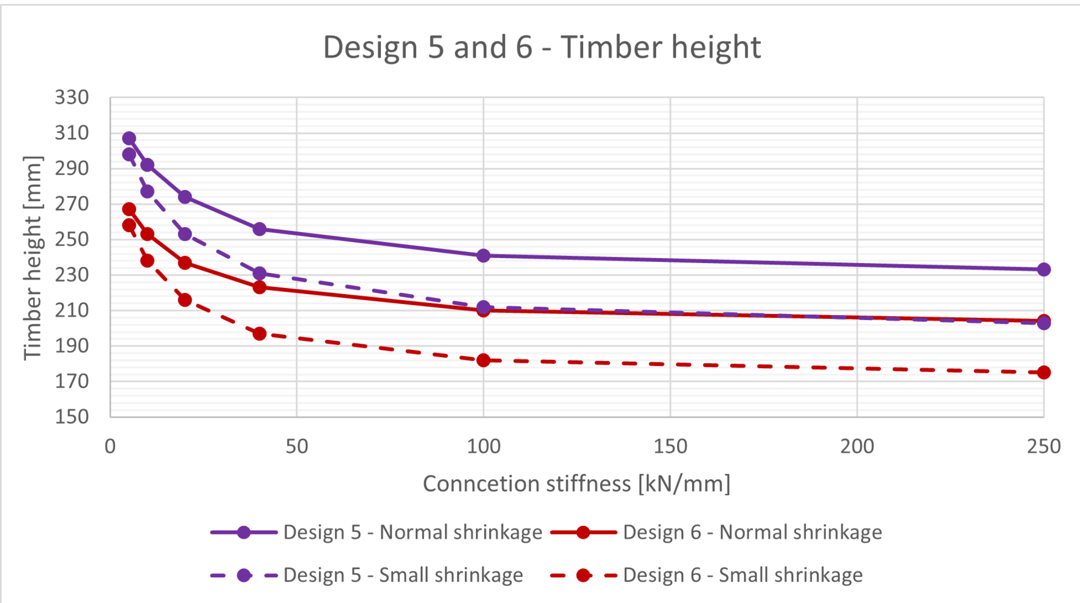

Figure 7.15: Required timber height for Design 5 and 6.

Unlike when varying the width, the difference between *normal* and *small* shrinkage gets continuously larger for each increase in stiffness, and has the largest influence for the stiffest connection. The possible reduction in height when using *small* shrinkage compared to *normal* shrinkage is then around 13 %. Overall, the shrinkage has a smaller impact in these designs compared to when the timber width is varied. Additionally, it is noted that the required height does not vary as drastically with the connection stiffness as in the analysis with varying timber width.

Figure 7.16 shows the required area per meter beam for the two different spacings, along with the result from the beam width variation analysis. In the graph it can be seen that the most material-efficient solution is found for the larger cc-distance (700 mm), Design 5, which requires around 18 % less material than the spacing of 500 mm, Design 6.

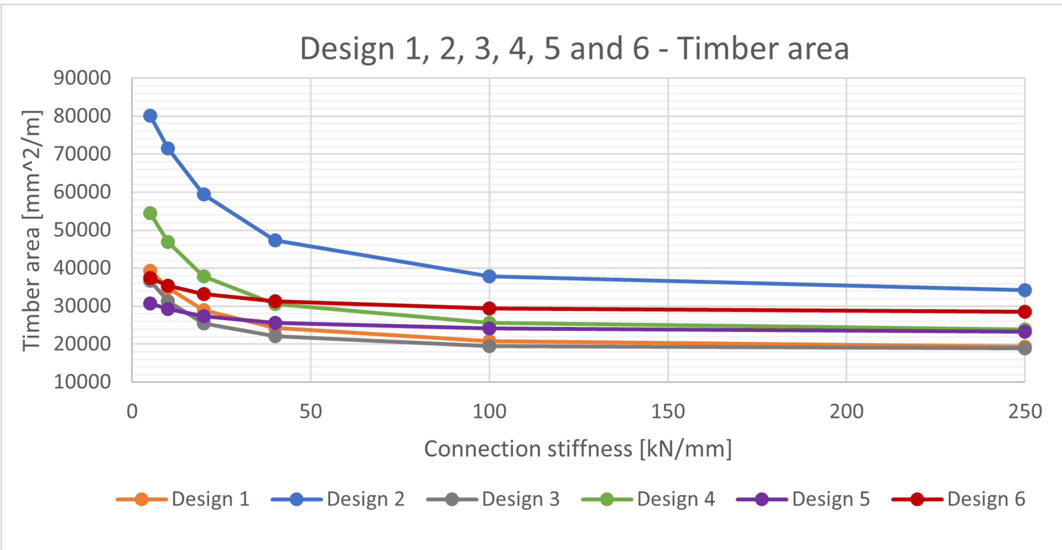

Figure 7.16: Required timber area for Design 1, 2, 3, 4, 5 and 6, with *normal* concrete shrinkage

A comparison between the most efficient solution for the analysis with varying width, Design 3, and this analysis, Design 5, is made. For the lowest connection stiffness, the total required area is around 16 % smaller in the latter (36 700 mm^2/m versus 30 700 mm^2/m). However, for the stiffer connections, the new design instead use 23 % more timber (18 900 mm^2/m verus 23 300 mm^2/m). The variation is explained by the fact that increasing the height is the most material-efficient design solution. For the weakest connections, the required timber height for Design 5 is 307 mm and for the strongest connections down to 233 mm, displayed in Figure 7.15. Thus, the switch in material efficiency between the two solutions occur at a timber height of 270 mm, which was used in Design 3.

7.5.3 Concrete thickness variation

In Design 7, the cross-section is optimized by changing the concrete thickness, see geometrical properties in Table 7.14. However, it was quickly concluded that increasing the concrete thickness had a relatively small impact on the long-term deflections and it was hard to find designs which fulfilled the deflection criterion. Since the concrete thickness has a large impact on the moment of inertia of the concrete slab, the conclusion may be surprising. However, the reason for this behaviour is due to the fact that in the quasi-permanent load case, the self-weight of the TCC element is the dominant load and thus, an increase in concrete thickness also increase the design load notably.

Changing the concrete thickness is the only geometrical variation that affect the concrete volume and thus the shrinkage impact is substantial. Figure 7.17 shows the result from the two investigated cases, with *normal* and *small* shrinkage. As was seen in the first part of the parametric study, stiffer connections increase the influence of the shrinkage, and that behaviour is clearly seen in this analysis as well. Additionally, it was found that for very thin concrete layers (smaller than around 60 mm), the loss in stiffness when reducing the concrete thickness was overshadowed by the gain in terms of the reduced self-weight. Thus, thinner concrete layers reduce the deflection. Since too thin concrete layers are not feasible to use in design, the conclusion does not have a practical impact, but it explains why the required thickness for the stiffest connections with *small* shrinkage quickly drops to zero.

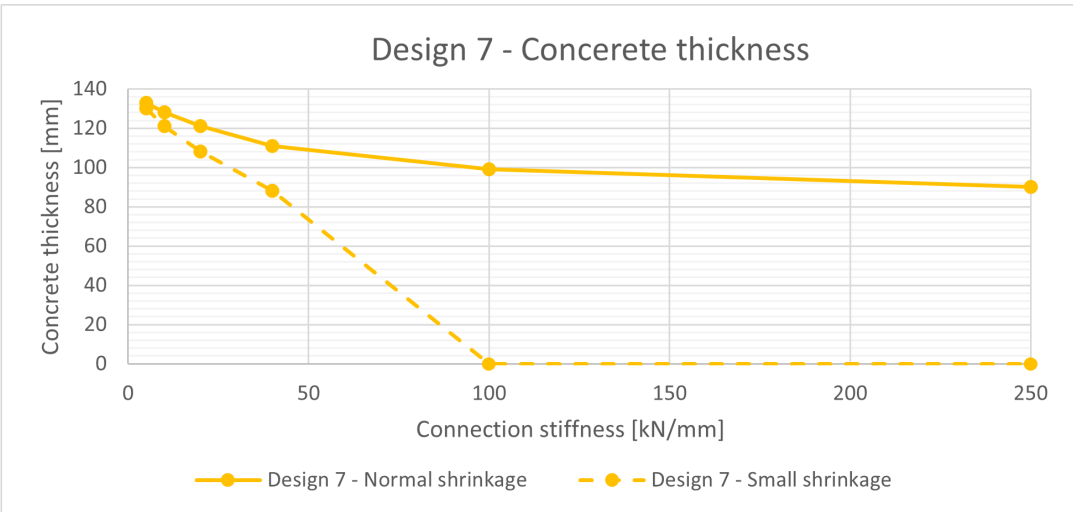

Figure 7.17: Required concrete thickness for Design 7.

For the case with *normal* shrinkage, the increase in required concrete area compared to a concrete thickness of 80 mm varies between 65-10 %, with the largest increase for the least stiff connections. However, since this solution requires less timber, the increased concrete volume must be weighted towards the lower timber usage. Figure 7.18 puts the timber usage in Design 7 in relation to the previous designs.

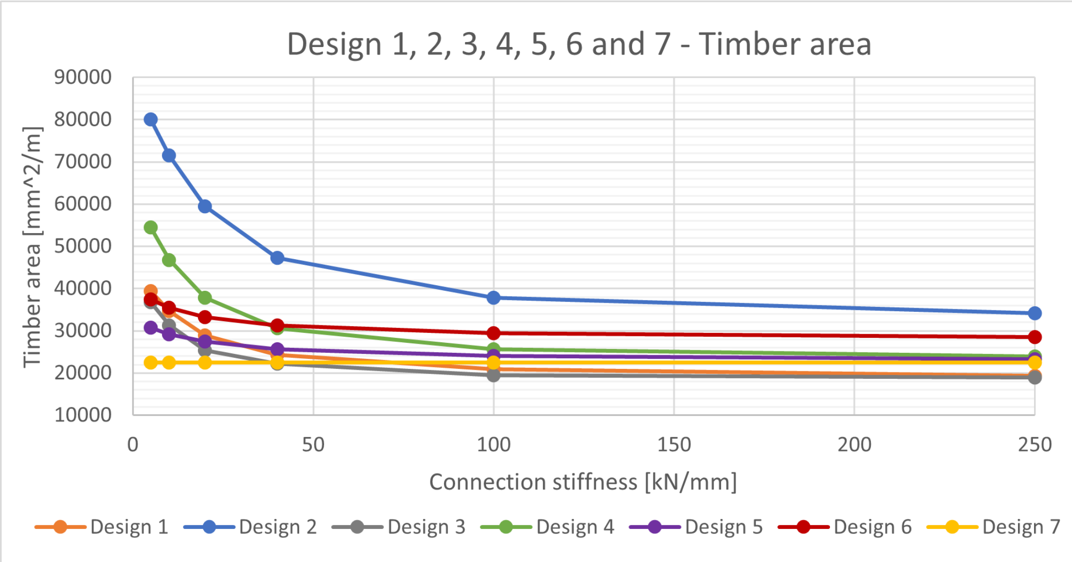

Figure 7.18: Required timber area for Design 1, 2, 3, 4, 5, 6 and 7, with *normal* concrete shrinkage

It is clear that no notable reductions in timber usage is achieved and for stiffnesses over 40 kN/mm, the new design is not even the most timber-efficient. Due to the various difficulties and the inefficient material-optimization, increasing the concrete thickness is not regarded as a generally preferred solution to decrease the long-term deflections of the cross-section.

7.5.4 Concrete width variation

The geometrical behaviour when changing the concrete width differs from when changing its thickness since the volume of concrete for the complete floor system is unaffected. However, the timber usage is reduced when increasing the concrete width. That is explained by the fact that the concrete layer will be continuous when placing several TCC elements next to each other. Therefore, increasing the concrete width also increases the spacing between the timber beams and thus reduces the volume of the timber, given that the timber cross-section is constant.

For the concrete slab, the moment of inertia is slightly increased when extending the concrete width, leading to a stiffer element. However, the increase in both self-weight of the concrete as well as the contributing area for the variable load override the increased stiffness substantially. As a result, the deflections of a TCC element becomes larger when increasing the width of the concrete slab. Design 8 and 9 investigate the behaviour for timber heights of 270 and 225 mm with varying concrete width, as presented in Table 7.14.

The resulting widths can be seen in Figure 7.19. As expected, the higher timber beam allows for wider concrete slabs due to its increase in stiffness. Like for the analysis with changing thickness of the concrete layer, an increased connection stiffness has a large influence on the shrinkage impact, which consequently increases. For the stiffest connections, the possible increase in width is 25 and 35 % for Design 8 and 9, respectively, when changing from *normal* to *small* shrinkage. The corresponding reduction in timber area is 20 and 25 %.

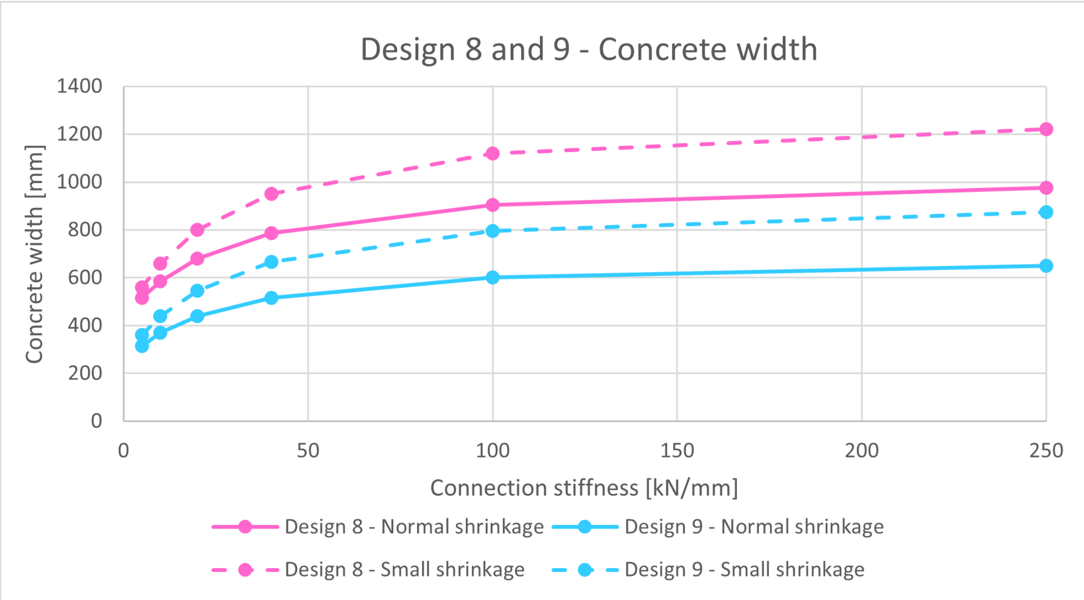

Figure 7.19: Required concrete width for Design 8 and 9.

The case with a higher timber beam, Design 8, is notably more material efficient, as is illustrated in Figure 7.20. Design 9 requires between 35-25 % more timber, with the largest increase being for low stiffness connectors. Compared to the best previous designs, Design 8 holds up well for all connection stiffness types.

Figure 7.20: Required timber area for Design 1, 2, 3, 4, 5, 6, 8 and 9, with *normal* concrete shrinkage

7.5.5 Design conclusions

In the second part of the parametric study, nine designs were investigated for different connection stiffnesses. Additionally, the impact of shrinkage was analysed for each design. Consistently throughout the analysis, the shrinkage was seen to have the largest influence in the design when using stiff connections. This is coincident with the result of the first part of the parametric study. However, the shrinkage impact seems to depend on the geometry and which parameters that were changed.

The largest impact of shrinkage was unsurprisingly found when changing the concrete thickness. A notable difference in dimensions was also noted for the designs with varying concrete width and timber width. In the former, the concrete width (spacing between the timber beams) could be increased up to 35 % when using *small* shrinkage whilst the possible decrease in timber width in the latter case was up towards 30 %. The geometrical property that showed the least influence of shrinkage was the timber height, for which the difference in dimensions was less than 15%. It can therefore be concluded that when the TCC height is restricted and the timber width or concrete width (cc-distance between the timber beams) needs to be varied, it is suitable to give extra attention to the concrete shrinkage effect.

Studying the required timber area for all of the designs, disregarding Design 7, the largest variations are found for low-stiffness connections. The most efficient one, Design 5, has a timber area of 30 700 mm^2/m whilst the least efficient solution, Design 2, has a corresponding area of 80 100 mm^2/m. The difference is reduced with increased stiffness and for the stiffest connections, the most efficient cross-section, Design 3, uses 18 900 mm^2/m compared to 34 200 mm^2/m for Design 2. Overall, Design 2 stands out in material consumption, indicating that a low timber beam with long spacing is not efficient.

The most material-efficient solution in each of the design steps, Design 3, 5 and 8, is presented in Figure 7.21. In addition to the previously presented values for *normal* shrinkage, the area corresponding to the design with *small* shrinkage is included as well. For low stiffnesses the material consumption is not majorly impacted by the shrinkage. However, with high stiffness-connectors, the timber area can be reduced by approximately 23 %, from 18 900 mm^2/m to 14 600 mm^2/m for Design 3. Corresponding reductions for Design 5 and 8 are 13 % and 20 %, respectively.

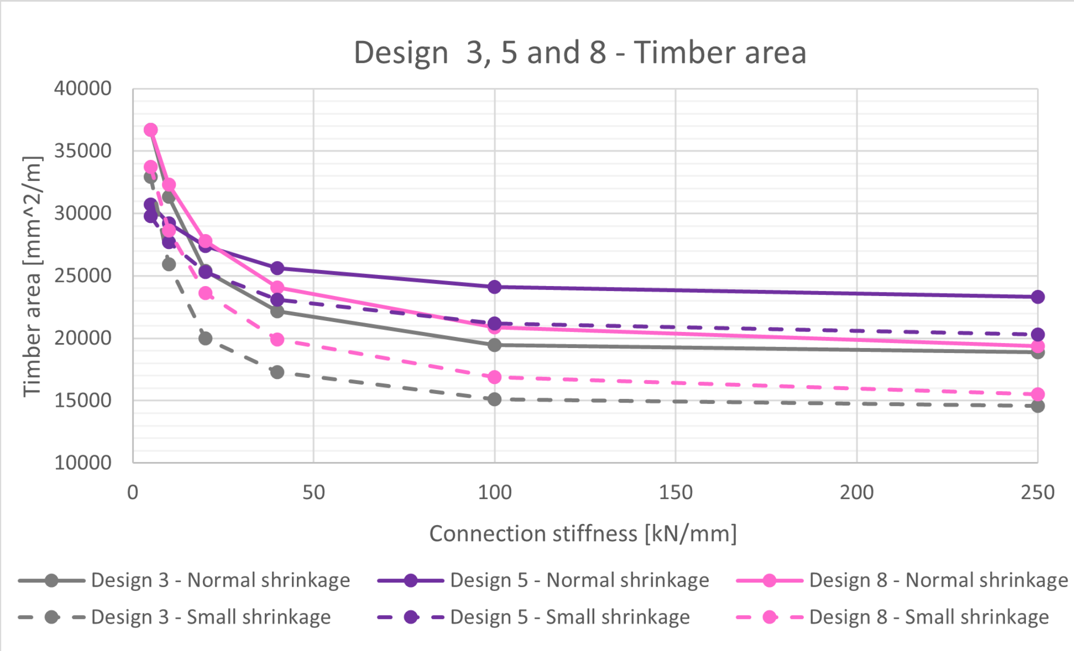

Figure 7.21: Required timber area for Design 3, 5 and 8

The most efficient cross-section property to vary based on the study is the timber height. The conclusion is motivated by the relatively small variation in timber height between the connection stiffnesses in Design 5 and 6, which indicates that the beam height is efficient in increasing the stiffness. Additionally, for all analysis run with two different timber heights, that is Design 1 and 2, 3 and 4 as well as 8 and 9, the most material-efficient solution was in all cases for the 270 mm high beam.

The least efficient dimension change in the study was when varying the concrete thickness, which significantly increased the concrete volume whilst the possible timber area reduction was basically neglectable. The two other studies, changing the width of the timber or concrete (cc-distance between timber beams) showed similar impacts on the total timber usage, and neither solution can be declared more efficient than the other. However, increasing the concrete width may induce stability problems in-between the timber girders, which has not been included in this study. Contrary, increasing the timber width may increase the stability and make the element less slender, which might be a limiting aspect.

8

Discussion

The modelling procedure and the result of the parametric study is in this chapter connected to the literature study and put in a practical application perspective.

8.1 Slip modulus

The values for slip modulus determination presented in Eurocode 5, SS-EN 1995-1-1:2004 (2009), was in the literature review found to significantly underestimate the stiffness of the connector. Therefore, testing is a way to increase the accuracy of the applied connection stiffness. Even so, the current approach is bad at considering non-linear connection types, for example dowels, and the testing procedure influence the results.

In this study, a simplification with linear connection stiffness was used for efficiency since the main focus was on evaluating the long-term behaviour in SLS. Since the load levels are reasonably low in that state, linear behaviour is more probable than in a test to failure. However, the result might still have been affected by this simplification.

8.2 Modelling

The main output of the FE-analysis is the deflections, and no consideration of other aspects such as stress limitations or dynamic behaviour has been taken. That limitation was made since the literature study depicted this as the critical aspect of a TCC element. One advantage of a numerical solution is that significantly more detailed result in addition to the deflection and stresses can be analysed.

The FE-modelling procedure of the creep behaviour is similar to that applied by the γ-method in Eurocode 5, SS-EN 1995-1-1:2004 (2009). The "effective modulus method" reduces the modulus of elasticity by ϕ or k_{def} for concrete and the timber and connection respectively. When no shrinkage is applied, the analytical (γ-method) and numerical (FE-model) approach should therefore give similar result. One difference is that the γ-method is limited in terms of possible connector spacing configurations and boundary conditions, for which the numerical solution could be used. However, when making significant changes to the geometry, the model should preferably be verified again.

The most important difference between the analytical analysis and the FE-model in this study is the application of shrinkage, which is not possible in the γ-method. Thus, unlike for the creep, the long-term behaviour when considering shrinkage strains should differ between the analysis.

The FE-model was made with solid elements since that was the simplest way to try out different connection types. However, a more efficient model could be achieved by using for example a shell element for the concrete slab and a beam element for the timber beam. In practical design, that is probably the most efficient approach to capture the deflections, since such an analysis does not require solid modelling.

8.3 Shrinkage

The long-term FE-models concluded that the shrinkage of concrete could have a large impact on the long-term behaviour of the element, and similar results were found in the literature study as well. The influence of shrinkage is the most significant for stiff connections since the high composite action does not allow for much slip between the timber and concrete. For the geometry used in the first part of the parametric study, a stiff connection and a *normal* concrete shrinkage strain (0.04 %) caused a deflection corresponding to 35 % of the deflection limit, compared to when *no* shrinkage strain was applied. Similarly, in the second part of the parametric study, the timber area in the most material-efficient cross-sections could be reduced by 13-23 % when halving the shrinkage strain from *normal* to *small* (0.02 %). The impact was largest when the timber height was set and the width of timber and/or concrete was changed.

Even though the shrinkage was found to have a significant impact on the deflections for medium- and high-stiffness connections, the γ-method presented in Eurocode 5 neglect its strain. The un-conservative approach may lead to unexpectedly large deflections. However, the concrete shrinkage effect is counteracted if the timber also shrinks, as a result of decreasing moisture content.

In the first part of the parametric study, it was shown that the deflection effect of the shrinkage could be cancelled out if the concrete and timber sustain equal strain. A *normal* concrete shrinkage corresponds to a moisture content change of 4 % in the longitudinal direction of the timber. Since the timber moisture content often is higher at delivery than its equilibrium state in a finished building, it might be possible to benefit from the timber shrinkage in terms of reducing the deflections. That is a very interesting subject to study further, but a conservative design approach might do best in neglecting the benefits from timber shrinkage.

Another way to reduce the deflection caused by concrete shrinkage is to cast the concrete slab separately and letting it shrink freely before connecting it to the timber beam. Since the shrinkage strain is developed the fastest shortly after casting, approximately 30-40 days is enough for the concrete to have shrunk 50 % of its total strain (for similar geometries as used in the parametric study). The procedure is only possible when using prefabricated concrete elements. If the concrete instead is cast on-site, the shrinkage could instead be reduced by changes in the mixture to get a low-shrinkage concrete.

8.4 Creep

For the timber and connection, the creep behaviour was studied by comparing service class 2 and 3. The concrete impact was investigated by applying different concrete creep factors, 1.5 and 2.5. There is a large difference in approach for the creep considerations presented in Eurocode 2, SS-EN 1992-1-1:2005 (2008), and Eurocode 5, SS-EN 1995-1-1:2004 (2009). For the timber and connection, the service classes give fixed values in terms of the creep factor, k_{def} whilst the concrete creep factor is instead calculated through a formula for a specific time.

The service class was shown to have a large influence on the result, with relative deflection differences between 50-60 %. Unlike for the shrinkage, the connection stiffness did not show any significant impact on the difference between the service classes. However, that does not mean that the connection stiffness does not matter for the deflections, but its influence is similar for all connection stiffnesses.

Since the applied service class makes a large difference in results, careful considerations should be made to ensure a good choice. In previously performed experiments of TCC elements, conditions fulfilling the definitions for service class 2 has shown creep behaviour corresponding to service class 3 in Eurocode 5. Therefore, a conservative design approach could be to consider a higher service class than the actual conditions in the structure, especially in climates with heavily varying relative humidity. In severe cases, neither of the service classes might be good enough to fully account for the mechano-sorptive effect. Due to the large impact of the service class, TCC elements may not be the best choice in structures with demanding environmental conditions.

The accuracy of the service class method is an interesting field of study. For example, the large difference in creep factor between service class 2 and 3 results in a stiffness reduction of 67 % for the timber (the modulus of elasticity is divided by 3.0 instead of 1.8) and 92 % for the connection (5.0 instead of 2.6). In situations where the conditions is somewhere in-between the definition of service class 2 and 3, neither of the two may give satisfactory approximations of the deflections. Additionally, as has been discussed previously, service class 3 might not be conservative enough in very severe environmental conditions.

In the analysis for the concrete creep impact, the difference between creep factor 1.5 and 2.5 was between 5 and 9 % for the studied cross-section. Similar to the service class, the connection stiffness was not found to have a significant impact on the relative increase. The results show that the effect of the concrete creep is not as severe as the creep of timber and connection.

The reason that the service class has a larger influence on the result than the concrete creep factor is that the stiffness of the timber cross-section is higher and therefore a reduction in its modulus of elasticity has a larger effect on the deflections. The moment of inertia of the timber is for the design in the first part of the parametric study approximately 5 times larger than that of the concrete, thanks to the height of the timber beam. As such, despite the concrete having around 2-3 times the modulus of elasticity of the timber, the total stiffness of the timber is higher. If another cross section would be studied, for example a slab-type where the moment of inertia from the concrete is contributing to a larger extent, the concrete creep would possibly have a larger influence. In addition to the reduction in stiffness for the timber, the service class also affect the connection stiffness. For service class 3, the slip modulus is reduced by 80 % of its initial value. In short, the service class is very decisive for the long-term deflections of a TCC element.

8.5 Design considerations

In the second part of the parametric study, increasing the concrete thickness was seen to have a relatively small positive impact on the deflections. This is due to the high self-weight of the concrete, which for an 80 mm thick concrete slab in the quasi-permanent load case is more than double the imposed load of an office floor, 2.0 and 0.9 kN/m^2 respectively. Therefore, it was concluded that the concrete mass is significant when studying the long-term effects of a TCC element. However, in buildings designed for higher imposed loads than office spaces, for example shopping areas, the relative influence of the self-weight becomes smaller.

One way to reduce the self-weight of the concrete whilst keeping the cross-section unchanged is to use lightweight concrete instead. Then, the density is reduced from around 24 to 16 kN/m^3, which is a significant reduction. The drawbacks of lightweight concrete are a lower stiffness and larger shrinkage than regular concrete mixes. However, the gain in reduced load of the structure may very well override the drawbacks and reduce the long-term deformations, as seen in literature.

The additional mass of a TCC element compared to pure timber floors should however not only be considered problematic. As presented in the report, the advantages of using a TCC element is for example a better vibration and acoustic performance, enhanced by the concrete mass. Therefore, TCC elements is an interesting alternative in buildings with high demands on such aspects, which is not easily achieved by pure timber solutions. In the parametric study, the design was limited to "T"-cross-sections and thus no slab type TCC elements were evaluated. Since the acoustic demands is more cumbersome to achieve with pure CLT slabs, a solution is sometimes to add concrete on top of the slabs. In such cases, the CLT slab needs to be designed to carry the increased self-weight of the structure. A more material-efficient solution would be to include the increased stiffness of the concrete to the structural behaviour, rather than only adding it as a noise insulator.

Another interesting field for which TCC elements could be a good alternative is in high-rise timber buildings. In such constructions, the lightweight framework may entail stability and dynamical problems when subjected to horizontal loads such as wind. To solve these problems, concrete is sometimes added to the structure only to increase its mass. A better utilization of the concrete could in such cases be to use it in TCC elements.

9

Conclusion

The long-term behaviour of a TCC element is a complex field of studies. To make the work less extensive, simplified analysis methods could be applied in design. The current approach suggested by Eurocode 5, the γ-method, is the most commonly applied analytical solution procedure. However, its applicability is limited both in terms of design variations as well as in terms of accuracy. A notable simplification in the γ-method is the neglection of concrete shrinkage.

Several design variations that affect the behaviour of TCC elements are possible. One key choice is the connection set-up, which affect the slip modulus and thus the composite action of the cross-section. The stiffest connections create high composite action and small deflections, but often result in brittle raptures. Less stiff connections are generally more ductile but causes larger deflections due to the lower composite action. Because of the different drawbacks, a clear recommendation on connector type can not be established.

In the parametric study as well as in the literature study, the concrete shrinkage was found to potentially have a significant impact on the deflections. For medium- and high-stiffness connections in the first part of the parametric study, the deflection increase caused by *normal* concrete shrinkage (0.04 %) corresponded to 30-35 % of the total allowed deflection. Additionally, the second part of the parametric study showed that the timber consumption for the best designed cross-section could be reduced by 13-23 % when decreasing from *normal* to *small* (0.02 %) concrete shrinkage. It was also seen that shrinkage is extra important to consider when the height of the TCC element is fixed, and the focus is to change the width of the timber beam or the concrete width (cc-distance of the timber beams) instead.

Neglecting the concrete shrinkage in design, as the γ-method suggest, is a non-conservative design approach. However, it might be a reasonable assumption in some cases. If the timber is installed with a higher moisture content than the equilibrium conditions, its shrinkage counteracts the effect of the concrete shrinkage. Additionally, the concrete shrinkage can be reduced by adding shrinkage reducing admixtures or by prefabricating the slabs and letting the concrete shrink freely before assembly. In design, the conditions should be carefully evaluated before neglecting the impact of concrete shrinkage, to make sure that the deflections will not become unexpectedly large.

The applied service class, which affect the timber and connection creep, has a large influence on the estimated deflections. Between service class 2 and 3, the deflections increase with 52-62 % for the geometry in the first part of the parametric study. Further, several experiments found in the literature study show that the deflection is underestimated when assuming service class 2, even when the conditions fulfil the corresponding Eurocode 5 definitions. An especially critical situation is when the moisture content is varying since this causes an additional mechano-sorptive creep. Assuming service class 3 as a conservative design method is a safety approach, unless there are certainties that the creep won't exceed service class 2.

The concrete creep factor has a much smaller impact on the behaviour than the service class. In the first part of the parametric study, the deflection difference between a concrete creep factor of 2.5 and 1.5 was 5-9 %. Thus, for similar cross-sectional configurations as those used in this study, the possible deflection gains by reducing the creep factor is quite limited for the common creep factors.

The result of the second part of the parametric study showed that the long-term deflections are distinctly affected by the concrete area since the self-weight was the dominating load-case. Therefore, the design suggestion for similar load conditions is to minimize the concrete area as much as possible, while still maintaining the composite action and the benefits of a TCC. Additionally, using lightweight concrete has in previous studies been shown to decrease the long-term deflections.

The most efficient geometrical modification was to increase the timber height, which resulted in the most material-efficient cross-sections. Thereafter, changing the timber width and concrete width (timber beam spacing) had similar effect on the long-term deflections.

Even though the structural performance in terms of deflection might not be directly improved by the added concrete layer in a TCC, compared to a pure timber beam, other improvements are achieved such as better sound insulation and fire performance. Additionally, the increased self-weight that the concrete bring could in high-rise buildings improve the global performance and reduce the risk of tilting due to horizontal loads.

9.1 Further research

The result in this study showed that the concrete thickness did not have a clear positive impact on the long-term deflections. Therefore, a continuation of the work could be to run the second, more detailed, part of the parametric study for longer span lengths and increased imposed loads. In those conditions, the concrete volume would not be as significant in terms of loading on the structure. Then, an increased concrete thickness might be more beneficial than in the studied case. Additionally, if such studies are made, a better understanding of when TCC elements are appropriate to use would be acquired.

In the literature study, the deflections were found to be the decisive condition to fulfil in design. The parametric study was therefore focused on evaluating them. However, in real design, the stresses need to be verified as well. An addition to this study could be to further analyse the long-term behaviour in terms of stress redistribution occurring over time. Since timber and concrete have different rate of creep development, it would in a detailed analysis not be enough to only consider the final creep factor.

Based on the literature study, the mechano-sorptive creep could have a crucial impact on the long-term deflections. In Eurocode 5, this effect can be taken into account by using a more severe service class than what the average surrounding climate is corresponding to, but previous research has found that this approach may not be sufficient for TCC elements. Thus, to better understand the impact of moisture content variations for TCC elements, a more detailed analysis of the timber and connection creep is an interesting field of study.

A similar study to evaluate the performance of slab type TCC elements would be a good compliment to the captured behaviour of "T"-cross-section. Since concrete is sometimes added on top of CLT slabs in order to improve the acoustic and vibration behaviour, it would be interesting to evaluate if the concrete has an impact on the structural performance worth considering during construction.

References

Ceccotti, A. (1995). Timber-concrete composite structures. In H. Blass et al. (Eds.), *Timber engineering step 2* (First ed., pp. 1–12). The Netherlands, Almere: Centrum Hout.

Ceccotti, A. (2002). Composite concrete-timber structures. *Progress in Structural Engineering and Materials*, *4*, 264–275. doi: 10.1002/pse.126

Ceccotti, A., Fragiacomo, M., & Giordano, S. (2006). Long-term and collapse tests on a timber-concrete composite beam with glued-in connection. *Materials and Structures*, *40*, 15–25. doi: 10.1617/s11527-006-9094-z

Cusson, D., & Margeson, J. C. (2010). Development of low-shrinkage high-pe rformance concrete with improved durability. In *6th intl conference on concrete under severe conditions environment and loading* (pp. 869–878). doi: DOI: 10.1201/b10552-110

Dias, A. M. (2005). *Mechanical behaviour of timber-concrete joints* (Doctoral dissertation, Delft University of Technology). Retrieved from `http://resolver.tudelft.nl/uuid:fc148f88-9ad7-4322-8dda-af121c940b62`

Dias, A. M. (2018). *Design of timber-concrete composite structures: A state-of-the-art report by COST Action FP1402/WG 4* (A. Dias, J. Schänzlin, & P. Dietsch, Eds.). Aachen: Shaker Verlag.

Dias, A. M., & Jorge, L. F. (2011). The effect of ductile connectors on the behaviour of timber-concrete composite beams. *Engineering Structures*, *33*, 3033–3042. doi: 10.1016/j.engstruct.2011.05.014

Dowling, N. E. (2013). *Mechanical Behavior of Materials: Engineering Methods for deformation, Fracture, and Fatigue* (4th ed.; M. J. Horton, H. Stark, & S. Disanno, Eds.). Harlow, England: Pearson.

Eisenhut, L., Seim, W., & Kühlborn, S. (2016). Adhesive-bonded timber-concrete composites – Experimental and numerical investigation of hygrothermal effects. *Engineering Structures*, *125*, 167–178. doi: 10.1016/j.engstruct.2016.05.056

Fragiacomo, M., Gutkowski, R. M., Balogh, J., & Fast, R. S. (2007). Long-Term Behavior of Wood-Concrete Composite Floor/Deck Systems with Shear Key Connection Detail. *Journal of Structural Engineering*, *133*(9), 1307–1315. doi: 10.1061/ASCE0733-94452007133:91307

Granello, G., & Palermo, . A. (2019). Creep in timber: research overview and comparison between code provisions. *New Zealand Timber Design Journal*, *27*(1), 6–22. Retrieved from http://hdl.handle.net/10092/18124

Haedicke, W., Schober, K.-U., Rautenstrauch, K., Müller, J., & Doehrer, A. (2007). Long-term behaviour of timber-concrete composite structures. In *Vsu.* Sofia. Retrieved from https://www.researchgate.net/publication/280977742

Hailu, M. (2015). *Long-term Performance of Timber-Concrete Composite Flooring Systems* (Doctoral dissertation, University of Technology, Sydney). Retrieved from https://opus.lib.uts.edu.au/bitstream/10453/38958/2/02whole.pdf

International Organization for Standardization. (1983). *ISO 6891: Timber structures - Joints made with mechanical fasteners - General principles for the determination of strength and deformation characteristics.* Stockholm: SIS Förlag AB.

Jaaranen, J., & Fink, G. (2021). Cohesive-frictional interface model for timber-concrete contacts. *International Journal of Solids and Structures*, *230-231*. Retrieved from https://doi.org/10.1016/j.ijsolstr.2021.111174

Jockwer, R. (2022). *Timber concrete composite floor systems for more efficient structures, of SBUF and VGR Project No. 13979* (Tech. Rep.). Sweden: Chalmers University of Technology.

Jorge, L. F., Schänzlin, J., Lopes, S. M., Cruz, H., & Kuhlmann, U. (2010). Time-dependent behaviour of timber lightweight concrete composite floors. *Engineering Structures*, *32*, 3966–3973. Retrieved from https://doi.org/10.1016/j.engstruct.2010.09.007

Kavaliauskas, S., Kazimieras Kvedaras, A., & Gurkðnys, K. (2005). Evaluation of long-term behaviour of composite timber-concrete structures according to EC. *Technological and Economic Development of Economy*, *XI*(4), 292–296. Retrieved from http://www.tede.vgtu.lt doi: http://dx.doi.org/10.3846/13928619.2005.9637710

Khorsandnia, N., Valipour, H. R., Shrestha, R., Gerber, C., & Crews, K. (2013). Review on long-term behaviour of timber-concrete composite floors. In B. Samali, M. Attard, & C. Song (Eds.), *From materials to structures: Advancement through innovation* (pp. 1053–1058). Sydney: Taylor & Francis Group. doi: 9710.1201/b15320-188

Lukaszewska, E. (2009). *Development of Prefabricated Timber-Concrete Composite Floors* (Doctoral dissertation, Luleå University of Technology, Luleå). Retrieved from https://www.diva-portal.org/smash/record.jsf?pid=diva2%3A991048&dswid=4106

Ogrin, A., & Hozjan, T. (2021). Timber-Concrete Composite Structural Elements. In G. Meng (Ed.), *Engineered wood products for construction* (chap. 14). IntechOpen. doi: 10.5772/intechopen.99624

Ottosen, N. S., & Petersson, H. (1992). *Introduction to the Finite Element Method.* Harlow, Essex: Pearson Education Limited.

Schänzlin, J., & Fragiacomo, M. (2007). Extension of EC5 Annex B formulas for the design of timber-concrete composite structures. In *Meeting forty of the working commission w18-timber structures, cib, international council for research and innovation in building and construction.* Bled, Slovenia. CIB-W18/40-10-1.

Simulia - Abaqus 6.14. (2014). *Abaqus Analysis User's Manual: 38.1.1 Contact formulations in Abaqus/Standard.* Retrieved from `http://130.149.89.49:2080/v6.14/books/usb/default.htm`

Soutsos, M., & Domone, P. (2017). *Construction materials: their nature and behaviour / edited by Marios Soutsos and Peter Domone* (Fifth ed.; M. Soutsos & P. Domone, Eds.). Boca Raton: CRC Press.

SS 230120:2010. (2010). *Nordic visual strength grading rules for timber (INSTA 142)* (2nd ed.). Stockholm: SIS Förlag AB. Retrieved from `www.sis.se`

SS-EN 1992-1-1:2005. (2008). *Eurocode 2: Design of concrete structures-Part 1-1: General rules and rules for buildings* (1st ed.). Stockholm: SIS Förlag AB.

SS-EN 1995-1-1:2004. (2009). *Eurocode 5: Design of timber structures-Part 1-1: General-Common rules and rules for buildings.* Stockholm: SIS Förlag AB. Retrieved from `www.sis.se`

SS-EN 338:2016. (2016). *Structural timber - Strength classes* (4th ed.). Stockholm: SIS Förlag AB. Retrieved from `www.sis.se`

Swedish Wood. (n.d.). *Wood grades.* Retrieved from `https://www.swedishwood.com/wood-facts/about-wood/wood-grades/`

Swedish Wood. (2016a). *Del 1 Limträhandbok Fakta om limträ.* Stockholm: Skogsindustrierna Svenskt Tra. Retrieved from `www.traguiden.se,`

Swedish Wood. (2016b). *Design of timber structures: Rules and formulas according to Eurocode 5, Volume 2* (2nd ed., Vol. 2; E. Borgström, Ed.). Swedish Forest Industries Federation, Swedish Wood. Retrieved from `www.swedishwood.com.`

Swedish Wood. (2016c). *Design of timber structures: Structural aspects of timber construction, Volume 1* (2nd ed., Vol. 1; Borgström; Eric, Ed.). Stockholm: Swedish Forest Industries Federation. Retrieved from `www.swedishwood.com`

Swedish wood. (2019). *The CLT Handbook: CLT structures-facts and planning*

(E. Borgström & J. Fröbel, Eds.). Stockholm: Skogsindustrierna Svenskt Tra. Retrieved from `www.traguiden.se,`

Tannert, T., Endacott, B., Brunner, M., & Vallée, T. (2017). Long-term performance of adhesively bonded timber-concrete composites. *International Journal of Adhesion and Adhesives*, *72*, 51–61. doi: 10.1016/j.ijadhadh.2016.10.005

Yeoh, D. (2010). *Behaviour and design of timber-concrete composite floor system* (Doctoral dissertation, University of Canterbury, Christchurch, New Zealand). Retrieved from `https://ir.canterbury.ac.nz/bitstream/handle/10092/4428/thesis_mainbody.pdf?sequence=2&isAllowed=y`

Zhan, P. m., & He, Z. h. (2019). Application of shrinkage reducing admixture in concrete: A review. *Construction and Building Materials*, *201*, 676–690. Retrieved from `https://doi.org/10.1016/j.conbuildmat.2018.12.209`

A

Concrete creep and shrinkage formulas in Eurocode

The Eurocode approach to calculate concrete shrinkage and creep is presented in the following appended MathCad-documents.

Calculation of concrete shrinkage strain at time t

This Mathcad document can be used to calculate how the concrete shrinkage strain varies in time. The values marked with a star* should be set by the user. In this example values from the cross-section used in the first parametric study have been used. The time for which the concrete shrinkage strain is calculated for is set to 1400 days.

Time the concrete shrinkage is calculated for:

$t := 1400\text{day}$ *

Concrete

$E_c := 33\text{GPa}$ * Modulus of elasticity of concrete

$f_{cm.c} := 38\text{MPa}$ * Mean compressive strength of concrete at age 28 days

$f_{ck.c} := f_{cm.c} - 8\text{MPa} = 30 \cdot \text{MPa}$ Characterisitc compression strength of concrete

$w_c := 700\text{mm}$ * Concrete width

$h_c := 80\text{mm}$ * Concrete height

$\text{Cementclass} := 2$ *
1 = S = Slow cement strength development
2 = N = Slow cement strength development
3 = R = Slow cement strength development

$t_s := 28\text{day}$ * Age of the concrete when drying starts (end of curing)

Timber

$w_{tim} := 90\text{mm}$ * Timber width

Climate

$RH := 70\%$ * Ambient relative humidity

CS Geometry properties

$A_c := w_c \cdot h_c = 5.6 \times 10^4 \cdot mm^2$ Concrete (gross) area

$u := 2 \cdot w_c - w_{tim} = 1.31 \times 10^3 \cdot mm$ Concrete perimeter that is exposed to drying

$h_0 := \frac{2 \cdot A_c}{u} = 85.496 \cdot mm$ Notional size of cross section

The shrinkage of concrete consists of both a drying shrinkage, $\varepsilon_{ct}(t)$, and an autogenous shrinkage, $\varepsilon_{ca}(t)$. The final concrete shrinkage, $\varepsilon_{cs}(t)$, can be calculated according to

$\varepsilon_{cs}(t) = \varepsilon_{cd}(t) + \varepsilon_{ca}(t)$

Drying shrinkage

The variation of the drying shrinkage by time can be calculated as

$\varepsilon_{cd}(t) = \beta_{ds}(t,t_s) * k_h * \varepsilon_{cd,0}$

where

$\beta_{ds}(t,t_s)$ is the time function of the drying shrinkage

k_h is a factor that considers the size of the cross section

$\varepsilon_{cd,0}$ is the basic value of the drying shrinkage

Calculation of k_h

$$k_h := \begin{cases} 1.0 & \text{if } \frac{h_0}{mm} \le 100 \\ \left[1 - \frac{(1-0.85)}{(100-200)}\cdot\left(100 - \frac{h_0}{mm}\right)\right] & \text{if } 100 < \frac{h_0}{mm} \le 200 \\ \left[0.85 - \frac{(0.85-0.75)}{(200-300)}\cdot\left(200 - \frac{h_0}{mm}\right)\right] & \text{if } 200 < \frac{h_0}{mm} \le 300 \\ \left[0.75 - \frac{(0.75-0.70)}{(300-500)}\cdot\left(300 - \frac{h_0}{mm}\right)\right] & \text{if } 300 < \frac{h_0}{mm} < 500 \\ 0.7 & \text{if } \frac{h_0}{mm} \ge 500 \end{cases} = 1$$

Calculation of $\varepsilon_{cd,0}$:

To calculate $\varepsilon_{cd,0}$ the parameter β_{RH}, α_{ds1} and α_{ds2} first need to be determined

$$\beta_{RH} := 1.55\cdot\left[1 - \left(\frac{RH\cdot 100}{100}\right)^3\right] = 1.018$$

$$\alpha_{ds1} := \begin{cases} 3 & \text{if Cementclass} = 1 \\ 4 & \text{if Cementclass} = 2 \\ 6 & \text{if Cementclass} = 3 \end{cases} = 4$$

$$\alpha_{ds2} := \begin{cases} 0.13 & \text{if Cementclass} = 1 \\ 0.12 & \text{if Cementclass} = 2 \\ 0.11 & \text{if Cementclass} = 3 \end{cases} = 0.12$$

Now $\varepsilon_{cd,0}$ can be calculated

$$\varepsilon_{cd0} := 0.85\left[\left(220 + 110\cdot\alpha_{ds1}\right)\cdot e^{-\alpha_{ds2}\cdot\left(\frac{f_{cm.c}}{MPa\cdot 10}\right)}\right]\cdot 10^{-6}\cdot\beta_{RH} = 3.621\times 10^{-4}$$

Calculation of $\beta_{ds}(t,t_s)$:

$$\beta_{ds.t.ts} := \frac{\left(\frac{t}{day} - \frac{t_s}{day}\right)}{\left(\frac{t}{day} - \frac{t_s}{day}\right) + 0.04 \cdot \sqrt{\left(\frac{h_0}{mm}\right)^3}} = 0.977$$

Finally the drying shrinkage at time t can be calculated according to

$$\varepsilon_{cd.t} := \beta_{ds.t.ts} \cdot k_h \cdot \varepsilon_{cd0} = 3.539 \times 10^{-4}$$

Autogenous shrinkage

The variation of the autogenous shrinkage by time can be calculated as

$\varepsilon_{ca}(t) = \beta_{as}(t) * \varepsilon_{ca}(\infty)$
where
$\beta_{as}(t)$ is the time function of the autogenous shrinkage
$\varepsilon_{ca}(\infty)$ is the final value of the autogenous shrinkage

First the two parameters, $\beta_{as}(t)$ and $\varepsilon_{ca}(\infty)$, are calculated

$$\varepsilon_{ca.\infty} := 2.5 \cdot \left(\frac{f_{ck.c}}{MPa} - 10\right) \cdot 10^{-6} = 5 \times 10^{-5}$$

$$\beta_{as} := 1 - e^{-0.2 \cdot \left(\frac{t}{day}\right)^{0.5}} = 0.999$$

Now the autogenous shrinkage at time t can be calculated

$$\varepsilon_{ca.t} := \beta_{as} \cdot \varepsilon_{ca.\infty} = 4.997 \times 10^{-5}$$

Total shrinkage at time t

$$\varepsilon_{cs.t} := \varepsilon_{cd.t} + \varepsilon_{ca.t} = 4.039 \times 10^{-4}$$

Calculation of concrete creep factor at time t

This Mathcad document can be used to calculate how the creep coefficient for concrete varies in time. The values marked with a star* should be set by the user. In this example values from the cross section used in the first parametric study have been used. The time for which the creep coefficient is calculated for is set to 1400 days.

At what time the creep factor is calculated for:

$t := 1400\text{day}$ *

Concrete

$E_c := 33\text{GPa}$ * Modulus of elasticity of concrete

$f_{cm.c} := 38\text{MPa}$ * Mean compressive strength of concrete at age 28 days

$f_{ck.c} := f_{cm.c} - 8\text{MPa} = 30\cdot\text{MPa}$ Characterisitc compression strength of concrete

$w_c := 700\text{mm}$ * Concrete width

$h_c := 80\text{mm}$ * Concrete height

$t_0 := 200\text{day}$ * Age of concrete when it is loaded

$t_s := 28\text{day}$ * Age of the concrete when drying starts (end of curing)

Timber

$w_{tim} := 90\text{mm}$ * Timber width

Connection

$K_{con} := 25000\dfrac{\text{N}}{\text{mm}}$ * Slip modulus of each connection

Climate

$RH := 70\%$ * Ambient relative humidity

Cross section Geometry properties

$A_c := w_c \cdot h_c = 5.6 \times 10^4 \cdot mm^2$ Concrete (gross) area

$u := 2 \cdot w_c - w_{tim} = 1.31 \times 10^3 \cdot mm$ Concrete perimeter that is exposed to drying

$h_0 := \frac{2 \cdot A_c}{u} = 85.496 \cdot mm$ Notional size of cross section

To calculate the creep coefficient at time t the following equation can be used according to Eurocode 2 (SS-EN 1992)

$\varphi(t,t_0) = \beta_c(t,t_0) * \varphi_0$

Where
$\beta_c(t,t_0)$ = time function of the creep coefficient
φ_0 = notional creep coefficient

Calculation of $\beta_c(t,t_0)$

$\beta_c(t,t_0)$ can be calculated according to

$\beta_c(t,t_0) = [(t-t_0)/(\beta_H + (t-t_0))]^{0.3}$

$$\beta_H := \begin{cases} \min\left[1.5 \cdot \left[1 + (0.012 \cdot RH \cdot 100)^{18} \frac{h_0}{mm} + 250\right], 1500\right] & \text{if } f_{cm.c} \le 35MPa \\ \min\left[1.5 \cdot \left[1 + (0.012 \cdot RH \cdot 100)^{18}\right] \cdot \frac{h_0}{mm} + 250\left(\frac{35}{\frac{f_{cm.c}}{MPa}}\right)^{0.5}, 1500 \cdot \left(\frac{35}{\frac{f_{cm.c}}{MPa}}\right)^{0.5}\right] & \text{if } f_{cm.c} > 35MPa \end{cases}$$

From this β_c (t,t_0) can be calculated

$$\beta_c := \left[\frac{\left(\frac{t}{day} - \frac{t_0}{day}\right)}{\beta_H + \left(\frac{t}{day} - \frac{t_0}{day}\right)}\right]^{0.3} = 0.922$$

Calculation of φ_0

φ_0 can be calculated according to

$\varphi_0 = \varphi_{RH} * \beta(f_{cm,c}) * \beta(t_0)$

where

φ_{RH} is a factor that considers the relative humidity
$\beta(f_{cm,c})$ is a factor that considers the concrete strength
$\beta(t_0)$ is a factor that considers the age of the concrete when it was loaded

$$\varphi_{RH} := \begin{cases} \left(1 + \dfrac{1 - \frac{RH \cdot 100}{100}}{0.1 \cdot \sqrt[3]{\frac{h_0}{mm}}}\right) & \text{if } f_{cm.c} \le 35MPa \\ \left[\left[1 + \dfrac{1 - \frac{RH \cdot 100}{100}}{0.1 \cdot \sqrt[3]{\frac{h_0}{mm}}} \cdot \left(\dfrac{35}{\frac{f_{cm.c}}{MPa}}\right)^{0.7}\right] \cdot \left(\dfrac{35}{\frac{f_{cm.c}}{MPa}}\right)^{0.2}\right] & \text{if } f_{cm.c} > 35MPa \end{cases} = 1.616$$

$$\beta_{fcmc} := \frac{16.8}{\left(\frac{f_{cm.c}}{MPa}\right)^{0.5}} = 2.725$$

$$\beta_{t0} := \frac{1}{\left[0.1 + \left(\frac{t_0}{day}\right)^{0.2}\right]} = 0.335$$

When both φ_{RH} , $\beta(f_{cm,c})$ and $\beta(t_0)$ are calculated the notional creep coefficient, $\varphi_{0,}$ can be calculated

$$\varphi_0 := \varphi_{RH} \cdot \beta_{fcmc} \cdot \beta_{t0} = 1.475$$

Finally the creep coefficient can be calculated

$$\varphi_{t.t0} := \varphi_0 \cdot \beta_c = 1.36$$

In Eurocode 2 this factor is used to reduce the modulus of elasticity of the concrete

<u>Reduction of the Youngs modulus due to creep</u>

$$E_{c.fin} := \frac{E_c}{\left(1 + \varphi_{t.t0}\right)} = 13.983 \cdot GPa$$

B

Validation of modelling technique

The validation of the FEM modelling procedure is done by modelling different experimental setups found in literature, and the results from the experiments can be compared with the results from the FEM-model. The γ-method ("gamma"-method) can also be used to validate the FEM-modelling technique, by comparing the results from the FEM-model with the results from the γ-method for a specific experimental setup. This means that the deflection in the FEM-model can be validated both based on the real results from the experiment, and also with the value that would be obtained if the γ-method would be used to model the experimental setup. The FEM model is both verified in the short-term and for a long-term analysis. Since there are few experiments found in literature, that has been performed for a longer period than one year, the long-term verification will be based on fewer experiments. In this report three experimental setups will be used to validate the modelling technique, one experiment from Lukaszewska (2009) (experimental setup 1) and two experiments from Hailu (2015) (experimental setup 2 and 3).

The short-term deflection can be validated by all three experiments, whereas the long-term deflection can be validated by experimental setup 2 and 3. The percentage difference in deflection between the FEM-model and experiment, and FEM-model and γ-method can be calculated by using Equation B.1. It is also interesting to verify the results by comparing the composite-efficiency, which is calculated according to Equation B.2.

$$\Delta = \frac{|FEM - A|}{A} \cdot 100 \tag{B.1}$$

Where A can be either the experimental deflection or deflection from γ-method, depending on what is compared, and FEM is the deflection from the FEM-model.

$$Composite - efficiency = \frac{\delta_{no} - \delta_{partial}}{\delta_{no} - \delta_{full}} \cdot 100 \tag{B.2}$$

It is important to note that the composite-efficiency of the experiments are based on theoretical values for no and full interaction, gained from the corresponding reports.

B.1 Experimental setup 1 - Short-term

The long-term test performed by Lukaszewska (2009) (experimental setup 1) was performed for 339 days. During this time only a small proportion of the creep has been developed. The proposed model in Abaqus does only take the final creep factor into account, and therefore it would be a too large source of error to use this experiment as a validation of the modelling technique in the long-term. Therefore, this experiment is only used to validate the model for short-term deflection.

In the following sections below a description of the experiment setup together with how the validation was done is described.

B.1.1 Execution of experiment

A 4.8 m TCC beam, with the material cast in situ concrete and glulam, was subjected to two point loads of 6.65 kN each according to Figure B.1. The cross section of the beam can be seen in Figure B.2 together with its corresponding dimensions.

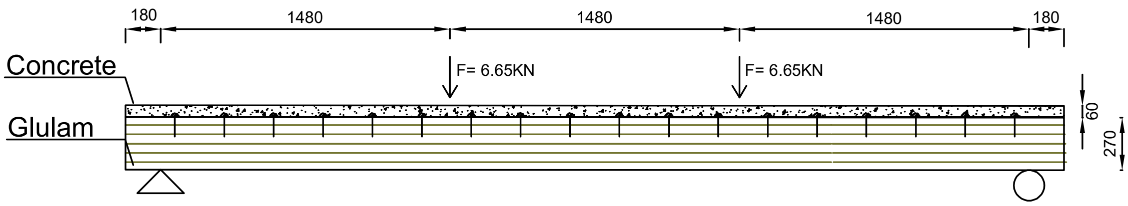

Figure B.1: Experimental setup 1 (dimension in mm)

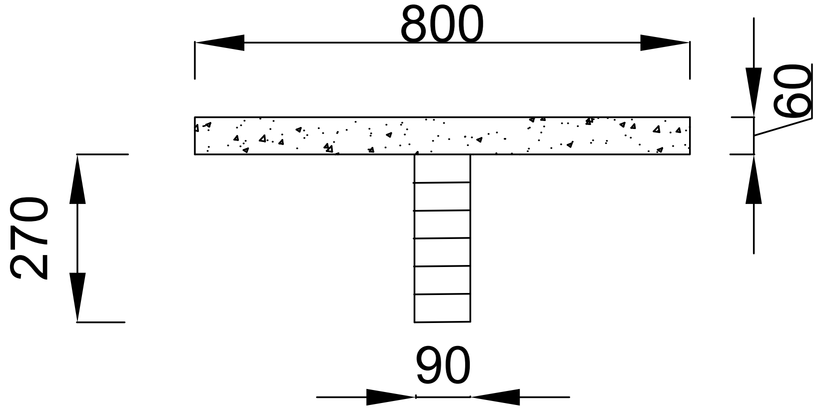

Figure B.2: Cross section of the TCC beam for experimental setup 1 (dimensions in mm)

The material properties for the concrete and timber were tested separately, and from these bending tests the modulus of elasticity of timber and concrete were equivalent to C20/25 and GL28c. Push out tests were performed to determine the slip modulus of each connection. The material properties that were used in the model can be seen in Table B.1, B.2 and B.3.

Table B.1: Material properties concrete in Experiment 1

Modulus of elasticity [MPa]	35380
Density [kg/m^3]	2400

Table B.2: Material properties timber in Experiment 1

Modulus of elasticity parallel to grain (E1) [MPa]	13500
Modulus of elasticity edgewise, perpendicular to grain (E2) [MPa]	300
Modulus of elasticity flatwise, perpendicular to grain (E3) [MPa]	300
Shear modulus flatwise, parallel to grain (G12) [MPa]	650
Shear modulus edgewise, parallel to grain (G13) [MPa]	650
Shear modulus flatwise, perpendicular to grain (G23) [MPa]	-
Poisons ratio [MPa]	0
Density [kg/m^3]	620

Table B.3: Material properties connection in Experiment 1

Slip modulus per screw [N/mm]	8000

B.1.2 Modelling of experiment in Abaqus

The modelling procedure described in Chapter 6 is used when modelling the experiment. Three different composite actions is modelled, no interaction, full interaction and partial interaction. Partial interaction is corresponding to the composite action of the experiment. The reason that the two extremes are modelled is to be able to compare the composite efficiency between the FEM-model and the experiment and γ-method. Since only the short-term test is modelled, the long-term effects do not need to be considered.

B.1.3 Modelling of experiment by γ-method

γ-method is used to validate the model, and this analytical approach has been described in Section 5.1. This procedure is used to analytically capture the behaviour of the experiment performed by Lukaszewska.

B.1.4 Results

The results for both the FEM-model, experiment and γ-method are presented in Table B.4, for three different composite actions together with the composite efficiency. To be able to easily verify the FEM-model towards both the experiment and the γ-method, a percentage difference is also presented. The measured experimental short-term deflection does not include the initial deflection from the self-weight, instead it is only the deflection that appeared when the sustained load (two point-loads) was applied.

Table B.4: Result for short-term validation, experimental setup 1

	FEM	Experiment	γ-method	Δ FEM vs. Exp	Δ FEM vs. γ-method
No int.	9.1 mm	-	9.9 mm	-	-8%
Partial int.	5.87 mm	5.4 mm	5.92 mm	+8.7%	-0.8%
Full int.	2.82 mm	-	2.48 mm	-	+13.7%
Comp. eff.	50.7%	57%	53.6%	-6.3%-points	-2.9%-points

B.1.5 Discussion

It can be seen in Table B.4 that the deflection from the FEM-model is 8.7% larger compared to the experimental value, which means that in this case the FEM-model overestimates the short-term deflection. When the experiment setup was modelled by using the γ-method very similar results were obtained for the deflection as for the FEM-model. This means that the FEM-model behaves similarly as the γ-method in the short-term when modelling partial interaction. At the same time the difference between the FEM-model and the γ-method is larger for the two extremes, no- and full interaction. When studying the composite efficiency it is seen that the FEM-model is more likely to underestimate the composite efficiency, which also would indicate that the FEM-model gives a bit larger deflections.

B.2 Experimental setup 2 - Short- and long-term

This experiment is presented in a report by Hailu, and was performed for a period of 1400 days. This is considered to be a sufficient period of time to verify the model both in short-term and long-term. In Section 6.5 it is described how the long-term effects can be taken into account. All the long-term effects are not considered, such as any effect due to change in moisture content.

B.2.1 Execution of experiment

In the experiment a TCC beam with a span length of 5.8 meters, and the material in-situ concrete and LVL, was tested and can be seen in Figure B.3. The cross section off the TCC element can be seen in Figure B.4 together with the corresponding dimensions of the concrete and timber. 200 days after the concrete was poured the long-term test started and was continued for 1400 days. The load that was applied at the start of the test was a distributed load of 1.74 kPa equivalent to 1.05 kN/m. The temperature was held almost constant around 20°C but the humidity varied between 50% and 100%, which is equivalent to service class 3.

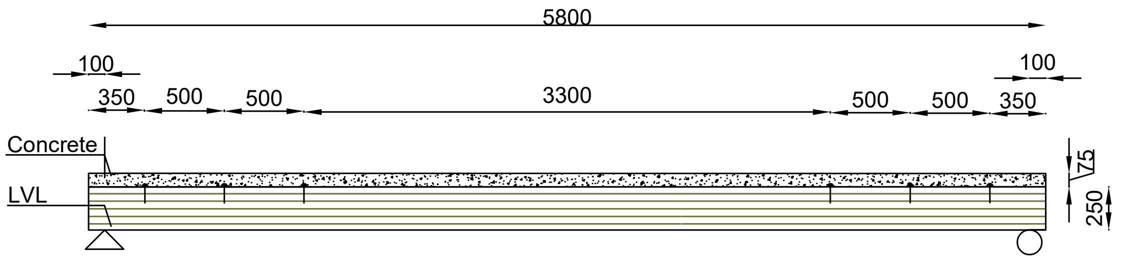

Figure B.3: Experimental setup 2 (dimensions in mm)

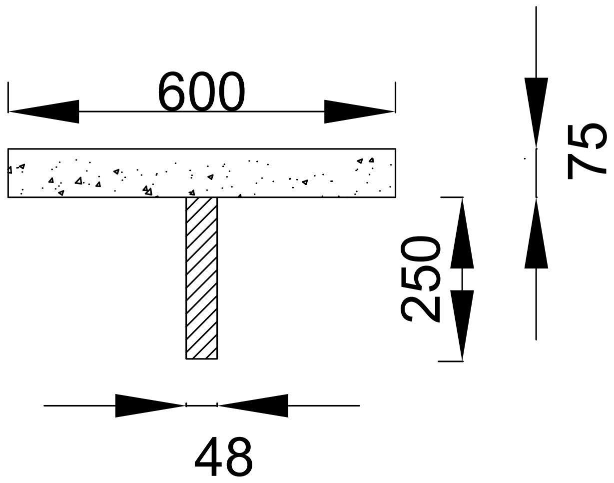

Figure B.4: Cross section of the TCC beam for experimental setup 2 (dimensions in mm)

The material properties for the concrete and timber were tested separately, and from these bending tests the modulus of elasticity of both concrete and timber were determined to 33 933 MPa and 13 482 MPa respectively. Another test was also performed to determine the strength properties of the concrete, where the compressive strength of the concrete was determined, which is needed to calculate the shrinkage and creep of concrete. A push out test of the TCC beam was performed, by which the slip modulus could be determined for each connection. All data necessary for the FEM modelling of this experimental setup was not presented by Hailu, and therefore some assumptions have been done (for example the stiffness properties for timber). The properties of the three different TCC components, that have been used in the FEM-model and γ-method, are presented in Table B.5, B.6 and B.7.

Table B.5: Material properties concrete for experimental setup 2 (also valid for experimental setup 3)

Modulus of elasticity, E_c [MPa]	33933
Density [kg/m^3]	2400

Table B.6: Material properties LVL for experimental setup 2 (Values taken from Swedish Wood (2016b))

Modulus of elasticity parallel to grain, E_1 [MPa]	13482
Modulus of elasticity edgewise, perpendicular to grain, E_2 [MPa]	430
Modulus of elasticity flatwise, perpendicular to grain, E_3 (E3) [MPa]	130
Shear modulus flatwise, parallel to grain, G_{12} [MPa]	600
Shear modulus edgewise, parallel to grain, G_{13} [MPa]	600
Shear modulus flatwise, perpendicular to grain, G_{23} [MPa]	-
Poisons ratio [MPa]	0
Density [kg/m^3]	620

Table B.7: Material properties connection for experimental setup 2

Slip modulus per screw, K_{con} [N/mm]	36900

B.2.2 Modelling of experiment in Abaqus

The same modelling technique was used as described in Chapter 6. Some simplifications are made such that the variation of the relative humidity and the corresponding change in moisture content of the timber is not considered. The concrete shrinkage at a specific time can be calculated with the MathCad-document presented in Appendix A . When calculating the shrinkage for this experimental setup it is seen that 85-90% of all the concrete shrinkage has already occurred at time=200days. Since the test starts 200 days after the concrete is poured the contribution to the deflection from the shrinkage will be limited. Therefore, the concrete shrinkage is not considered when modelling the experiment.

Creep of timber is based on service class 3, with kdef = 2.0 for LVL, with this factor also the creep of the connection can be calculated. The long-term modulus of elasticity and shear modulus for timber in different directions are presented in Table B.8 and B.9, and calculated with k_{def} = 2.0. It is important to keep in mind that this is the final creep factor, and probably all the creep has not been developed at the specific time for the connection and the timber yet in the experiment.

The concrete creep is considered by calculating a creep factor for time t=1400 days. To calculate the concrete creep factor, information regarding age of concrete and ambient relative humidity is needed. This creep factor can be calculated according to Appendix A, which for this experimental setup is 1.33. A final long-term modulus of elasticity can be calculated with this final creep factor to 14570 MPa. The input data for the long-term effects and the final value of the long-term modulus of elasticity for concrete is presented in Table B.10.

Table B.8: Material properties for timber in long-term

Service class	3
k_{def}	2
Modulus of elasticity parallel to grain, long-term, $E_{1,fin}$ [MPa]	4494
Modulus of elasticity edgewise, perpendicular to grain, long-term, $E_{2,fin}$ [MPa]	143
Modulus of elasticity flatwise, perpendicular to grain, long-term, $E_{3,fin}$ [MPa]	43
Shear modulus flatwise, parallel to grain, long-term, $G_{12,fin}$ [MPa]	200
Shear modulus edgewise, parallel to grain, long-term, $G_{13,fin}$ [MPa]	200
Shear modulus flatwise, perpendicular to grain, long-term, $G_{23,fin}$ [MPa]	-

Table B.9: Material properties for connection in long-term

Service class	3
k_{def}	2
Slip modulus, long-term, $K_{con,fin}$ [N/mm]	7380

Table B.10: Material properties for concrete in long-term

Age of concrete when loaded,t_0 [days]	200
Time duration of long-term test [days]	1400
Ambient relative humidity [%]	70
Creep coefficient of concrete at time 1400 days [-]	1.33
Long-term modulus of elasticity, $E_{c,t=1400}$ [MPa]	14 570

B.2.3 Modelling of experiment by Gamma-method

The same procedure is used to calculate the short-term deflection by the γ-method as was described for experimental setup 1. Since the long-term modelling used in Abaqus for this experiment does not consider concrete-shrinkage or any moisture content changes in the timber, results in that the same long-term effects are considered in the γ-method and the Abaqus model. This means that the long-term properties of timber, concrete and connection are the same as those implemented in the Abaqus model, $E_{1,fin}$, $E_{c,t=1400}$ and $K_{con,fin}$.

B.2.4 Results

The results for both the FEM-model, experiment and γ-method are presented in Table B.11 for short-term and in Table B.12 for long-term. To be able to easily verify the FEM-model against both the experiment and the γ-method, a percentage difference is presented in the tables. As for experimental setup 1 the measured experimental short-term deflection does not include the initial deflection from the self-weight, instead it is only the deflection that appeared when the sustained load was applied. As for the short-term deflection, the long-term-deflection does not include the deflection from the self-weight. At the same time the self-weight of the TCC slab has a large contribution to the long-term effects, for example creep. Therefore, it is very important to take the self-weight into account in the model, but to be able to compare with the experimental results the initial deflection from self-weight is subtracted.

Table B.11: Result for short-term validation, experimental setup 2

	FEM	Experiment	γ-method	Δ FEM vs. Exp	Δ FEM vs. γ-method
No int.	10.2 mm	-	9.9 mm	-	+3%
Partial int.	4.75 mm	4.39 mm	4.42 mm	+8.2%	+7.5%
Full int.	3.39 mm	-	2.85 mm	-	+19%
Comp. eff.	80%	84% *	77.7%	-4%-points	+2.3%-points

*This value is based on theoretical values for full and no interaction, together with the experimental value for partial interaction.

Table B.12: Result for long-term validation, experimental setup 2

	FEM	Experiment	γ-method	Δ FEM vs. Exp	Δ FEM vs. γ-method
No int.	45.0 mm	-	44.0 mm	-	+2.4%
Partial int.	25.6 mm	34.0 mm	25.0 mm	-24.7%	+2.4%
Full int.	16.3 mm	-	13.8 mm	-	+18.2%
Comp. eff.	67.8%	-	62.8%	-	+5%-points

B.2.5 Discussion

As for the short-term results from Lukaszewska the deflection for partial interaction is conservative when comparing the FEM-model with the experimental values, and is 7,5% larger. It can also be seen from the short-term result that the difference between the FEM-model and γ-method is not very large, except for full interaction where the FEM-model presents 19% larger deflection. The composite efficiency of the FEM-model differs less from the experimental one than the γ-method.

The long-term test was held for 1400 days which was considered to a sufficient time to be able to verify the model in long-term. When studying the results in Table B.12 it is seen that the deflection from the FEM-model is 24.7% smaller compared to the experimental value, which is considered to be a relatively large difference. Eventough the final creep of all the three materials is considered, obviously these effects are not enough to get a proper results. The main reason that the deflection is different between the experiment and the FEM-model is probably due to the climate conditions that the beam is subjected to. The relative humidity and moisture content of the timber is varying a lot, and therefore the mechano-sorptive creep will have a large influence. This is also probably the main reason for the large difference, since the mechano-sorptive creep is not taken into account in the FEM-model explicitly. When instead the long-term deflection is compared with the one from γ-method it can be seen that they are very similar for both no, full and especially for partial interaction. Since the same long-term effects have been used in the γ-method and in the Abaqus model this would also be the expected result. Therefore it can be concluded that the FEM-model for this case, with no concrete shrinkage and no moisture content changes in the timber, the model is almost equivalent as using the γ-method.

B.3 Experimental setup 3 - Short- and long-term

As for experimental setup 2 this experiment (experimental setup 3) was also performed by Hailu (2015). The only difference between this experiment and experimental setup 2 is the location of the connectors, otherwise the conditions are almost the same. It was seen by Hailu during the bending test of the LVL that it had another modulus of elasticity than experimental setup 2. Therefore the only new in-data compared to experimental setup 2 is another modulus of elasticity of LVL and another connector stiffness and connector spacing. The new connector spacing is presented in Figure B.5, and the new material properties are defined in Table B.13 and B.14.

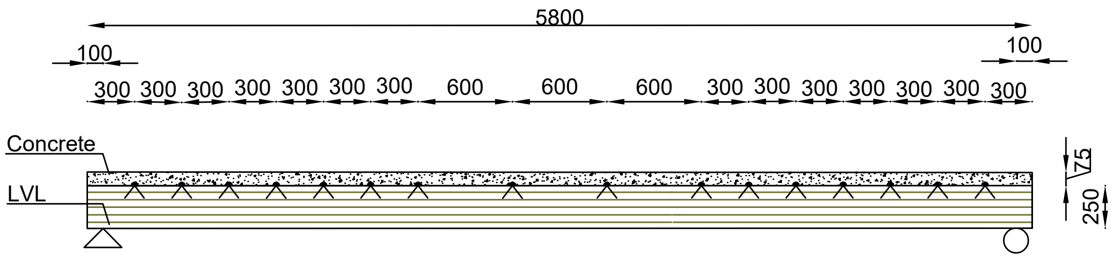

Figure B.5: Experimental setup 3 (dimensions in mm)

Table B.13: Updated connector stiffness

Initial Slip modulus per connection, K_{con}	54900
Final Slip modulus per connection, $K_{con,fin}$	10980

Table B.14: Updated data for LVL

Modulus of elasticity parallel to grain, E_1 [MPa]	12312
Modulus of elasticity parallel to grain, long-term, $E_{1,fin}$ [MPa]	4104

B.3.1 Results

The short-term deflection and the long-term deflection for experimental setup 3 are presented in Table B.15 respectively B.16. As for the other two experimental setups, the deflection from the self-weight is not presented in the results for the short-term test. This means that the deflection for short-term is the initial deflection that appeared when the sustained load was applied. Also in the long-term deflection the initial deflection from the self-weight is subtracted.

Table B.15: Result for short-term validation, experimental setup 3

	FEM	Experiment	γ-method	Δ FEM vs. Exp	Δ FEM vs. γ-method
No int.	10.7 mm	-	10.4 mm	-	+2.7%
Partial int.	4.1 mm	4.17 mm	3.6 mm	-2.2%	+13%
Full int.	3.6 mm	-	3.1 mm	-	+16%
Comp. eff.	93%	90% *	93%	+2.8%-points	+0.1%-points

*This value is based on theoretical values for full and no interaction, together with the experimental value for partial interaction.

Table B.16: Result for long-term validation, experimental setup 3

	FEM	Experiment	γ-method	Δ FEM vs. Exp	Δ FEM vs. γ-method
No int.	45.0 mm	-	46.0 mm	-	-2.6%
Partial int.	20.1 mm	33 mm	19 mm	-39%	+4.7%
Full int.	16 mm	-	15 mm	-	+9%
Comp. eff.	86%	-	86%	-	+0.5%-points

B.3.2 Discussion

For this beam the short-term deflection of the experiment is very well captured with the FEM-model, with only a difference of 2.2%. The composite efficiency for the FEM-model, experiment and γ-method is very similar. When comparing the long-term effects of this beam it can be seen that the long-term deflection from the experiment is 33mm, and the FEM-model and γ-method gives respectively 20.1 mm and 19.2 mm. This is a large difference, and as for experimental setup 2 no mechano-sorptive creep is considered and is probably one of the main reasons for the large difference. At the same time when comparing the long-term deflection with experimental setup 2 it is seen that the long-term deflection from the experiment is 33mm, which is only 1 mm smaller compared to experimental setup 2. In the report by Hailu this is discussed as an unexpected result since the both the connector spacing is smaller and the slip modulus of them higher. Therefore, it cannot be concluded that the modelling technique works worse for this experimental setup than experimental setup 2.

C

Parametric study

The result in parametric study part 1 and 2 are presented in the following tables.

C.1 Parametric study - Part 1

Table C.1: Concrete shrinkage - connection stiffness

	K_0	K_1	K_4	K_{10}	K_{25}	K_{75}	K_{200}	K_∞
no shrinkage [mm]	-42.5	-33.1	-23.4	-18.4	-15.7	-14.2	-13.8	-13.3
normal shrinkage [mm]	-42.5	-35.6	-28.3	-24.6	-22.5	-21.5	-21.1	-20.8
Relative increase [%]	0	7.5	21.1	33.5	43.8	50.6	53.2	56.0

Table C.2: Concrete shrinkage - connection stiffness 2500 N/mm

	L_{2000}	L_{3000}	L_{4000}	L_{5000}	L_{6000}	L_{7000}	L_{8000}	L_{9000}	L_{10000}
no [mm]	-1.0	-3.0	-7.3	-15.0	-27.0	-44.6	-69.0	-101.6	-144.1
normal [mm]	-1.1	-3.4	-8.4	-17.3	-31.1	-51.0	-78.1	-114.0	-160.3
Relative [%]	12.7	15.1	15.9	15.8	15.1	14.2	13.2	12.2	11.2

Table C.3: Concrete shrinkage - connection stiffness 7500 N/mm

	L_{2000}	L_{3000}	L_{4000}	L_{5000}	L_{6000}	L_{7000}	L_{8000}	L_{9000}	L_{10000}
no [mm]	-0.9	-2.5	-5.8	-11.3	-20.0	-32.8	-51.3	-76.7	-110.9
normal [mm]	-1.2	-3.4	-7.8	-15.0	-25.8	-41.4	-62.9	-91.9	-130.0
Relative [%]	27.6	34.9	35.5	33.0	29.6	26.0	22.7	19.8	17.2

Table C.4: Concrete shrinkage - connection stiffness 15000 N/mm

	L_{2000}	L_{3000}	L_{4000}	L_{5000}	L_{6000}	L_{7000}	L_{8000}	L_{9000}	L_{10000}
no [mm]	-0.9	-2.2	-4.9	-9.6	-17.0	-28.5	-45.2	-68.6	-100.5
normal [mm]	-1.2	-3.4	-7.5	-13.9	-23.7	-37.8	-57.6	-84.6	-120.5
Relative [%]	43.0	53.1	51.5	45.5	38.8	32.7	27.6	23.3	19.9

Table C.5: Concrete shrinkage - connection stiffness 25000 N/mm

	L_{2000}	L_{3000}	L_{4000}	L_{5000}	L_{6000}	L_{7000}	L_{8000}	L_{9000}	L_{10000}
no [mm]	-0.8	-2.1	-4.5	-8.7	-15.7	-26.5	-42.5	-65.1	-96.1
normal [mm]	-1.3	-3.4	-7.2	-13.3	-22.6	-36.2	-55.3	-81.5	-116.5
Relative [%]	56.6	67.3	62.8	53.6	44.3	36.5	30.1	25.1	21.2

Table C.6: Concrete shrinkage - moisture content

	MC_0	MC_2	MC_4	MC_6	MC_8
no [mm]	-19.8	-16.9	-13.9	-11.0	-8.1
normal [mm]	-25.6	-22.7	-19.8	-16.9	-14.0
Absolute [mm]	5.85	5.85	5.85	5.85	5.85
Relative [%]	29.6	34.7	42.0	53.0	72.0

Table C.7: Timber creep - connection stiffness

	K_{7500}	K_{20000}	K_{45000}	K_{100000}
SC 2 [mm]	-21.1	-15.9	-13.1	-11.6
SC 3 [mm]	-32.9	-25.3	-20.7	-18.1
Relative [%]	56.0	58.5	57.6	55.7

Table C.8: Timber creep - length, creep factor 1.5

	L_{2000}	L_{4000}	L_{6000}	L_{8000}	L_{10000}
SC 2 [mm]	-0.8	-5.8	-21.1	-53.1	-109.9
SC 3 [mm]	-1.2	-8.8	-32.9	-84.2	-174.9
Relative [%]	53.1	51.9	56.0	58.5	59.3

Table C.9: Timber creep - length, creep factor 2.5

	L_{2000}	L_{4000}	L_{6000}	L_{8000}	L_{10000}
SC 2 [mm]	-0.9	-6.2	-22.2	-55.9	-115.8
SC 3 [mm]	-1.3	-9.6	-35.5	-90.1	-186.3
Relative [%]	55.0	55.9	59.6	61.1	61.0

Table C.10: Concrete creep - connection stiffness

	K_{7500}	K_{20000}	K_{45000}	K_{100000}
C 1.5 [mm]	-32.9	-25.3	-20.7	-18.1
C 2.5 [mm]	-35.5	-26.9	-21.9	-19.1
Relative 1.5-2.5 [%]	7.8	6.4	5.9	5.8

Table C.11: Concrete creep - length, SC2

	L_{2000}	L_{4000}	L_{6000}	L_{8000}	L_{10000}
C 1.5 [mm]	-0.8	-5.8	-21.1	-53.1	-109.9
C 2.5 [mm]	-0.9	-6.2	-22.2	-55.9	-115.8
Relative 1.5-2.5 [%]	4.9	5.8	5.4	5.2	5.4

Table C.12: Concrete creep - length, SC3

	L_{2000}	L_{4000}	L_{6000}	L_{8000}	L_{10000}
C 1.5 [mm]	-1.2	-8.8	-32.9	-84.2	-174.9
C 2.5 [mm]	-1.3	-9.6	-35.5	-90.1	-186.3
Relative 1.5-2.5 [%]	6.2	8.5	7.7	7.0	6.5

C.2 Parametric study - Part 2

Table C.13: Design 1 - timber thickness

Connection stiffness [kN/mm]:	5	10	20	40	100	250
Width, *Normal shrinkage* [mm]	102	90	75	63	54	50
Deflection [mm]	16.61	16.58	16.56	16.52	16.57	16.67
Width, *Small shrinkage* [mm]	94	78	60	49	42	39
Deflection [mm]	16.63	16.54	16.57	16.49	16.54	16.67

Table C.14: Design 2 - timber thickness

Connection stiffness [kN/mm]:	5	10	20	40	100	250
Width, *Normal shrinkage* [mm]	178	159	132	105	84	76
Deflection [mm]	16.67	16.63	16.62	16.63	16.67	16.66
Width, *Small shrinkage* [mm]	178	136	101	75	60	55
Deflection [mm]	16.67	16.66	16.63	16.64	16.66	16.63

Table C.15: Design 3 - timber thickness

Connection stiffness [kN/mm]:	5	10	20	40	100	250
Width, *Normal shrinkage* [mm]	68	58	47	41	36	35
Deflection [mm]	16.58	16.55	16.65	16.51	16.65	16.48
Width, *Small shrinkage* [mm]	61	48	37	32	28	27
Deflection [mm]	16.57	16.55	16.62	16.42	16.65	16.57

Table C.16: Design 4 - timber thickness

Connection stiffness [kN/mm]:	5	10	20	40	100	250
Width, *Normal shrinkage* [mm]	121	104	84	68	57	53
Deflection [mm]	16.61	16.63	16.60	16.59	16.64	16.64
Width, *Small shrinkage* [mm]	108	85	62	48	41	39
Deflection [mm]	16.66	16.59	16.55	16.64	16.63	16.49

Table C.17: Design 5 - timber height

Connection stiffness [kN/mm]:	5	10	20	40	100	250
Height, *Normal shrinkage* [mm]	307	292	274	256	241	233
Deflection [mm]	16.58	16.62	16.61	16.67	16.59	16.59
Height, *Small shrinkage* [mm]	298	277	253	231	212	203
Deflection [mm]	16.60	16.66	16.63	16.61	16.59	16.57

Table C.18: Design 6 - timber height

Connection stiffness [kN/mm]:	5	10	20	40	100	250
Height, *Normal shrinkage* [mm]	267	253	237	223	210	204
Deflection [mm]	16.62	16.66	16.65	16.59	16.62	16.59
Height, *Small shrinkage* [mm]	258	238	216	197	182	175
Deflection [mm]	16.58	16.64	16.62	16.63	16.59	16.58

Table C.19: Design 7 - concrete thickness

Connection stiffness [kN/mm]:	5	10	20	40	100	250
Thickness, *Normal shrinkage* [mm]	133	128	121	111	99	90
Deflection [mm]	16.66	16.66	16.59	16.65	16.64	16.66
Thickness, *Small shrinkage* [mm]	130	121	108	88	-	-
Deflection [mm]	16.55	16.66	16.64	16.66	<16.67	<16.67

Table C.20: Design 8 - concrete width

Connection stiffness [kN/mm]:	5	10	20	40	100	250
Width, *Normal shrinkage* [mm]	515	585	680	785	905	975
Deflection [mm]	16.64	16.65	16.65	16.65	16.67	16.66
Width, *Small shrinkage* [mm]	560	660	800	950	1120	1220
Deflection [mm]	16.64	16.62	16.66	16.64	16.67	16.66

Table C.21: Design 9 - concrete width

Connection stiffness [kN/mm]:	5	10	20	40	100	250
Width, *Normal shrinkage* [mm]	315	370	440	515	600	650
Deflection [mm]	16.55	16.65	16.67	16.65	16.67	16.66
Width, *Small shrinkage* [mm]	360	440	545	665	795	875
Deflection [mm]	16.66	16.65	16.59	16.63	16.63	16.67

DEPARTMENT OF ARCHITECTURE AND CIVIL ENGINEERING
CHALMERS UNIVERSITY OF TECHNOLOGY
Gothenburg, Sweden 2022
www.chalmers.se